Vitamin D receptor activation modulates the allergic immune response

vorgelegt von

Diplom-Biochemiker

Björn Hartmann

Von der Fakultät III – Prozesswissenschaften
der Technischen Universität Berlin
zur Erlangung des akademischen Grades
Doktor der Naturwissenschaften
Dr. rer. nat.
genehmigte Dissertation

Promotionsausschuss:

Vorsitzender: Prof. Dr. rer. nat. Peter Neubauer

Gutachter: Prof. Dr. rer. nat. Roland Lauster

Gutachter: Prof. Dr. med. Margitta Worm

Gutachter: Prof. Dr. rer. nat. Leif-Alexander Garbe

Tag der wissenschaftlichen Aussprache: 22.02.2011

durchgeführt an der

Charité, Klinik für Dermatologie, Venerologie und Allergologie, Berlin

Berlin 2011

D 83

“A vitamin is a substance that makes you ill if you don’t eat it.”

(Albert Szent-Gyorgyi, Nobel Prize in Physiology or Medicine, 1937)

Meinen Eltern

1. List of Abbreviations

1αOHase	25-hydroxyvitamin D_3-1α-hydroxylase (CYP27B1)
7-DHC	7-dehydrocholesterol
A647	Alexa 647
aa	amino acid (only with numbers)
AD	atopic dermatitis
ADHR	autosomal dominant hypophosphatemic rickets
AEC	3-amino-9-ethylcarbazole
AID	activation-induced cytidine deaminase
alum	aluminium hydroxide and magnesium hydroxide
AMP	antimicrobial peptide
AP	alkaline phosphatase
AP	alternative pocket (regarding VDR)
AP-1	activator protein 1
APC	allophycocyanin or antigen presenting cell
AU	arbitrary units
BALB/c	a mouse strain
BCL6	B cell lymphoma 6
BLIMP1	B lymphocyte-induced maturation protein 1
BCR	B cell receptor
bio	biotinylated
bp	base pair (only with numbers)
BSA	bovine serum albumin
CBP/p300	CREB-binding protein
CCL	CC chemokine ligand
CCR	CC chemokine receptor
CCS	charcoal stripped fetal calf serum
CD	cluster of differentiation
CD40L	CD40 ligand
cDNA	complementary DNA
CDK	cyclin-dependent kinase
CE	cornified envelope
CFSE	5(6)-carboxyfluorescein diacetate *N*-succinimidyl ester

C_H	constant heavy chain
CK-II	casein kinase II
CSR	class switch recombination
C_T/C_P	threshold cycle value/crossing point
CTACK	cutaneous T cell-attracting chemokine (CCL27)
C-terminal	carboxyl-terminal or COOH-terminal
CTLA-4	cytotoxic T-lymphocyte antigen 4 (CD152)
CYP24A1	25-hydroxyvitamin D_3-24-hydroxylase
CYP27A1	vitamin D_3-25-hydroxylase
d	day(s); deoxy; distilled (as in dH2O)
DAPI	4',6'-diamidino-2-phenylindole
DBD	DNA-binding domain
DBP	vitamin D-binding protein
DC	dendritic cell
DMF	*N,N*-dimethylformamide
DMSO	dimethylsulfoxide
DNA	deoxyribonucleic acid
DNase	deoxyribonuclease
DR	direct repeat
ds	double-stranded (as dsDNA)
DSB	double-strand DNA breaks
e.c.	epicutaneous
EDTA	ethylenediaminetetraacetic acid
ELISA	enzyme-linked immunosorbent assay
ELISPOT	enzyme-linked immunospot
ER	everted repeat (only with numbers); endoplasmic reticulum
ERK	extracellular signal-regulated kinase
ERp57	endoplasmic reticulum protein of 57 kDa
FACS	fluorescence-activated cell sorting
FCS	fetal calf serum
FcεR	receptor for IgE (FcεRI high affinity/ FcεRII (CD23) low affinity)
FGF23	fibroblast growth factor 23
FITC	fluorescein isothiocyanate
FL-	fluorescence

FO	follicular zone
FSC	forward scatter channel
g	acceleration of gravity
GM-CSF	granulocyte macrophage colony stimulation factor
GP	genomic pocket
GRp58	glucose regulated protein of 58 kDa/PDIA3
H	helix (only with numbers)
h	hour (only with numbers)
HBD	human β-defensin
HDAC	histone deacetylase
HE	hematoxylin and eosin
HIGM2	Hyper-IgM syndrome, type 2
HPRT	hypoxanthine-guanine phosphoribosyltransferase
HRP	horseradish peroxidase
HSV	herpes simplex virus
i.p.	intraperitoneal
IDEC	inflammatory dendritic epidermal cell
IFN	interferon (e.g., IFN-γ)
Ig	immunoglobulin (also IgA, IgD, IgE, IgG, IgM)
IL-	interleukin (e.g., IL-4)
IP	inverted repeat
IRF4	interferon-regulatory factor 4
ISC	immunoglobulin secreting cell
IκB	inhibitor of NF-κB
JAK or Jak	Janus kinase
JN	1α,25-dihydroxy-lumisterol D_3
JNK	JUN amino-terminal kinase
kb	kilobase (only with numbers)
K_d	distribution coefficient; dissociation constant
LAGeSo	State Office of Health and Social Affairs
LBD	ligand-binding domain
LBP	ligand-binding pocket
LC	Langerhans cell
LU	laboratory unit

mAb	monoclonal antibody
MACS	magnetic-activated cell sorting
MAPK	mitogen-activated protein kinase
MARRS	membrane associated, rapid response, steroid-binding
MCP-1	monocyte chemotactic protein 1
MDC	macrophage-derived chemokine (CCL22)
M-DC	myeloid DC
MEK	mitogen-activated protein kinase kinase
MEKK1	mitogen-activated protein kinase kinase kinase 1
MFI	median fluorescence intensity
mg	milligram (only with numbers)
MHC	major histocompatibility complex
min	minute (only with numbers)
ml	milliliter (only with numbers)
MP	milk powder
mRNA	messenger RNA
MZ	marginal zone
n	number in study or group
n.d.	not detectable
n.s.	not significant
NBNT cells	non-B non-T cells
NCoA	nuclear receptor coactivator
NCoR	nuclear receptor corepressor
NF	nuclear factor
NFAT	nuclear factor of activated T cells
NF-IL-6	nuclear factor of interleukin-6
NF-κB	nuclear factor κB
NK cell	natural killer cell
NKT cell	natural killer T cell
NLS	nuclear localization signal
NR	nuclear receptor
N-terminus	amino terminus or NH_2-terminus
NTP	nucleoside 5'-triphosphate
nVDRE	negative VDRE

OVA	ovalbumin
P	probability
PAX5	paired box protein 5
PBAF	polybromo-associated BAF, chromatin-remodeling complexes of the SWI/SNF family
PBMC	peripheral blood mononuclear cell
PBS	phosphate-buffered saline
PBS-T	PBS with Tween20
PCR	polymerase chain reaction
PE	phycoerythrin
PerCP	peridinin-chlorophyll proteins
PI	propidium iodide
PKC	protein kinase C
PL	phospholipase
PLA_2	phospholipase A_2
PLC	phospholipase C
PMTs	photomultiplier tubes
*p*NPP	*para*-nitrophenylphosphate
pSTAT	phosphorylated signal transducer and activator of transcription
PTH	parathyroid hormone
PTHrP	parathyroid hormone-related protein
qPCR	quantitative PCR
R	receptor (e.g., IL-4R)
r	recombinant, (e.g., rIL4)
RANKL	receptor activator of NF-κB ligand (also known as CD254, OPGL and TRANCE)
RBC	red blood cell
RNA	ribonucleic acid
RNase	ribonuclease
RT	room temperature
RXR	retinoid X receptor
s	second (use only with numbers)
S. aureus	*Staphylococcus aureus*
s.c.	subcutaneous
SDLN	skin-draining lymph nodes

SEM	standard error of the mean
SMRT	silent mediator for retinoid and thyroid hormone receptor
Src	tyrosine kinase
SRC-1	steroid receptor coactivator 1
SSC	side scatter channel
STAT	signal transducer and activator of transcription
SWI/SNF	SWItch/Sucrose NonFermentable
Sε	genomic epsilon switch region
TBS	Tris-buffered saline
TBS-T	TBS with Tween 20
TCR	T cell receptor for Ag
TEWL	transepidermal water loss
TGF	transforming growth factor
T_H cell	T helper cell
TIO	tumor-induced osteomalacia
TLR	Toll-like receptor
TMB	3,3',5,5'-tetramethylbenzidine
TNF	tumor necrosis factor (e.g., TNFα)
TNP	trinitrophenyl
TRAF	TNF-receptor-associated factor
T_{reg}	regulatory T cell
Tris	tris(hydroxymethyl)aminomethane
TSLP	thymic stromal lymphopoietin
UV	ultraviolet
VDJ	variable (V), diversity (D), and joining (J)
VDR	vitamin D receptor
VDRE	1α,25-hydroxyvitamin D_3 response element, vitamin D response element
VDS	vitamin D sterol
VV	vaccinia virus
wk	week (only with numbers)
XLH	X-linked hypophosphatemic rickets
XBP1	X-box-binding protein 1
ZK159222	(5*Z*,7*E*,22*E*)-(1*S*,3*R*,24*R*)-1,3,24-trihydroxy-26,27-cyclo-9,10-secocholesta 5,7,10(19),22-tetraene-25-carboxylic acid butyl ester

ZK203278	(5*Z*,7*E*)-(1*S*,3*R*,24a*S*)-24a-(thiazol-2-yl)-24a-homo-9,10-secochola-5,7,10(19)-triene-1,3,24a-triol
β-ME	β-mercaptoethanol
εGLT	epsilon germline transcript
µg	microgram (only with numbers)
µl	microliter (only with numbers)

1. Abstract

Vitamin D, known as “the sunshine vitamin”, has become increasingly recognized as a pluripotent autocrine and paracrine hormone to regulate biological functions beyond its classical effects on bone and calcium homeostasis. Much of the growing interest in vitamin D is provoked by new data on nonclassical immunomodulatory effects of calcitriol, the active form of vitamin D, and by the growing worldwide trend to nutritional vitamin D insufficiency. Epidemiological data indicate a significant association between vitamin D deficiency and increased incidence or risk of several autoimmune and cardiovascular diseases as well as cancer. Moreover, an important modulatory role of vitamin D in asthma and other allergic disorders is now clearly recognized. Based on the critical role of vitamin D and the vitamin D receptor (VDR) in the immune system and skin homeostasis VDR targeted therapies have gained great interest over the last years.

Unfortunately, the effective therapeutic doses of calcitriol required for the treatment of most disorders can have toxic side effects, especially hypercalcemia. This limitation of calcitriol therapy has stimulated the development of dissociated vitamin D analogs that retain the therapeutically important properties of the natural ligand, but have reduced calcemic activity.

This thesis aimed to investigate the impact of a novel low-calcemic VDR agonist on the allergic immune response *in vitro* and *in vivo*. As recently reported for calcitriol, the low-calcemic VDR agonist strongly inhibited the stimulated IgE response of human peripheral B cells. IgG and to a lesser extent IgA were affected as well. The mechanisms leading to reduced levels of immunoglobulins involved a reduction of immunoglobulin-secreting cells and diminished gene expression of activation-induced deaminase (AID). Importantly, the VDR agonist was well tolerated *in vivo* and impaired the humoral IgE response in a type I allergy mouse model in a therapeutic setting (i.e. treatment subsequent to allergic sensitization). Moreover, treatment with the VDR agonist improved the clinical symptoms in a mouse model of allergic skin inflammation, mimicking atopic dermatitis (AD) in humans. In this setting, an induction of $Foxp3^+$ cells and increased expression of skin barrier genes, known to play a crucial role in AD, likely contributed to the improvement of allergen-induced dermatitis.

In conclusion, these data provide evidence that VDR activation by a low-calcemic agonist modulates the humoral immune response including IgE *in vitro* and *in vivo*. Hence, VDR targeting by a low-calcemic ligand may prove a promising strategy for the treatment of AD and allergic diseases.

2. Zusammenfassung

Vitamin D, auch bekannt als das „Sonnenschein-Vitamin“, ist ein pluripotentes, autokrin und parakrin wirkendes Hormon, das neben den klassischen Funktionen im Knochen und der Kalziumhomöostase, auch weitere biologische Prozesse beeinflussen kann. Das wachsenden Interesse an Vitamin D wird unter anderem durch neue Erkenntnisse zu den sogenannten nicht-klassischen, immunmodulatorischen Effekten von Calcitriol, der aktiven Form des Vitamin D, und die weltweit zunehmende, nahrungsbedingte Vitamin D-Insuffizienz verursacht. Epidemiologische Daten deuten darauf hin, dass es einen signifikanten Zusammenhang zwischen der Vitamin D-Defizienz und der steigenden Inzidenz von verschiedenen Autoimmun- und Krebserkrankungen sowie kardiovaskulären Erkrankungen gibt. Darüber hinaus ist eine wichtige modulatorische Funktion von Vitamin D im Hinblick auf die Entwicklung und Ausprägung von Asthma und anderen allergischen Erkrankungen deutlich erkennbar.

Vitamin D und Vitamin D-Rezeptoren (VDR) haben in den letzten Jahren, aufgrund ihrer wichtigen Funktion im Immunsystem und der Homöostase der Haut, eine wichtige Stellung für therapeutische Ansätze erlangt. Jedoch können die therapeutisch wirksamen Dosen von Calcitriol, die für die Behandlung der meisten Erkrankungen erforderlich wären, toxische Nebenwirkungen, insbesondere Hyperkalzämie, verursachen. Die daraus resultierende Limitierung einer Therapie mit Calcitriol hat die Entwicklung selektiver Vitamin D-Analoga, die die therapeutisch entscheidenden Eigenschaften des natürlichen Liganden bei gleichzeitig verminderter hyperkalzämischer Aktivität besitzen, vorangetrieben.

Diese Arbeit hatte das Ziel, den Einfluss eines neuen, niedrigkalzämischen VDR-Agonisten auf die allergische Immunantwort *in vitro* und *in vivo* zu untersuchen. Wie bereits für Calcitriol gezeigt wurde, führte auch der niedrigkalzämische VDR-Agonist zu einer Hemmung der IgE-Immunantwort in humanen peripheren B-Zellen. Des Weiteren waren auch die Isotypen IgG und, in geringerem Ausmaß, IgA beeinflusst. Als Mechanismen, die zur Abnahme in der IgE-Produktion führten, konnten eine Verminderung der Anzahl Immunglobulin-sezernierender Zellen sowie eine verringerte Genexpression der aktivierungsinduzierten Cytidin-Deaminase (AID) nachgewiesen werden. Weitere Analysen ergaben, dass der VDR-Agonist *in vivo* gut verträglich ist und auch hier die humorale IgE-Immunantwort durch therapeutische Applikation in einem Typ I-Allergie Mausmodell inhibierte. Darüber hinaus führte die therapeutische Anwendung des VDR-Agonisten in einem allergischen Hautentzündungsmodell der Maus zu einer signifikanten Verbesserung der

Ekzemausprägung. Dabei könnten der beobachtete Anstieg von Foxp3$^+$-Zellen in der Haut sowie die verstärkte Genexpression von Hautbarriere-Genen, beides wichtige Parameter in der Pathogenese der atopischen Dermatitis, zur Verbesserung des Hautbildes beigetragen haben.
Zusammenfassend zeigen die hier dargestellten Ergebnisse, dass die Aktivierung des VDRs durch niedrigkalzämische VDR-Agonisten die humorale Immunantwort, einschließlich IgE, *in vitro* und *in vivo* reguliert. Die VDR-Aktivierung könnte darüber hinaus, durch Modulation spezifischer Immunantworten und der positiven Wirkung auf die Barrierefunktion der Haut, auch von Vorteil für die Behandlung allergisch bedingter Hauterkrankungen wie der atopischen Dermatitis sein. Somit stellen niedrigkalzämische VDR-Agonisten einen vielversprechenden Ansatz für neue immunmodulatorische Therapien dar.

3. Introduction

3.1. Vitamin D and physiology

Vitamins are defined as small organic compounds derived from nutritional origin and required in tiny amounts by an organism for diverse biochemical reactions. Although vitamin D_3 can be obtained by nutritional uptake or dietary supplements, photochemical synthesis following exposure to sunlight in the skin serves as the major source of this secosteroid compound which, under usual circumstances, contributes to more than 90% to the serum concentration of vitamin D_3[1]. Therefore, by definition vitamin D_3 is not a true vitamin[2].

Solar ultraviolet B (UV-B) radiation (wavelength: 280 – 320 nm) penetrates throughout the epidermis of skin and converts 7-dehydrocholesterol (7-DHC) in a photochemical reaction with a maximum spectral effectiveness from 297 to 302 nm to the secosteroid pre-vitamin D_3 (Figure 1)[1, 3, 4]. The epidermal layers with the highest capacity for conversion to pre-vitamin D_3 are the stratum spinosum and basale[3, 5]. In a next step, pre-vitamin D_3 is converted in a time- and temperature-dependent nonenzymatic isomerization to the secosteroid vitamin D_3 (cholecalciferol, calciol, calciferol) (Figure 1)[1, 3]. Experimental evidence indicates that about 50% of the pre-vitamin D_3 can isomerize to vitamin D_3 within 2.5 hours in the skin[1]. Thereby, the effectiveness of cutaneous synthesis of vitamin D_3 is determined by the content of 7-DHC in the skin, mainly regulated by the activity of the 7-DHC-Δ^7-reductase[6]; the wavelength and exposure doses of the UV-B radiation[7-9]; the solar zenith angle and time of day[10]; the skin pigmentation and use of sunscreens[11-13]; the temperature[3]; and the age[14]. As UV-B exposure higher than the suberythemogenic dose causes photoisomerization of pre-vitamin D_3 to inactive isomers, such as lumisterol, tachysterol, toxisterols, and 7-DHC[15], and of vitamin D_3 to suprasterols I, II and 5,6-*trans*-vitamin D_3[9], the photochemical synthesis of pre-vitamin D_3 and vitamin D_3 in the skin is a self-limiting process to prevent vitamin D_3 intoxication.

Vitamin D_3 (cholecalciferol) itself is biologically inert and requires a stepwise activation by several hydroxylation steps[1]. In the course of this process, vitamin D_3 is preferentially translocated into the circulation by binding to serum carrier proteins, in particular, vitamin D-binding protein (DBP)[16-18]. Vitamin D_3 from dietary sources, fortified foods and supplements is incorporated into chylomicrons and absorbed into the lymphatic system[19]. Vitamin D_3 is transported by the abundant, multifunctional DBP, also known as Gc-globulin[16, 17], to the liver where it is enzymatically metabolized in a first step to 25-hydroxyvitamin D_3 (25-hydroxycholecalciferol, calcidiol) (Figure 1). This side chain hydroxylation is catalyzed by the microsomal cytochrome P450-containing vitamin D_3-25-hydroxylase CYP2R1, the major

player *in vivo*, with the highest affinity and specificity for vitamin D_3, and by the mitochondrial cytochrome P450-containing CYP27A1[20, 21]. Recently, additional microsomal cytochrome P450 mixed function oxidases from different species, namely CYP2D11, CYP3A4, CYP2D25, and CYP2J2/3, were found to be capable of 25-hydroxylation[20-22].

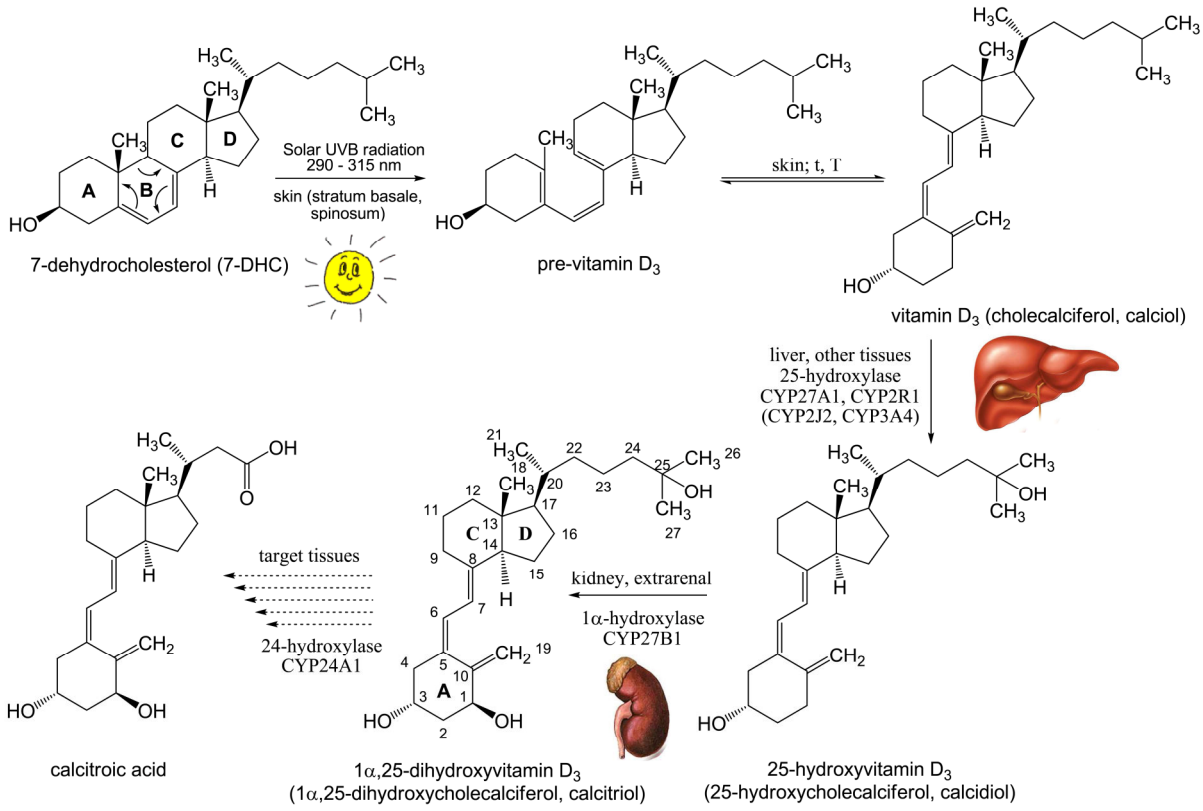

Figure 1 Vitamin D_3 synthesis, sequential activation and catabolism. Vitamin D_3 is mainly produced in the basal and suprabasal layers of the skin by the photolytic cleavage of 7-dehydrocholesterol (7-DHC) to pre-vitamin D_3 followed by a time (t)- and temperature (T)-dependent isomerization to vitamin D_3 (cholecalciferol). Vitamin D_3 is mainly transported to the liver via the serum vitamin D binding protein (DBP), where it is converted by the 25-hydroxylase (CYP27A1) to 25-hydroxyvitamin D_3 (25-hydroxycholecalciferol), the major circulating metabolite of vitamin D_3. The final activation step, 1α-hydroxylation, occurs primarily, but not exclusively, in the kidney by the CYP27B1 (see text), forming 1α,25-dihydroxyvitamin D_3 (calcitriol), the hormonal and biologically active form of the vitamin. The inactivation of the active compound is carried out by the 24-hydroxylase (CYP24A1), which catalyzes a series of oxidation steps resulting in side chain cleavage, e.g. to calcitroic acid.

After the first hydroxylation step, 25-hydroxyvitamin D_3 enters the circulation where it is tightly bound to the DBP (K_d = 5 x 10^{-8} M)[17]. Caused by this tight binding and the high plasma concentration of DBP (5 – 6 µM, 0.3 – 0.5 mg/ml) virtually all 25-hydroxyvitamin D_3 in the circulating blood is bound to the DBP[17]. Only approximately 0.04% (equivalent to 12.4 ± 4.5 pM)[1, 17] of this metabolite is found in free form resulting in a half-life of about

15 days[23]. The serum concentration of 25-hydroxyvitamin D_3, the major circulating form of vitamin D_3, is between 25 nM to 200 nM and determines plus 25-hydroxyvitamin D_2 a patient's vitamin D status[23-25]. Currently, serum levels of less than 20 ng/ml (50 nM) are considered to indicate vitamin D deficiency. Vitamin D insufficiency is now recognized as a 25-hydroxyvitamin D_3 serum concentration of 21 – 29 ng/ml. Levels of 30 ng/ml (75 nM) to 60 ng/ml (150 nM) are considered by many investigators as preferred range, while levels much greater than 150 ng/ml (374 nM) are believed to be toxic, associated with hypercalcemia, hypercalciuria and, often, hyperphosphatemia[24, 25].

Subsequent to the transport to the kidneys, 25-hydroxyvitamin D_3 bound to the DBP is endocytosed in the proximal tubular epithelium via the endocytic receptor pathway recognizing DBP by cubilin and megalin[26-28]. The endocytosed complexes are delivered to lysosomes where DBP is degraded[27] and 25-hydroxyvitamin D_3 finally hydroxylated by the 25-hydroxyvitamin D_3-1α-hydroxylase CYP27B1 (1αOHase) to the main biologically active form 1α,25-dihydroxyvitamin D_3 (1α,25-dihydroxycholecalciferol, calcitriol)[29, 30] (Figure 1). This reaction is tightly regulated by the parathyroid hormone (PTH), calcium, phosphate, calcitonin, fibroblast growth factor 23 (FGF23), and calcitriol itself[1, 20, 24, 31, 32]. Calcitriol binds DBP with an affinity of 2 x 10^{-7} M, and has a serum half-life of 10 – 20 hours[23]. Thus, the calcitriol concentration in the circulation ranges from 75 pM to 200 pM whereas 0.4% of the ligand are in the free form[1, 16, 17].

Interestingly, numerous reports considerably evidence additional extrarenal sites of calcitriol synthesis from 25-hydroxyvitamin D_3 (summarized in Table 1) followed by autocrine, intracrine and paracrine hormonal effects[1, 33-37]. More importantly, several immune cells including, human monocytes and macrophages[38-42], dermal and monocyte-derived dendritic cells (DCs)[43-45], B cells[46, 47], and T cells[45, 48] express CYP27B1 (1αOHase) which enables them to locally hydroxylate 25-hydroxyvitamin D_3 upon activation by immune stimuli resulting in the autocrine production of calcitriol (Table 1).

A number of cell types, including epidermal keratinocytes, macrophages, DCs, prostate epithelial cells, and osteoblasts, express both vitamin D_3-metabolizing enzymes, vitamin D_3-25-hydroxylase (CYP27A1) and 25-hydroxyvitamin D_3-1α-hydroxylase (CYP27B1)[1, 45, 49-54]. Hence, these cells are capable to produce their own calcitriol from the precursor vitamin D_3, which was shown for human keratinocytes *in vitro*[55-57] and *in vivo*[58]. In contrast, dermal fibroblasts only express the vitamin D_3-25-hydroxylase (CYP27A1) and might play an important role in supplying calcitriol precursors, e.g. vitamin D_3 and 25-hydroxyvitamin D_3 for keratinocytes and, probably, for the serum[59].

Tissue and cells producing calcitriol	
B cells	Osteoblasts
Colon	Osteoclasts
Dendritic cells	Pancreatic islets
Endothelial cells	Parathyroid glands
Human brain (Schwann cells and oligodendrocytes)	Placenta, decidua
Macrophages	Prostate
Mammary, breast	Skin, keratinocytes
Monocytes	T cells

Table 1 Sites of CYP27B1-mediated extrarenal calcitriol production in humans, adapted from[33, 34].

The catabolism of calcitriol and 25-hydoxyvitamin D_3 is attributed to the multifunctional mitochondrial 25-hydroxyvitamin D_3-24-hydroxylase (CYP24A1), which is widely expressed and transcriptionally induced by the action of both ligands in a very rapid and sensitive manner[20, 21, 60]. The main biologically active metabolite calcitriol is catabolized by multi-step inactivation pathways (C-23 and C-24 pathways) to less lipophilic calcitroic acid in target cells which is then excreted in the bile (Figure 1)[20, 21]. 24-Hydroxylation of 25-hydroxyvitamin D_3 generates 24*R*,25-dihydroxyvitamin D_3, which has lower binding affinity to the nuclear vitamin D receptor (VDR)[60]. Nevertheless, it has been shown to exert biological activities in parathyroid gland, bone metabolism and to activate the human osteocalcin gene[61-63].

3.2. Vitamin D receptor and signaling

The natural ligand 1α,25-dihydroxyvitamin D_3 (calcitriol), and its synthetic analogs exert its hormonal functions by binding to the vitamin D receptor (VDR, NR1I1), first discovered in the chick intestine[64-66]. The VDR belongs to the family of nuclear receptor (NR) proteins[67, 68], and can act as both a classical ligand-dependent transcription factor in a genomic manner and membrane receptor within seconds to minutes in a nongenomic manner[69-71]. The VDR is structured in at least three functional domains, including a variable amino N-terminal activation domain (A/B), a highly conserved DNA-binding domain (DBD) and a conserved carboxy C-terminal ligand-binding domain (LBD)[31, 67] (Figure 2). The N-terminal A/B domain is very short and not thoroughly defined until know[72]. To date, besides the VDRA with 427 amino acids (aa), an N-terminal isoform of the human VDR (VDRB) has been identified that differ only by a 50 aa extension of the A/B domain[73, 74]. However, a region immediately N-terminal of the zinc fingers of the DBD (residues 18 – 22) serves as coactivator interface[75].

Therefore, the human VDR can interact with basal transcription factors such as TFIIB (Figure 2).

The DBD includes regions termed P- and D-box within two typical cysteine (Cys)-rich zinc finger motifs, two α-helices and a C-terminal extension that contains the so-called T- and A-box[76, 77]. A defining feature of each zinc finger in the DBD is its compact, interdependent structure in which four conserved cysteine residues tetrahedrally coordinate one zinc ion (Zn^{2+}) to form a zinc finger DNA binding motif[72, 76] (Figure 2).

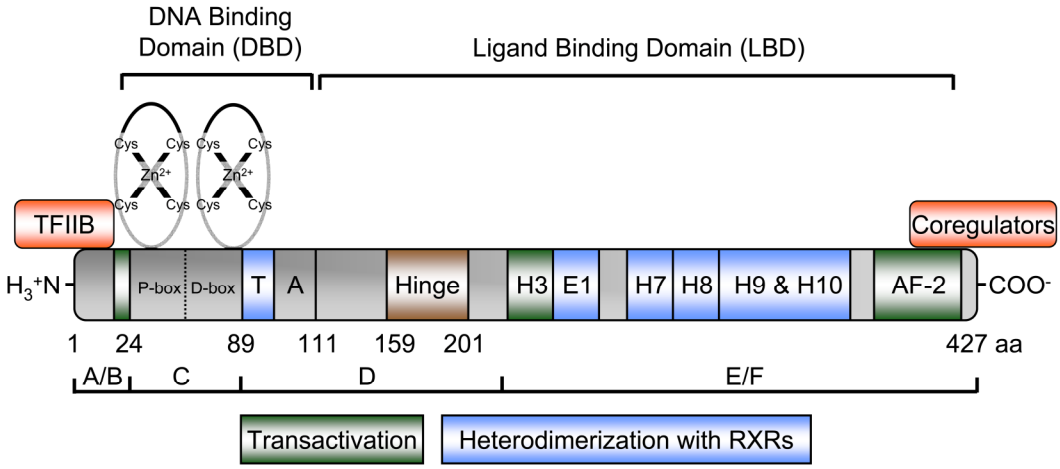

Figure 2 Domain structure of the human vitamin D receptor (VDR); see text for details.

The first N-terminal α-helix contains P-box residues beginning with the third conserved cysteine residue and binds the major groove of DNA to make specific contact with DNA response elements[72, 76, 77]. The second α-helix forms a right angle with the first so-called recognition helix. Conserved residues in the second zinc finger labeled as D-box dictates the half-site spacing. The reverse β-turn formed by six residues at the base of the second zinc finger, the so-called T-box, may form a critical dimerization interface for DNA-directed interaction between the VDR and retinoid X receptor (RXR)[72, 78]. The D domain harbors the hinge region, a long α-helical structure between the DBD and LBD allowing flexibility and changes in structural conformation upon ligand activation[72, 77, 78] (Figure 2).

The LBD of the VDR consists of a three-stranded β-sheet and 12 α-helices (H1 – H12) arranged to create a three-layer antiparallel sandwich-like structure that mediates ligand binding in a large hydrophobic core as well as dimerization, and ligand-dependent transactivation function (Figure 3B)[70, 75]. The C-terminal flexible helix H12 (domain F; residues 404 – 427) constitutes the activation function-2 (AF-2) domain that contributes

together with helix H3, H4 and H5 to the activation of transcription by forming high affinity interfaces for nuclear coregulators such as coactivator (NCoA) molecules (Figure 2)[70, 75].

Recently, Mitzwicki and colleagues proposed the so-called vitamin D sterol (VDS)-vitamin D receptor (VDR) conformational ensemble model[70, 71, 79]. The VDS-VDR conformational ensemble model is separated into three interconnected parts: the VDS conformational ensemble (Figure 3A), the VDR two pocket model (Figure 3B), and the VDR (helix 12) conformational ensemble (Figure 3C)[71]. The VDS-VDR conformational ensemble model proposes that two overlapping, functionally distinct ligand-binding pockets (LBPs) exist in the VDR, the genomic and alternative pocket (Figure 3B)[70, 71].

Vitamin D_3 or its active form calcitriol are unusually conformationally flexible containing three flexible regions, the A-ring, seco-B ring, and side chain (Figure 3A)[69, 70, 80]. Therefore, calcitriol exists in two principal conformations. These conformations result from 360° rotation around the 6,7 carbon-carbon single bond of the seco-B ring resulting in the 6-s-*cis*-conformer (the steroid-like shape) and the 6-s-*trans*-conformer (the extended shape) (Figure 3A)[81]. The "bowl-shape" and "planar-shape" 6-s-*trans*-conformers of calcitriol can also form a stable complex with the VDR[71]. The 6-s-*cis*-conformation is preferred for rapid nongenomic biological responses, e.g. shown for the 6-s-*cis*-locked 1α,25-dihydroxy-lumisterol D_3 (JN) that binds in the alternative pocket (AP) (Figure 3B)[70, 80, 82]. The conformationally flexible natural ligand calcitriol is a full agonist for both rapid and genomic responses[80, 83]. Recent results from structure-function analyses suggest that the major physicochemical traits of a potent and efficient VDR genomic agonist are: the ability to form hydrogen bonds (H-bonds) with the VDR Ser_{237} and Arg_{274} residues; the ability to conform to a "bowl-shaped" molecular geometry; and a molecular volume that is similar to that calculated for calcitriol. Alternatively, for a efficient non-genomic agonist: the ability to form H-bonds with Ser_{237} and Arg_{274}; the ability to conform to a more linear, "planar-like" molecular geometry, and a molecular volume that is $\leq$ to that calculated for calcitriol are major traits[71].

VDR nuclear localization signals (NLS, residues 49 – 55, 79 – 105) direct the receptor mainly into the nucleus[84, 85]. Upon ligand-binding to the LBD, VDR is stabilized by the phosphorylation of Ser_{51} in the DBD by protein kinase C (PKC)[86], and Ser_{208} in the hinge region by casein kinase II (CK-II)[87]. As a transcription factor, the occupied VDR is tightly associated with its heterodimeric partner, RXR – which has three main isoforms: α, β and γ[76, 88] – and binds to vitamin D responsive elements (VDREs) in the promoters of vitamin D-regulated genes to up- or downregulate transcription[31, 70].

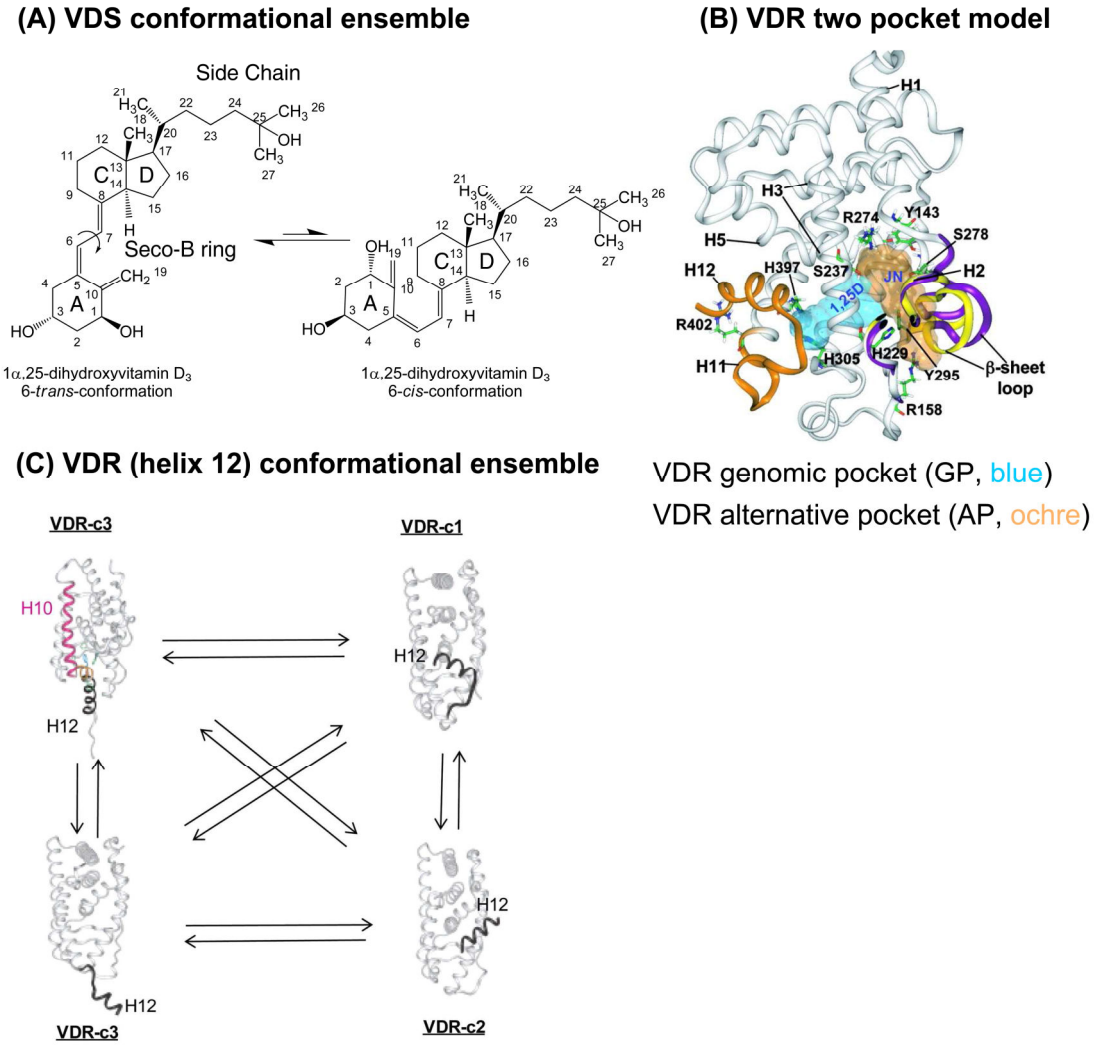

Figure 3 The vitamin D sterol (VDS)-vitamin D receptor (VDR) conformational ensemble model, adapted from[82, 89]. (A) Conformations of 1α,25-dihydroxyvitamin D_3. (B) Ribbon diagram from molecular modeling of the VDR LBD. The more hydrophobic VDR genomic pocket (GP, blue Connolly surface) is occupied by 6-s-*trans*-1α,25-dihydroxyvitamin D_3 and 1α,25-dihydroxy-lumisterol D_3 (JN) is docked in the putative overlapping more hydrophilic VDR alternative pocket (AP, ochre Connolly surface). The C-terminal end of helix 11 (H11) and H12 are colored orange and H12 is shown in the closed, transcriptionally active conformation. H2 and the β-sheet are colored yellow, whereas the purple ribbons indicate their final position after JN was docked in the A pocket. Important amino acid residues are labelled. (C) Dynamic conformational heterogeneity of the helix 12 (black ribbon, labeled H12) of the human VDR molecule in the absence of ligand projected using NR x-ray data (see Protein Data Bank). In VDR-c1, helix 12 is in the closed, active conformation. In the VDR-c2 conformational isomer, H12 is bound to the NCoA surface. It is proposed that in VDR-c3, H12 is in the opened conformation, where the ligand binding pocket is accessible to ligand (bottom, VDR-c3 structure) or is occupied by H11 residues (orange ribbon in the top VDR-c3 structure), thereby exposing the C-terminal H11 Arg_{402} residue. Certainly, synthetic or natural ligands can do the same[70, 82, 89].

VDREs composed of two binding sites arranged either as a direct repeat of two hexameric half-elements with a spacer of commonly three nucleotides (DR3), inverted palindromes interspaced by nine nucleotides (IP9) or an everted repeat of two half-elements with a spacer of six nucleotides (ER6) motif[31, 75]. The consensus sequence considered for a VDRE half site is (A/G)G(G/T)TCA, with RXR occupying the 5′ half-element and VDR the 3′ half-element[31, 75]. Positive VDREs promote the binding of a coactivator complex to the ligated VDR-RXR heterodimer that includes not only steroid receptor coactivator 1 (SRC-1), but also CBP/p300, nuclear receptor coactivator-62 (NCoA-62) and a SWI/SNF chromatin remodeling complex anchored by polybromo-associated BAF (PBAF) resulting in transcriptional activation[75]. In contrast, negative VDREs (nVDRE), which closely resemble the consensus sequence, bind either VDR-RXR heterodimers or VDR homodimers and mediate repression of transcription by recruiting histone deacetylases (HDAC) and NR corepressors (NCoR)/silent mediator for retinoid and thyroid hormone receptor (SMRT) corepressors[31, 75]. Another group of nVDREs, composed of E-box type motifs with the sequence 5'-CATCTG-3', was identified in the human CYP27B1, as well as in the human PTH and PTHrP promoters[32, 90, 91].

Besides genomic responses, a wide range of rapid, non-genomic responses have been shown for the classical VDR, which can be associated with caveolae in the plasma membrane[92, 93]. Caveolae, a subset of membrane (lipid) rafts, are flask-shaped membrane invaginations containing scaffolding caveolin proteins, sphingolipids and cholesterol that serve as interaction platforms for signaling components[94]. Thereby, calcitriol mediated rapid responses include the modulation of several signaling molecules such as PKC, mitogen-activated protein kinase (MAPK), phospholipase A_2 (PLA_2), phospholipase C (PLC), store-operated Ca^{2+} channels and Src kinases[70, 95]. More recently, another membrane receptor for calcitriol, which is a distinct gene product from the classical nuclear VDR, was discovered. This 57 kDa protein is named 1,25D_3-MARRS (membrane associated, rapid response, steroid-binding), and is identical to a previously cloned member of the thioredoxin family of proteins, ERp57 (endoplasmic reticulum protein of 57 kDa) or alternatively GRp58 (glucose regulated protein of 58 kDa)/PDIA3[96-99]. In addition, localization in the endoplasmic reticulum (ER) and in the nucleus has been shown for MARRS (ERp57/PDIA3), which also contains a domain that can bind to DNA[99-101]. Nevertheless, some of these non-genomic signals can modulate the expression of genes, either through effects on the function of the VDR in the nucleus or independently of VDR[70].

3.3. Vitamin D and the immune system

The VDR is expressed in a wide range of tissues and cells (Table 2) reflecting its capability to influence about 3% of the humane genome[34, 102].

Tissue and cell distribution of VDR	
Adipose	Monocytes/Macrophages
Adrenal	Muscle, cardiac
Bone, osteoblasts	Muscle, embryonic
Brain, general	Muscle, smooth
Brain, amygdale	Ovary
Brain, hypothalamus	Pancreas β-cell
Brain, glial cells	Parathyroid
Breast	Parotid
Cartilage	Pituitary
Colon	Placenta
Dendritic cells	Prostate
Eggshell gland	Retina
Epididymus, seminiferous tubules	Skin
Gills (fish)	Sperm
Hair follicle	Stomach
Intestine	Testis
Kidney	Thymus
Liver	Thyroid
Lung	Tonsils, dendritic cells
Lymphocytes (B, T)	Uterus
Mast cells	Yolk sac

Table 2 Sites of vitamin D receptor (VDR) expression, adapted from[33, 34].

The classic physiological function of the hormonally active calcitriol is to maintain serum calcium and phosphorus levels within the normal physiologic range to support most metabolic functions, neuromuscular transmission, and bone mineralization[19, 24]. Inherited vitamin D-resistant syndromes such as vitamin D-dependent rickets type 1 to 3, vitamin D or calcium deficiency, X-linked hypophosphatemic rickets (XLH), autosomal dominant hypophosphatemic rickets (ADHR) and tumor-induced osteomalacia (TIO) result in hypocalcemia, hyperparathyroidism, hypophoshatemia, phosphaturia, rickets, and osteomalacia[19, 103]. During the past decades, the knowledge of the vitamin D metabolism has greatly evolved. The discovery of VDRs and vitamin D-activating enzymes in extrarenal tissues and cell types, strongly indicating a more diverse role of vitamin D metabolism, and the worsening, world-wide trend to vitamin D insufficiency or deficiency heightened the interest in vitamin D physiology[104, 105]. Thereby, besides causing osteoporosis and muscle weakness, vitamin D deficiency is also linked to an increased incidence of multiple malignancies, metabolic and cardiovascular diseases, neurological, and immune disorders

such as autoimmune diseases[24, 103-105]. The ubiquitous expression of VDR in multiple immune cells such as dendritic cells[45, 106], monocytes[107], macrophages[107], mast cells[108], and activated T and B cells[45, 48, 109-111] (Table 2) led to its recognition as a central immunomodulator. Thus, VDR signaling can modulate the innate and adaptive immunity.

It is known that activation of monocyte/macrophage toll-like receptor (TLR)2/1 stimulates expression of the VDR and 25-hydroxyvitamin D_3-1α-hydroxylase (CYP27B1) in an interleukin-15 (IL-15)-dependent manner[112]. In addition, interferon γ (IFNγ) and CD14/TLR4 activation is also reported to induce CYP27B1 expression in human monocytes[38]. In this way, 25-hydroxyvitamin D_3 is converted into the hormonally active form calcitriol in the mitochondria of monocytes/macrophages[41]. Consequently, calcitriol binds to the VDR and transcriptionally induces target genes such as the antimicrobial protein human cathelicidin (CAMP/hCAP18/LL-37)[113, 114]. The antimicrobial protein human β-defensin 4 (DEFB4, formerly HBD2) is also transcriptionally induced by calcitriol but requires co-stimulation by activators of NF-κB, such as IL-1β[115]. Remarkably, the regulation of the *camp* (encoding hCAP18) and *defb4* (encoding β-defensin 4) genes by calcitriol appears to be not conserved between human and mouse[113, 116]. Additionally, calcitriol can inhibit the expression of inflammatory cytokines, including IL-1β, IL-6, TNFα, IL-8, and IL-12 in monocytes[117-119]. Differentiation of monocytes, into either macrophages or immature and mature DCs, is accompanied by a reciprocal organization of CYP27B1 and VDR expression ensuring that mature antigen-presenting DCs are relatively insensitive to calcitriol, thereby shaping defined T cell responses[43, 107]. VDR signaling prevents DC maturation as evidenced by a decreased expression of DC markers (e.g. CD1a), major histocompatibility complex class II (MHC-II), co-stimulatory molecules (CD40, CD80, and CD86), and other maturation induced surface markers (e.g. CD83)[120-123]. Calcitriol also inhibits the production of the T helper 1 (T_H1) polarizing factor IL-12 and the T_H17 polarizing factor IL-23 in DCs whereas the release of the tolerogenic cytokine IL-10 and the chemokine CCL22, involved in the recruitment of CCR4-expressing regulatory T cells (T_{regs})[124, 125], is enhanced[120, 121]. Together, VDR activation promotes a tolerogenic phenotype and function in myeloid DCs (M-DCs)[126] and seems to foster the induction of $CD4^+$ $CD25^+$ T_{regs}[127].

VDR activation by its natural ligand also directly modulates the function of adaptive immune cells. It inhibits T cell proliferation[128], the production of inflammatory T_H1 cytokines such as IL-2[128-130] and IFNγ[131], the T_H17-derived cytokines IL-17 and IL-21[132], and CD8 T cell-mediated cytotoxicity[133], whereas IL-10 expression can be induced[132, 134] or inhibited[48, 135] in human T cells. Contradictory reports exist regarding T_H2-skewing effects of VDR activation

in murine $CD4^+$ T cells, showing an induction of the T_H2 cytokines IL-4[136], IL-5, and IL-10 as well as T_H2-specific transcription factors GATA3 and c-Maf[137] whereas others report an inhibition of IL-4 and IFNγ with stable GATA3 and c-Maf expression in mice[138]. Whether or not VDR triggering favors a shift toward T_H1 versus T_H2 dominance remains to be elucidated. More interestingly, VDR activation by calcitriol alone or in combination with dexamethasone has been shown to induce human T_{regs} expressing CTLA-4 and Foxp3[132] and murine naive $CD4^+$ T cells to differentiate into IL-10-producing T_{regs}, even in the absence of antigen-presenting cells (APCs)[139]. However, VDR triggering not only facilitates induction and expansion of T_{regs} and enhance their suppressive activity, but can promote their recruitment to sites of inflammation, too[140-143].

In human B cells, an inhibitory effect of calcitriol on immunoglobulin E (IgE) synthesis *in vitro*, at least in part mediated by diminished nuclear factor-κB (NF-κB) activation and inhibition of the epsilon germline transcript (εGLT), has been proven[144]. Additionally, a recent study has shown that the liganded VDR binds to the εGLT gene promoter and exhibits transrepressive activity[145]. In contrast, another report showed that VDR activation by calcitriol inhibits the proliferation, plasma cell differentiation and immunoglobulin secretion including IgG and IgM, memory B cell generation and induces B cell apoptosis[46]. Despite these suppressive functions of calcitriol on human B cells, it enhances IL-10 expression in activated B cells[47] and promotes expression of the skin-homing receptor CCR10 in terminally differentiating B cells[146]. Likewise it has been described in activated T cells[45].

3.4. Vitamin D in allergic diseases and atopic dermatitis

3.4.1. Type I allergic immune response

The term allergy can be used to refer an abnormal and harmful adaptive immune response directed against various non-infectious environmental antigens (allergens)[147]. There are two main types of allergen. The first type includes any non-infectious environmental protein that induces IgE- and T_H2 cell-mediated responses leading to anaphylaxis, allergic rhinitis (hay fever), some food allergies and allergic asthma. The second type of allergen is a non-infectious environmental molecule that can induce an adaptive immune response associated with a local inflammation, where IgE is thought not to be important, e.g. allergic contact dermatitis. Allergic diseases, also known as atopic disorders (from the Greek *atopos*, meaning out of place, abnormal), are common and afflict roughly 25% of people in the developed world.

In case of IgE dependent hypersensitivity, a single allergen exposure produces an acute reaction, which is known as an early-phase reaction or a type I immediate hypersensitivity reaction. Such a reaction can occur locally (for example, acute asthma or rhinoconjunctivitis) or systemically (anaphylaxis) within minutes of allergen exposure, followed by allergen-induced crosslinking of IgE bound to FcεRI (high-affinity receptor for IgE) on mast cells and basophils. The crosslinking results in the release of diverse preformed and newly synthesized mediators, including cytokines, chemokines, histamine, heparin, serotonin and proteases, causing vasodilation, increased vascular permeability with edema, and acute functional changes in affected organs. These events also promote the local recruitment and activation of leukocytes, contributing to the development of late-phase reactions. The late-phase reaction typically develops 2 – 6 h later and peaks 6 – 9 h after allergen exposure. Usually it completely resolves in 1 – 2 days. This type of reaction reflects the local recruitment and activation of T_H2 cells, eosinophils, basophils and other leukocytes, and persistent mediator production by resident cells (such as mast cells) resulting in edema, pain, warmth and erythema (redness) in the skin as well as airway narrowing and mucus hypersecretion in the lungs. Persistent or repetitive exposure to allergen leads to a chronic allergic inflammation, with presence of large numbers of innate and adaptive immune cells and alterations in the affected tissue. There are many factors affecting the probability of developing allergic diseases including genetic[148, 149], epigenetic[150, 151] and environmental components as proposed in the hygiene hypothesis[152, 153].

3.4.2. Role of T_H2 cells in the allergic immune response

T_H2 cells are indispensable for host immunity to extracellular parasites, such as helminths, but are also responsible for the development of asthma and other allergic inflammatory diseases[154]. The initiation of T_H2 cell responses takes place in the tissue sites where allergens or parasites are encountered. Activated APCs such as macrophages, Langerhans cells (LCs), DCs and basophils migrate from tissues to the draining lymph nodes to stimulate proliferation and differentiation of naïve $CD4^+$ (T_H0) into T_H2 cells under the influence of various cytokines such as thymic stromal lymphopoietin (TSLP), IL-4 and IL-25 (IL-17E) (Figure 4). Also other cell types like activated lung and intestinal epithelial cells can initiate T_H2 immune responses by acting on basophils, DCs and/or non-B non-T cells (NBNT cells) by producing TSLP, IL-25 and IL-33. Other immune cells, including natural killer (NK) cells, NKT cells, γδ T cells, macrophages, B cells, eosinophils and mast cells, may also participate in the initiation and amplification of T_H2 immune responses by creating a T_H2-biased cytokine

environment. T_H2 cell differentiation requires both, GATA-binding protein 3 (GATA3) expression and activated signal transducer and activator of transcription 5 (STAT5) activation; and is favored by low-strength T cell receptor (TCR) signaling. T_H2 cells produce various T_H2 cell-associated cytokines, including IL-2, IL-4, IL-5, IL-9, IL-13 and IL-25. T_H2 cells regulate B cell class switch recombination (CSR) to IgE through their production of IL-4 and IL-13[155] (Figure 4). Both of these cytokines use the common γ-chain (γ_c)-related IL-4 receptor α-chain (IL-4Rα) to signal through three cytokine-receptor combinations. IL-4 signals through the type I receptor IL-4Rα-γ_c, and both IL-4 and IL-13 can signal through the type II receptor IL-4Rα-IL-13Rα1[156]. Ligation of the IL-4R activates the Janus family tyrosine kinase JAK1 (through IL-4Rα), JAK3, IRS1 and TYK1 (through γ_c) (Figure 4). IL-13R triggering leads to the activation of JAK1 and TYK2. Subsequently, activated JAKs phosphorylate tyrosine residues in the intracellular domains of IL-4Rα, which serve as docking sites for STAT6 monomers (Figure 4). STAT6 gets tyrosine phosphorylated itself by the receptor-associated JAK kinases, dimerizes and translocates to the nucleus, where it can activate the transcription of target genes[155, 157] (Figure 4). Additionally, IL-21 signals via the IL-21R, which is structurally related to the IL-2Rβ associated with γ_c; and activates STAT3 subsequently stimulating the IgE production in human beings[158, 159]. Another important signal to facilitate T cell-dependent class switch recombination to IgE is provided by the membrane-bound trimeric CD40L (CD154) on T_H2 cells (Figure 4). CD40-CD40L interaction in B cells mainly allows the recruitment of tumour-necrosis factor-associated factors (TRAFs) 2, 3 and 6 that promote the activation of nuclear factor-κB (NF-κB), activator protein 1 (AP1) (Figure 4), nuclear factor of interleukin-6 (NF-IL-6), MEKK1 [mitogen-activated protein kinase kinase kinase/extracellular signal-regulated kinase (ERK)], JUN amino-terminal kinase (JNK) and p38, resulting in proliferation, differentiation, isotype switching, cytokine production, surface-molecule upregulation; protection from apoptosis; and promotion of humoral memory[155, 160].

3.4.3. Mechanism of IgE class switch recombination

STAT6 and NF-κB (p50/p65) are essential for the CSR to IgE as shown by STAT6-deficient ($STAT6^{-/-}$) mice that are severely impaired in IgE production and NF-κB $p50^{-/-}$ mice that have a preferentially impaired IgE switching[161-164]. Thereby, both transcription factors can bind to promoter regions of the epsilon germline transcript (εGLT) and *aicda*, encoding activation-induced cytidine deaminase (AID)[165-168] (Figure 4). Upon activation antibody class

switching in mature B cells occurs by a unique type of intrachromosomal deletional recombination within special G-rich tandem repeated DNA sequences [called switch, or S, regions located upstream of each of the heavy chain constant (C_H) region genes, except Cδ][169, 170]. Thus, the εGLT is transcribed as a sterile transcript, starting with the Iε exon, which is located immediately upstream of Sε and proceeds with Sε and Cε. The Iε exon is spliced to Cε yielding the human 1.7 kb εGLT[168, 171]. The sterile εGLT, which remains hybridized to the template strand of the switch region DNA, forms the "R loop" structure (RNA-DNA hybrid). During this process, AID is recruited by an unknown mechanism and deaminates several cytosine bases to uracil bases in the donor and acceptor S regions, which results in double-strand DNA breaks (DSBs) in both S regions by DNA-repair proteins and CSR by an end-joining type of recombination. Joining can then occur between breaks upstream of the Cε cluster of exons and downstream of the variable (V), diversity (D), and joining (J) gene segments, giving rise to an intact IgE heavy-chain gene[169, 172, 173]. The phenotype observed in patients with the autosomal recessive form of Hyper-IgM syndrome (HIGM2) and in AID$^{-/-}$ mice demonstrates the absolute requirement for AID in several crucial steps of B cell terminal differentiation necessary for efficient antibody responses[174, 175].

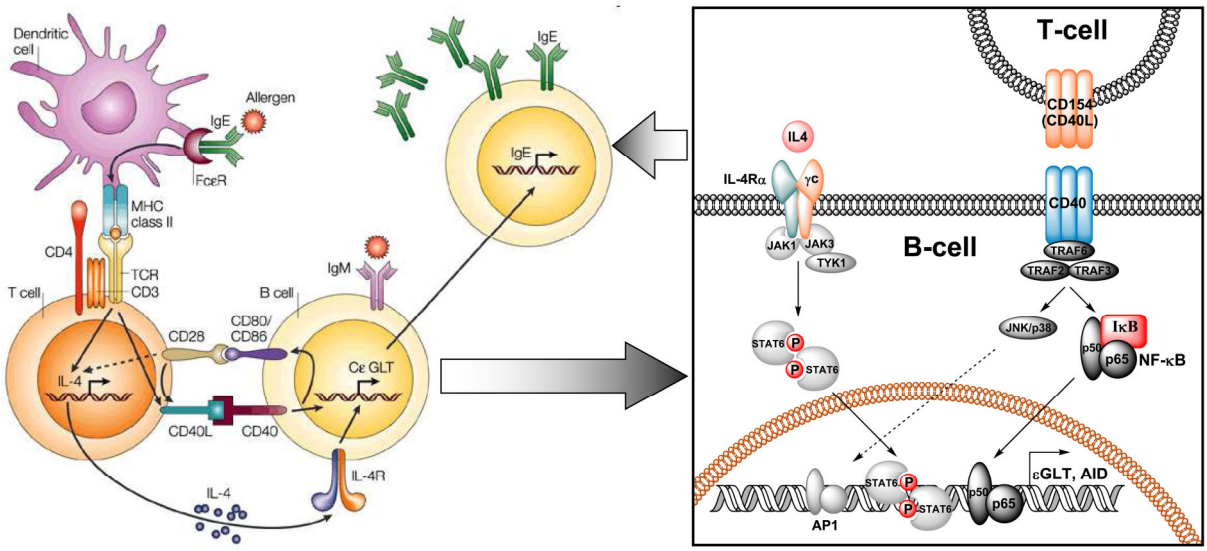

Figure 4 Classical interactions important for IgE class switch recombination, adapted from[155]. Antigen presenting cells, such as dentritic cells, take up allergens, which are presented to T cells by MHC class II. Subsequent activation of $CD4^+$ T cells leads to the induction of T_H2 cells, expressing IL-4 and CD40L (CD154). CD40-mediated activation of B cells synergizes with IL-4 to induce class switch recombination to IgE by enhancing the transcription of εGLT and *aicda* (encoding AID), which results in rearrangement of the IgE locus and production of IgE antibodies.

3.4.4. Vitamin D in the context of IgE and atopic dermatitis (AD)

IgE is a stringently regulated key molecule in type I hypersensitivity that is usually present in very low concentrations, in the range of $1-400$ ng/ml in non-atopic human[170]. Epidemiological data suggest that vitamin D insufficiency, reflected by less than 30 ng/ml of the circulating precursor 25-hydroxyvitamin D_3, is associated with elevated IgE levels in asthmatic children[176]. Hyppönen *et al.* reported a significant but nonlinear relationship between serum 25-hydroxyvitamin D_3 and IgE, suggesting the possibility of a threshold effect[177]. Interestingly, type I sensitized VDR knockout mice have higher serum IgE concentrations than wild type controls in an allergic asthma model[178]. Accordingly, allergen-specific immunotherapy has been suggested to be more efficient upon calcitriol treatment[179]. Additionally, reports show a beneficial association between higher maternal vitamin D intake during pregnancy and protection from childhood asthma and allergic diseases in the offspring[180-182]. In contrast, further studies have shown that the prevalence of atopic diseases was equal or even higher in subjects who received vitamin D supplementation during infancy[183, 184]. Another study by Oren *et al.* reported no significant associations between vitamin D status and the prevalence of asthma or allergic rhinitis in an obese population[185]. Nevertheless, these conflicting data indicate that there might be a complex relationship between external supply, endogenous production, metabolism, signaling pathways on one hand and the development of allergy on the other hand.

However, there is also a debate on the role of vitamin D metabolism and its potential beneficial effects on atopic dermatitis (AD), a common skin disease that is often associated with other atopic disorders. Thereby, a negative correlation between serum 25-hydroxyvitamin D_3 levels and severity of atopic dermatitis in children has been reported[186]. A randomized controlled trial by Sidbury *et al.* showed a favorable impact of vitamin D supplementation on winter-related AD[187]. Studies by Vähävihu *et al.* showed an improved vitamin D balance along with an altered antimicrobial peptide (AMP) expression in skin lesions followed by an improvement in AD after heliotherapy or narrowband UV-B treatment[188, 189].

3.4.5. Atopic dermatitis (AD)

AD is a chronic and relapsing eczematous skin inflammation associated with epidermal barrier dysfunction, intense pruritis, and cutaneous hyperreactivity to environmental triggers that frequently starts at infancy or early childhood (early-onset atopic dermatitis)[190, 191]. Infants with AD have an increased tendency to develop asthma and allergic rhinitis later in

life, a phenomenon known as the atopic march. Nevertheless, the disease can also start in adults, called late-onset atopic dermatitis. Histopathology of AD skin lesions reveals intense infiltrates of mononuclear cells in particular T cells in the dermis combined with intercellular edema in the epidermis (spongiosis)[190]. The lifetime prevalence of AD is estimated to 15 ~ 30% in children and 2 ~ 10% in adults while the incidence of AD has increased by 2- to 3-fold during the past 3 decades in industrialized countries[190, 192]. AD is a multifactorial, heterogenous disease with a variety of defects in the immune system, in antimicrobial defense mechanisms and epidermal barrier integrity that collectively contribute to the risk and severity of AD development[193, 194]. AD can be categorized into the extrinsic (allergic AD) and intrinsic types (non-allergic AD)[195-197]. The classical extrinsic type of AD with high prevalence (70 – 80% of AD patients) shows high total serum IgE levels and the presence of specific IgE for environmental and food allergens. Intrinsic or non-allergic AD exhibits normal total IgE values and the absence of specific IgE with an incidence of approximately 20 – 30% and female predominance. Early-onset atopic dermatitis usually emerges in the absence of detectable IgE-mediated allergic sensitization which often occurs several weeks or months after the lesions appear[190]. Therefore, the non-IgE associated form may represent a transitional phase of the IgE-associated form, at least in infancy[192]. The initial mechanisms inducing skin inflammation in patients with AD are mostly unknown. They may involve neuropeptide-induced, irritation-induced, or pruritus-induced scratching, which leads to the release of pro-inflammatory cytokines from keratinocytes[190]. They also entail T cell-mediated but IgE-independent reactions to allergens from pollens, house-dust-mite products, microbes, and food. Subsequent studies have shown that TSLP, expressed in keratinocytes of AD patients, can also promote pathogenesis of AD in the effector phase by acting on DCs or directly on skin-infiltrating T cells to induce T_H2 cytokine secretion[198, 199]. All these factors provide signals that drive a T_H2 polarization in the skin, the point of entry for atopic sensitization. Inflammation in atopic dermatitis is a biphasic process[190, 192, 196]. The initial acute eczematous skin lesions present clinically as intensely pruritic, erythematous papules associated with excoriation and exudation. Thereby, Langerhans cells (LCs) in lesional skin are activated by binding through allergens by means of specific IgE and the high affinity receptor FcεRI in the IgE-associated form but not in the non-IgE-associated form of AD. They produce monocyte chemotactic protein 1 (MCP-1), IL-16 and present allergen-derived peptides to recruited T cells that induce a T_H2 profile. The T_H2 cytokines IL-4, IL-5, and IL-13 predominate in the acute phase. Eosinophils are seen in the acute lesions but basophils and neutrophils are rarely present. Mast cells are present in various stages of degranulation. After

migration into the skin, the recruited monocytes differentiate into inflammatory dendritic epidermal cells (IDECs) and produce the pro-inflammatory cytokines IL-1, IL-6, and TNFα as well as IL-12 and IL-18, which contribute to the switch from T_H2 to $T_H1/0$ and thereby lead to the chronic phase of the disease. A hyperplastic epidermis with elongation of the rete ridges, prominent hyperkeratosis and minimal spongiosis characterizes chronic AD skin. In chronic AD skin lesions, macrophage-dominated mononuclear cell infiltrates in the dermis are detected. They display an increase of IFNγ and IL-12, as well as IL-5 and granulocyte macrophage colony stimulation factor (GM-CSF), which are characteristic for $T_H1/0$ dominance. The intrinsic type of AD is characterized by a lower expression of interleukin IL-4, IL-5, and IL-13, and a higher expression of IFNγ. T_{reg} cells, expressing the alpha chain of the IL-2 receptor (CD25) and the transcription factor Foxp3, can directly suppress allergic T_H2 immune responses[200, 201]. The number of T_{reg} cells is decreased in lesional skin of patients with AD, suggesting that there might be a role for T_{reg} cells in AD[202].

The skin barrier, as one part of the first line defense, is perturbed in the extrinsic, but not intrinsic type of AD[193-195]. Epidermal barrier dysfunction is a prerequisite for the penetration of allergens and microbes and causes increased transepidermal water loss, one hallmark of AD[190]. The epidermal barrier is formed by the cornified layer (stratum corneum) consisting of terminally differentiated, dead, cornified, flattened cells (corneocytes) and the cornified envelope (CE), which is mainly composed of the structural proteins, loricrin, involucrin, filaggrin and small proline-rich proteins[203]. By cross-linking these and other proteins, transglutaminases are likewise involved in the formation of the CE[203, 204]. Recently, loss-of-function genetic variants of the filaggrin gene (*FLG*) have been reported to be strong predisposing factors for extrinsic[205-207], but not intrinsic AD[206, 208]. Other reports show a reduced expression of antimicrobial peptides (AMPs), involucrin and loricrin in AD skin[193].

Numerous functions of the skin, including formation of the permeability barrier, are regulated by VDR signaling[209]. For instance, calcitriol has been reported to increase involucrin and transglutaminase expression in keratinocytes[210-212]. Silencing of the VDR and two VDR coactivators blocked keratinocyte differentiation as shown by decreased expression of filaggrin[213]. VDR null mice exhibit a defect in epidermal differentiation as shown by reduced levels of involucrin, filaggrin and loricrin, and loss of keratohyalin granules[214]. Additionally, CYP27B1 (1αOHase) null animals, which are unable to produce the biologically active calcitriol from its precursor 25-hydroxyvitamin D_3, showed a reduction in levels of the epidermal differentiation markers involucrin, filaggrin and loricrin, and displayed a markedly delayed recovery of normal barrier function following disruption of the barrier[215]. Disruption

of the permeability barrier, suppression of innate immune cells and the reduction in AMPs, such as cathelicidin and human β-defensins HBD2, and HBD3 in AD skin leads to the colonization and infection by *Staphylococcus aureus* (*S. aureus*), herpes simplex virus (HSV), and vaccinia virus (VV) in AD patients[193, 216-219]. The most important symptom of AD is persistent pruritus leading to itching induced by neuropeptides, proteases, kinins, and cytokines[190]. Moreover, keratinocyte-derived chemokines, TSLP, and IL-31 secretion are induced and augmented by *S. aureus* enterotoxins, leading to an increased inflammation in atopic dermatitis and provoke the generation of enterotoxin-specific IgE. Therefore, IL-31 is a major pruritogenic factor as shown by the overexpression of this cytokine and its receptor in lesional skin[220, 221]. Besides IgE antibodies against food and aeroallergens, autoantibodies against proteins from keratinocytes and endothelial cells such as manganese superoxide dismutase and calcium-binding proteins were found in the serum of patients with AD, correlating with disease severity[222-225]. Thus, AD seems to be at the frontier between allergy and autoimmunity[190].

Interestingly, a new unifying hypothesis, in which the natural history of atopic dermatitis has three phases including gene-gene and gene-environment interactions, emerges (Figure 5)[190]. Thereby, no classification distinguishing between an IgE-associated (extrinsic) and non-IgE-associated (intrinsic) form of AD exists. In the initial phase, genetically determined epidermal-barrier dysfunctions and the effect of environmental factors lead to non-atopic dermatitis, the first manifestation of AD in early infancy. In the transition phase, IgE-mediated sensitization to environmental allergens, influenced by genetic factors, is induced. In the third phase, pruritus-induced scratching damages the skin, which release autoantigens that can induce IgE autoantibodies in AD patients.

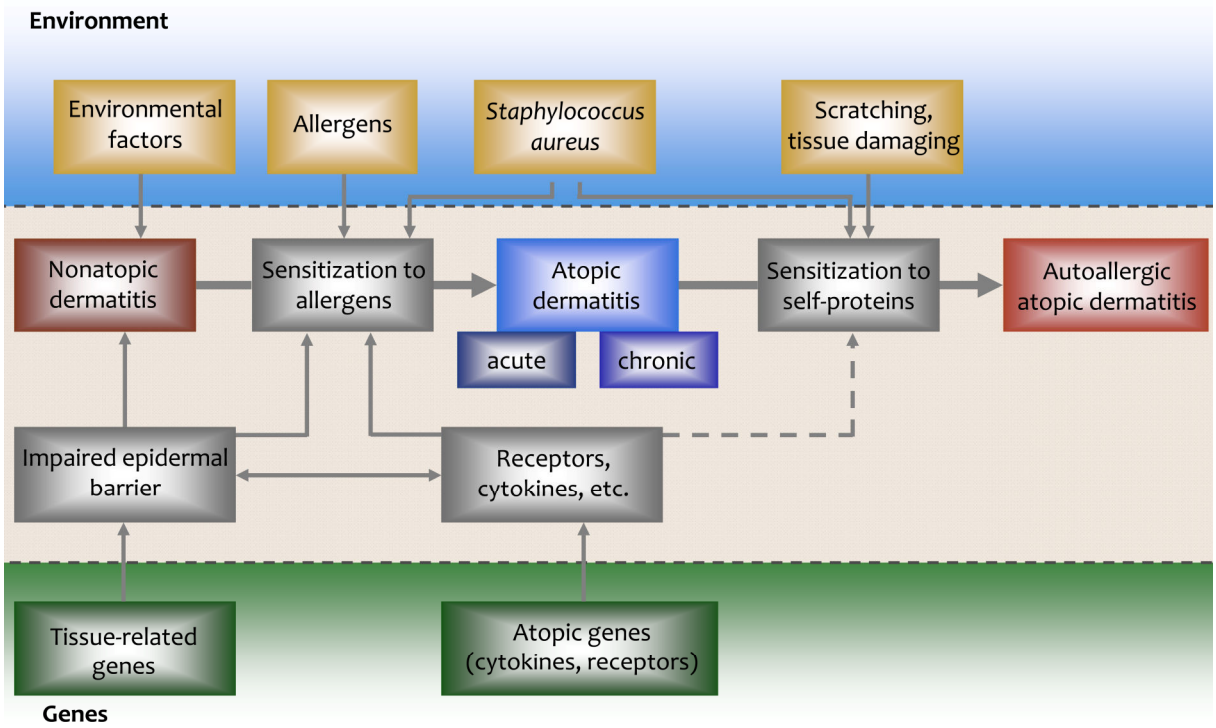

Figure 5 Proposed model for the three phases of the natural history of atopic dermatitis, adapted from[190], see text for details.

4. Objectives

Over the past years, the knowledge of the vitamin D endocrinology, including the pleiotropic functions of vitamin D receptor (VDR) activation in the immune system increased steadily. Recent epidemiologic data also indicated a role for the vitamin D metabolism in the allergic immune response. Unfortunately, the clinical use of the natural VDR ligand calcitriol is hampered by its toxic side effects, in particular hypercalcemia.

This work aimed to analyze the role of VDR activation in the allergic immune response *in vitro* and *in vivo* by using the novel low-calcemic VDR agonist ZK203278.

The first part of the work intended to investigate the *in vitro*-efficacy of the VDR agonist to activate the VDR and to modulate the stimulated IgE response in isolated human peripheral B cells in comparison to the natural ligand (calcitriol) and a known VDR antagonist. Thereby, mechanisms involved in the VDR-dependent modulation of human peripheral B cells were in the focus of this work. Second, the effect of the low-calcemic VDR agonist on the humoral IgE response in a mouse model of type I sensitization was studied in this work.

Finally, based on the crucial role of the VDR and VDR signaling in skin homeostasis and epidermal barrier function, the work aimed to investigate the clinical efficiency of VDR agonist treatment in a mouse model of allergen-induced eczema.

5. Materials and Methods

5.1. Materials

5.1.1. Antibodies

Antibody	Clone	Manufacturer
Anti-chicken egg albumin (OVA)	OVA-14	Sigma-Aldrich
Anti-human CD14 MicroBeads		Miltenyi Biotec
Anti-human CD14 PE	MφP9	BD Pharmingen
Anti-human CD19 FITC	4G7	BD Pharmingen
Anti-human CD19 MicroBeads		Miltenyi Biotec
Anti-human CD19 MultiSort Kit		Miltenyi Biotec
Anti-human CD19 PE	LT19	Miltenyi Biotec
Anti-human CD20 FITC	2H7	eBioscience
Anti-human CD23 APC	EBVCS-5	BD Pharmingen
Anti-human CD27 APC	M-T271	Miltenyi Biotec
Anti-human CD27 FITC	LG.7F9	eBioscience
Anti-human CD27 MicroBeads		Miltenyi Biotec
Anti-human CD27 PE	LG.7F9	eBioscience
Anti-human CD3 APC	SK7	BD Pharmingen
Anti-human CD38 FITC	HIT2	BD Pharmingen
Anti-human CD38 PE-Cy5	HIT2	eBioscience
Anti-human CD38 PerCP-Cy5.5	HIT2	BD Pharmingen
Anti-human CD40	626	Santa Cruz Biotechnology
Anti-human CD40	G28.5	DRFZ
Anti-human CD69 FITC	FN50	BD Pharmingen
Anti-human IgA	G20-359	BD Pharmingen
Anti-human IgA, IgG, IgM	Matched pairs	Jackson ImmunoResearch
Anti-human IgE	HP6061, HP6029b	Southern Biotech
Anti-human IgG	G18-145	BD Pharmingen
Anti-human IκBα Alexa Fluor 647	L35A5	Cell Signaling Technology Inc.
Anti-human pSTAT6 Alexa Fluor 647	pY641, 18	BD Pharmingen
Anti-human STAT6 PE	23	BD Pharmingen
Anti-mouse CD4	RM4-5	BD Pharmingen
Anti-mouse CD8	53-6.7	BD Pharmingen
Anti-mouse CD21/35 FITC	7G6	BD Pharmingen
Anti-mouse CD23 PE	B3B4	BD Pharmingen

Antibody	Clone	Manufacturer
Anti-mouse CD19 APC	1D3	BD Pharmingen
Anti-mouse IgA, biotin		Southern Biotech
Anti-mouse IgE	R35-72	BD Pharmingen
Anti-mouse IgE, biotin	EM95.3	DRFZ
Anti-mouse IgG_1, biotin	A85-1	BD Pharmingen
Anti-mouse IgG_{2a}, biotin	R19-15	BD Pharmingen
Anti-rat IgG, biotin		BD Pharmingen
Bio-conjugated OVA		DRFZ
Purified mouse anti-TNP IgE	C38-2	BD Pharmingen

5.1.2. Buffers and solutions

Buffer/Solution	Composition	Manufacturer
50x Tris-acetate-EDTA (TAE) buffer		Gibco, Invitrogen
1x Tris-EDTA (TE), pH 8.0	10 mM Tris	
	1 mM EDTA	
AEC-DMF buffer (pH 5.0)	64 mM CH_3COONa	
	45 mM CH_3COOH	
Blocking buffers	3% BSA/1x PBS	
	2% BSA/1x TBS	
	3% MP/1x PBS	
Coating buffer, pH 9.6	34.8 mM $NaHCO_3$	
	154 mM NaCl	
	15.1 mM Na_2CO_3	
FACS buffer	1% BSA or FCS/1x PBS	
Loading buffer, pH 8.0	1x TE	
	40% glycerine	Sigma-Aldrich
	0.25% bromphenol blue	Sigma-Aldrich
MACS buffer	0.2% BSA/1x PBS	
	20 mM EDTA	
Medium complete	500 ml Advanced RPMI 1640	Gibco, Invitrogen
	25 ml CCS	Biochrom AG
	4 mM L-glutamine	Biochrom AG
	100 U/ml penicillin	Biochrom AG
	100 µg/ml streptomycin	Biochrom AG

Buffer/Solution	Composition	Manufacturer
PBS, pH 7.4	137 mM NaCl	
	2.7 mM KCl	
	10 mM Na_2HPO_4	
	1.8 mM KH_2PO_4	
Sodium carbonate buffer, pH 9.6	28.6 mM $NaHCO_3$	
	15.1 mM Na_2CO_3	
Substrate buffer, pH 9.8	1 M diethanolamine	
	0.5 mM $MgCl_2$	
TBS, pH 7.4	100 mM Tris-Base	
	154 mM NaCl	
TMB buffer, pH 5.0	0.05 M Na_2HPO_4	
	0.02 M citric acid	

5.1.3. Chemical and biological reagents

Reagent	Specification	Manufacturer
1α,25-dihydroxyvitamin D_3 (calcitriol)	4 x 10^{-3} M in ethanol	Fluka
3,3',5,5'-tetramethylbenzidine (TMB)		Sigma-Aldrich
3-amino-9-ethylcarbazole	20 mg per tablet	Sigma-Aldrich
4',6'-diamidino-2-phenylindole (DAPI)-dihydrochloride		Roth
Acetic acid, CH_3COOH	≥ 99.7%	Sigma-Aldrich
Advanced RPMI 1640		Invitrogen
Agarose LE Agarose		Biozym Scientific GmbH
Albumin from chicken egg white (OVA)	Grade V	Sigma-Aldrich
Antibody diluent (Dako REAL™)		DAKO Diagnostika
Avidin/biotin blocking Kit		Vector
Bovine serum albumin (BSA)	Fraction V, pH 7.0	Serva
5(6)-carboxyfluorescein diacetate *N*-succinimidyl ester (CFSE)		Sigma-Aldrich
Charcoal stripped FCS (CCS)	S3113, heat-inactivated	Biochrom AG
Citric acid, $C_6H_8O_7$	≥ 99%	Merck
Detection System (Dako REAL™)	K 5005, AP/RED	DAKO Diagnostika
Diethanolamine, $(HOCH_2CH_2)_2NH$	≥ 98%	Sigma-Aldrich
Disodium carbonate, Na_2CO_3		Merck

Reagent	Specification	Manufacturer
Disodium hydrogen phosphate, Na_2HPO_4		Merck
Dimethylsulfoxide (DMSO)	Hybri-Max™	Sigma-Aldrich
DNAse		Macherey-Nagel
Dry milk powder (MP)	blotting grade, powdered	Carl ROTH®
Dulbecco´s phosphate-buffered saline (PBS), without Ca^{2+}/Mg^{2+}		PAA
Ethanol, CH_3CH_2OH	absolute	Merck
Ethidium bromide solution	10 mg/ml	Gibco/Invitrogen
Ethylenediaminetetraacetic acid (EDTA)	≥ 99%, anhydrous	Sigma-Aldrich
Extra Avidine Peroxidase		Sigma-Aldrich
FACS Flow		BD Pharmingen
FastStart DNA Master SYBR® Green		Roche
Fetal calf serum (FCS)	0314G, heat-inactivated	Biochrom AG
Ficoll	sterile, d = 1.077 g/mL	PAA
Goat serum normal	DakoCytomation, X097	DAKO Diagnostika
Heparan sulfate		Rotexmedica GmbH
Hydrochloric acid, HCl	≥ 37%	Merck
Hydrogen peroxide, H_2O_2	≥ 30%	Merck
Imject® Alum ($Al(OH)_3$, $Mg(OH)_2$)	40 mg/ml	Thermo Fisher Scientific
Isoflurane (Forane)	≥ 99.9% w/w	Abott
Kaiser's glycerol gelantine		Merck
L-glutamine	200 mM	Biochrom
Magnesium chloride, $MgCl_{2*}6H_2O$		Merck
N,N-dimethylformamide (DMF)	≥ 99%	Sigma-Aldrich
NucleoSpin® RNA II Kit		Macherey-Nagel
Papanicolaou, Harris' Hematoxylin solution		Merck
para-nitrophenylphosphate (*p*NPP)		Sigma-Aldrich
Penicillin/streptomycin	10000 U/ml, µg/ml	Biochrom AG
Potassium chloride, KCl		Merck
Potassium dihydrogen phosphate, KH_2PO_4		Merck
Propidium iodide		Sigma-Aldrich
ProTaqs Tris, pH 7.6		BIOCYC
Proteinase K		Macherey-Nagel
Recombinant human interleukin (IL)-21		Immunotools
Recombinant human interleukin (IL)-4		Miltenyi Biotec
Red blood cell (RBC) lysis buffer		eBioscience
RNeasy Mini Kit		Quiagen

Reagent	Specification	Manufacturer
Sodium acetate, CH_3COONa		Merck
Sodium bicarbonate, $NaHCO_3$		Merck
Sodium chloride, NaCl		Merck
Streptavidin-alkaline phosphatase (AP)		ZYMED
Streptavidin-horseradish peroxidase (HRP)		R&D Systems®
Sulfuric acid, H_2SO_4	≥ 96%	Merck
TaqMan® Reverse Transcription Reagents		Applied Biosystems
Toluidine blue		Merck
Tris(hydroxymethyl)aminomethane (Tris-Base)		Sigma-Aldrich
Tween20		Sigma-Aldrich
Quick-Load® 100 bp DNA Ladder		New England BioLabs®
ZK159222	10^{-2} M in ethanol	Bayer Schering Pharma AG
ZK203278	10^{-2} M in ethanol	Bayer Schering Pharma AG
β-Mercaptoethanol	14.3 M, ≥ 98%	Sigma-Aldrich

5.1.4. Labware

Labware	Specification	Manufacturer
12-, 24-, 48-, 96-well plates	multiwell suspension culture	Greiner Bio-One
autoMACS® columns		Miltenyi Biotec
Biopsy punch, sterile	4 mm diameter	Stiefel
Blade for Cryostat		Feather
Cell strainers	40 µm, 100 µm	BD Falcon
Cohesive bandage	Peha-haft®, 6 cm width	Hartmann
Coverslips		Menzel-Gläser
Cryo-spray	cryogenic spray	Bio Optica
Disposable wet razor		Wilkinson
ELISA plates	Immuno 96 MicroWell™ Solid Plates, MaxiSorp™	Nunc
Filter paper discs	7.5 mm	Epitest Ltd Oy
Finn chambers®		Epitest Ltd Oy
Hypodermic needle, sterile	Sterican	Braun
LightCycler® capillaries	20 µl	Roche
LS/LD columns		Miltenyi Biotec
Microscope slide	Superfrost™ Plus	R. Langenbrinck
Mortar and pestle		Carl ROTH®

Labware	Specification	Manufacturer
MultiScreen$_{HTS}$ IP	hydrophobic PVDF, 0.45 µm	Millipore
Petri dishes		Greiner Bio-One
Pre-Separation Filters	30 µm	Miltenyi Biotec
Shredder columns for tissue samples		Quiagen
Syringes, sterile	1, 2, 5, 10, 20, 50 ml	Braun
Tissue freezing medium	Tissue-Tek® O.C.T™ Compound	Sakura Finetek
Vinyl specimen mold		Sakura Finetek

Pipettes, reaction tubes, pipette tips and further standard labware were obtained from Eppendorf, Sarstedt, BD Falcon and Kimberly-Clark.

5.1.5. Technical equipment

Equipment	Model	Manufacturer
Analytical balances		Sartorius AG
CASY® Technology Cell Counter	Casy 1, Model TT	Roche Innovatis AG
Centrifuges	Varifuge RF	Heraeus Holding
	Megafuge 1.0R	Heraeus Holding
Clean bench	HeraSafe	Heraeus Holding
Cryostat	Chryotome FSE	Thermo Fisher Scientific
Digital camera	EOS20D	Canon
Electrical pipetting aid	Pipetus	Hirschmann Laborgeräte
ELISPOT Analyzer	CTL-ImmunoSpot® S4	C.T.L Cellular Technology
Flow cytometer/FACS	FACSCalibur™	BD Biosciences
	FACSAria II cell sorter	BD Biosciences
	MACSQuant® Analyzer	Miltenyi Biotec
Freezer (-20°C)/Fridge (4°C)	TKF380	EUREKA
Freezer (-80°C)	HeraFreeze	Heraeus Holding
Gel chamber		Bio-Rad Laboratories
Heating block	Thermomixer 5436	Eppendorf
Hot plate	nuova II	Thermolyne
Incubator	Heracell®	Heraeus Holding
Magnetic cell sorter	autoMACS™ Separator	Miltenyi Biotec
Magnetic stirrer	Magnetmix 2070	Hecht-Assistent
Microscope and camera	AxioPlan 2	Carl Zeiss AG
	AxioCam HRC	Carl Zeiss AG

Equipment	Model	Manufacturer
pH electrode		neoLab GmbH
pH meter	MV 870 Digital	Präcitronic
Pipetts	10 µl, 100 µl, 200 µl, 1000 µl	Eppendorf, Brandt
Plate reader	MRX Microplate Reader	Dynex Technologies GmbH
Plate washer		TECAN
Power supply	Power Pac300	Bio-Rad Laboratories
Shaker	IKA-Vibrax-VXR	IKA® Werke GmbH & Co. KG
Spectrophotometer	NanoDrop 1000	Thermo Fisher Scientific
Table top centrifuge	5417 C	Eppendorf
Table top centrifuge	5417 R	Eppendorf
Thermal cyclers	LightCycler® 1.5	Roche
	Px2	Thermo Electron Corporation
Ultrasonic bath	Sonorex TK52	Bandelin
Vortex mixer	Reax 2000	Heidolph
Water bath	U3	Julabo

5.1.6. Software

Software	Release	Developer
AxioVision	4.6.3	Carl Zeiss AG
CASY®measure	1.5	Schärfe System
Excel 2003, 2007		Microsoft Corporation
FCS Express	V3	De Novo Software
FlowJo	7.6.1	Tree Star, Inc.
Immunocapture	6.0	C.T.L Cellular Technology
ImmunoSpot	v4.0.13	C.T.L Cellular Technology
LightCycler® Software	Version 3	Roche
Prism	5.00	GraphPad
Revelation	G3.2	Dynex Technologies GmbH

5.2. Methods

5.2.1. Cellular methods

All cell culture procedures were performed under a tissue culture hood with sterile commodities and reagents.

5.2.1.1. Human cell isolation

Peripheral blood mononuclear cells (PBMC) were isolated from buffy coats of healthy donors by density gradient separation with lymphocyte separation medium (d = 1.077 g/ml) for 20 min at 900 *g*, room temperature (RT). B cells were purified by magnetic-activated cell sorting (MACS) using anti-CD19-coupled magnetic beads. Briefly, 1-2 x 10^8 PBMC were incubated with 300 µl MACS buffer, 100 µl autologous serum and 100 µl CD19 MicroBeads for 12 min at 4°C. After washing, CD19 positive B cells were isolated by the MACS® Column Technology according to the manufacture's instructions or by double positive selection with the autoMACS™ Separator. The enriched cell population contained more than 95% or 99% B cells as assessed by flow cytometry.

$CD19^+$ $CD27^-$ B cells were purified by the CD19 MultiSort Kit followed by depletion of $CD27^+$ and $CD14^+$ cells by CD27 and CD14 MicroBeads, according to the manufacture's protocols or by fluorescence-activated cell sorting (FACS) using the FACSAria. Sorted B cell populations were > 95% enriched. Cell number of single cell suspensions was measured by CASY®-Technology.

5.2.1.2. Murine splenocyte isolation

BALB/c mice were splenectomized with sterile surgical instruments and each spleen was kept in 1x phosphate buffered saline (PBS) at 4°C, separately. Each spleen was placed on a sterile 100 µm nylon mesh of a cup-shaped cell strainer in a petri dish under sterile conditions. The splenic capsule was gently mashed through the nylon mesh of the cell strainer with the rubber end of a plunger from a 5 ml syringe into ice-cold 1x PBS/2 mM ethylenediaminetetraacetic acid (EDTA). To rinse the clumps and elute any imbedded cells the procedure was repeated until the capsule appeared white. To create a single cell suspension dispersed cells were resuspended with chilled 1x PBS/2 mM EDTA and filtered through a second 40 µm cell strainer into a 50 ml conical tube. After washing several times with 1x PBS/2 mM EDTA the cell suspension was centrifuged for 10 min at 340 *g*, and 4°C. The supernatant was discarded and the cell pellet was loosening by flicking the tube. 2.5 ml red blood cell (RBC) lysis buffer

was added and incubated for 5 min on ice. After stopping the reaction with 30 ml chilled 1x PBS/2 mM EDTA cells were centrifuged for 10 min at 340 *g*, and 4°C. After discarding the supernatant the cell pellet was resuspended in 30 ml 1x PBS/2 mM EDTA and the cell number was measured by CASY®-Technology.

5.2.1.3. Cell culture conditions

Cells (1 x 10^6 cells/ml) were cultured in Advanced RPMI 1640 culture medium supplemented with 4 mM L-glutamine, 50 U/ml penicillin, 50 µg/ml streptomycin and 5% heat inactivated charcoal stripped fetal calf serum (CCS). Cells were stimulated with 1 µg/ml anti-CD40 (626) and 10 ng/ml rhIL-4 or additionally with 50 ng/ml IL-21 in the presence or absence of the synthetic VDR ligands ZK203278[226] (hereinafter referred to as VDR agonist), ZK159222[227] (hereinafter referred to as VDR antagonist) or calcitriol at concentrations ranging from 1 nM to 100 nM. All cell cultures were carried out at 37°C and 5% CO_2 in a humidified atmosphere. VDR ligands were dissolved in 100% sterile filtered ethanol and stored at -20°C. The vehicle control was performed in culture media containing the same volume of ethanol.

5.2.2. Animal work

5.2.2.1. Mouse model of type I allergy

To induce a profound IgE response *in vivo* mice were sensitized with ovalbumin (OVA) and a mixture of aluminium hydroxide and magnesium hydroxide (alum)[228]. OVA is known as a major allergen and is a 385 amino acid glycoprotein of approximately 45 kDa, which constitutes about 54% of the egg white proteins[231, 232]. The carbohydrate moieties of OVA account for about 3% of its molecular weight[229]. Alum was used as an adjuvant for the adaptive immune reaction exerting its function by inducing uric acid and activating inflammatory dendritic cells[230].

Female, 10-week-old BALB/c mice were kept in a specific pathogen-free environment under laboratory conditions at 21°C ± 1°C, humidity 55 ± 5% with chow and water provided *ad libitum*. All experimental procedures were performed in compliance with protocols approved by the local State Office of Health and Social Affairs (LAGeSo). The mice were sensitized intraperitoneally (i.p.) using 10 µg OVA adsorbed to 1.5 mg alum in 100 µl 1x PBS on days 0, 14 and 21 (Figure 6). The VDR agonist ZK203278 (6 µg/kg/d in 100 µl PBS/0.03% ethanol) or an equal volume of PBS/0.03% ethanol as vehicle was injected intraperitoneally for two consecutive 5-day-periods (day 33-37 and 40-44) separated by a 2-day-break (Figure 6). On day 47 mice were treated with the inhalational anesthesia isoflurane and

exsanguinated via the orbital sinus or plexus. Blood samples were collected in 1.5 ml reaction tubes with 2 µl heparan sulfate. Samples were centrifuged at 6800 *g*, 4°C and serum was aliquoted and stored at -80°C. Mice were sacrificed by cervical dislocation immediately after blood collection. Using surgical scissors, an incision on the left side of each animal between the last rib and the hip joint, was made. The spleen was grasped using sterilized medium forceps and pulled through the incision in the peritoneal wall. While holding the spleen with the medium forceps, the spleen was separated from connective tissue by using fine forceps or scissors and kept in 1x PBS at 4°C. Calcium serum concentrations were determined from pooled sera of each respective group on day 47 by the Charité, Institute of Laboratory Medicine and Pathobiochemistry.

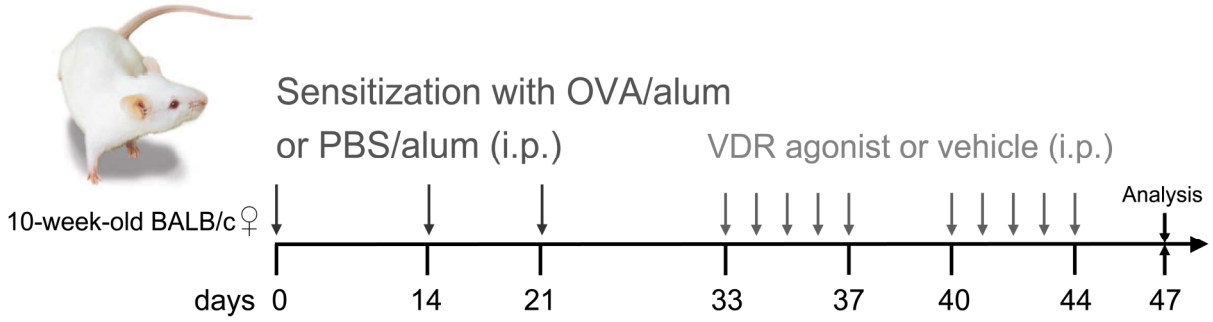

Figure 6 Experimental scheme of the mouse model of type I allergy and the treatment with the VDR agonist. 10-week-old female BALB/c mice were sensitized 3 times intraperitoneally with OVA/alum on day 0, 14 and 21. Mice were treated by intraperitoneal injections with either the VDR agonist or PBS (0.03% ethanol) as described above.

5.2.2.2. Mouse model of allergen-induced eczema

For the induction of AD skin lesions, a modified epicutaneous (e.c.) allergen application patch test, originally described by Wang G. *et al.,* Spergel *et al.* and Wang L.F. *et al.*, was used[231-233]. Therefore, mice were sensitized intraperitoneally (i.p.) using 10 µg OVA adsorbed to 1.5 mg alum in a total volume of 100 µl 1x PBS on day 0, 14 and 21 (Figure 7). Mice were shaved on the ventral side with a wet razor (Figure 8). Afterwards, 100 µg OVA adsorbed to 1.5 mg alum in a total volume of 20 µl 1x PBS was applied to a sterile patch and secured to the skin with an elastic cohesive bandage. The patch was placed for three 1-week-periods (with patch renewal after 3 days) separated by a 2-week interval between each application (Figure 7). The VDR agonist ZK203278 (6 µg/kg/d in PBS/0.03% ethanol) or an equal volume of PBS/0.03% ethanol as vehicle was injected intraperitoneally for two consecutive 5-day-periods separated by a 2-day-break after the first and second patch (Figure 7). On day 72 mice were exsanguinated under isoflurane inhalational anesthesia and sacrificed by cervical

dislocation. Photographs of the patch regions were taken. Skin samples from lesional skin were taken by biopsy punches (5 mm diameter) directly frozen into liquid nitrogen (RNA) or embedded in O.C.T compound and subsequently carefully frozen into liquid nitrogen. The frozen samples were stored at -80°C.

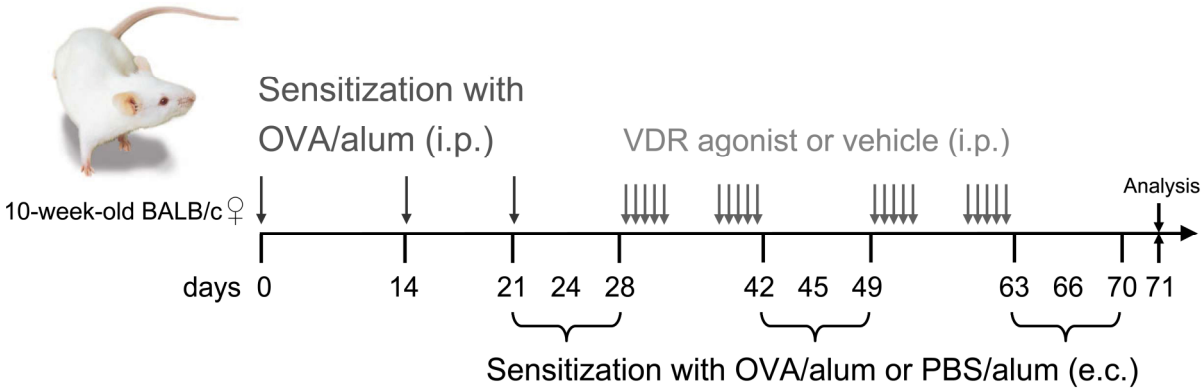

Figure 7 Experimental scheme of the mouse model of allergen-induced eczema and the treatment with the VDR agonist. Mice were sensitized intraperitoneally (i.p.) with 10 µg OVA/alum on days 0, 14, and 21 (dark grey arrows), and epicutaneously (e.c.) by patches with 100 µg OVA/alum (OVA-Patch) or PBS/alum (PBS-Patch) as a control, twice a week (gray arrows). E.c. sensitization comprised three 1-week exposures. Treatment with VDR agonist or vehicle started with removing the patch after the first week of exposure. 0.15 µg of VDR agonist in 100 µl PBS/0.03% ethanol was applied intraperitoneally five times a week for two weeks and was repeated after the second patching period. On day 71 mice were sacrificed and skin and blood samples were collected.

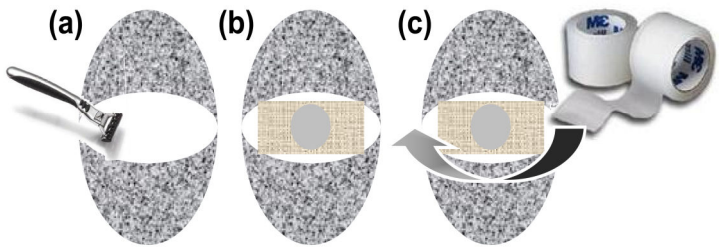

Figure 8 Schematic representation of the patching procedure. *(a)* Mice were shaved on the ventral side with a wet razor. *(b and c)* A sterile patch (filter paper disc in a metal chamber) was placed on the ventral side and secured to the skin with an elastic cohesive bandage.

5.2.2.3. Assessment of AD symptoms

Erythema, edema, excoriation, dryness and extension were used as typical hallmarks of human AD to evaluate clinical severity of the induced eczema, as described[234]. Each parameter was evaluated independently and blindly by six investigators. Severity for each parameter was rated according to scores as follows: 0, no reaction observed; 1, mild symptoms; 2, intermediate symptoms; 3, severe symptoms. The score values for each of these factors were then summed up and the total score was taken as index of eczema severity.

5.2.3. Immunological methods

5.2.3.1. Enzyme-linked immunosorbent assay (ELISA)

ELISA is an immunoassay based on the immunochemical "sandwich" principle to quantitate antigens or immunoglobulins in mostly cell-free media[235]. In the present study the ELISA technique was used to analyze immunoglobulins released by B cells. Thereby, the solid phase is coated with antibodies or antigen to capture the specific immunoglobulins released by the cells. In the next step the bound analyte is incubated with biotinylated secondary or enzyme-coupled antibodies. Biotinylated antibodies are detected by enzyme-conjugated streptavidin. Horseradish peroxidase (HRP) or alkaline phosphatase (AP) is used to convert chromogenic substrates. The resulting color is read by a spectrophotometer. The protein concentration in the sample is calculated by means of standard curve.

5.2.3.2. Human immunoglobulin ELISA

Human B cells were cultured for 8 days and immunoglobulin concentrations were determined in the cell free supernatants by ELISA. For IgE detection anti-human IgE (HP6061) diluted in sodium carbonat buffer was coated on 96-well MaxiSorp plates overnight at 4°C. After blocking with 2% bovine serum albumin (BSA)/Tris-buffered saline (TBS), samples and standards were incubated for 2 h at RT. Wells were washed and subsequently biotinylated anti-IgE (HP6029) diluted in 0.2 % BSA/TBS was used as detection antibody for 1.5 h at RT. After the final washing step captured IgE was detected by the enzymatic activity of streptavidin-AP and the colorimetric analysis of the cleaved *para*-nitrophenylphosphate (*p*NPP) in substrate buffer at 405 nm in a microplate ELISA reader.

For the detection of human IgM, IgA and IgG matched antibody pairs were used. Briefly, coating antibodies diluted in sodium carbonate buffer pH 9.6 were incubated over night at 4°C followed by blocking as described above. Wells were incubated with samples and serial dilutions of standard for 2 h at RT and subsequently detected with AP-conjugated anti-Ig antibody diluted in 0.2% BSA/TBS for 1.5 h at RT. Diluted human serum of an atopic individual served as standard in which the respective Ig-levels were determined by the Charité, Institute of Laboratory Medicine and Pathobiochemistry.

5.2.3.3. Murine immunoglobulin ELISA

To analyze total and OVA-specific murine immunoglobulins, MaxiSorp plates were coated with the appropriate antibody in coating buffer pH 9.6 over night at 4°C (Table 3). After washing with 1x PBS/0.05% Tween 20 (PBS-T) plates were blocked with either 3% milk powder (MP)/1x PBS or 3% BSA/1x PBS (OVA-IgE) for 1.5 h at RT. Standards and samples were diluted in 1% MP/1x PBS or in 1% BSA/1x PBS and applied in suitable concentrations for 2 h at RT. Plates were washed with PBS-T. Subsequently, indicated biotin conjugated detection antibodies or OVA (Table 3) diluted in 1% MP/1x PBS or in 1% BSA/1x PBS were applied for 2 h at RT. After washing, samples were incubated with streptavidin conjugated HRP for 30 min at RT. The colorimetric reaction was developed with 3,3',5,5'-tetramethylbenzidine (TMB, 1 tablet dissolved in 10 ml of TMB buffer with 4 µl of 30% hydrogen peroxide (H_2O_2)) and stopped with 1 M sulphuric acid resulting in a yellow color. The plates were read spectrophotometrically at 450 nm (reference wavelength 600 nm). Diluted mouse anti-trinitrophenyl (TNP) IgE κ isotype control (C38-2) was used for standard curve calculation of total IgE. The concentrations of OVA-specific antibodies were estimated by comparison to a standard curve prepared from pooled sera of OVA-sensitized mice. Data are expressed as laboratory units per ml (LU/ml). For OVA-IgG_1 OVA-14 was used as standard.

Analyte	Coating	Detection	
IgE	anti-mouse IgE (R35-72)	anti-mouse IgE *bio**	(EM95.3)
OVA-IgE	anti-mouse IgE (R35-72)	ovalbumin (OVA) *bio**	
OVA-IgG_1	ovalbumin (OVA)	anti-mouse IgG_1 *bio**	(A85-1)
OVA-IgG_{2a}	ovalbumin (OVA)	anti-mouse IgG_{2a} *bio**	(R19-15)
OVA-IgA	ovalbumin (OVA)	anti-mouse IgA *bio**	

* *biotinylated*

Table 3 Antibodies used for ELISA.

5.2.3.4. Enzyme-linked immunospot (ELISPOT)

The same immunochemical "sandwich" principle as for ELISA is shared by the ELISPOT technique. The main differences between these two assays are first live cells are cultured directly in ELISPOT plates and more importantly the frequency of secreting cells can be determined by enumerating these cells[236].

In this study the number of human antibody secreting cells was determined by ELISPOT. The surface of 96-well MultiScreen filter plates (0.45 µm) was activated for 1 min by incubation with 15 µl ethanol (υ = 100%). After washing with 1x PBS plates were coated with anti-human IgE (HP6061) or goat anti-human IgA or IgG diluted in sodium carbonat buffer over night at 4°C. Plates were washed with 1x PBS and blocked with 3% BSA/1x PBS for 2 h at RT. Human peripheral B cells were cultured for 6 days as described above in the presence or absence of VDR ligands. Subsequent to a washing step 300 µl of each cell suspension was applied and diluted serially. Cells were incubated over night (IgE) or for 3 h (IgG, IgA) at 37°C and 5% CO_2 in a humidified atmosphere. Afterwards, cells were removed and the plates were washed 6x with PBS-T. Detection was performed using biotin conjugated mouse anti-human IgE (HP6029), mouse anti-human IgA (G20-359) or mouse anti-human IgG (G18-145) in 0.2% BSA/1x PBS for 2 h at RT. Plates were washed and streptavidin-HRP (1:3000) was applied for 45 min at RT. The reaction was developed with a mixture of 1 tablet 3-amino-9-ethylcarbazole dissolved in *N,N*-dimethylformamide (DMF) with 65 mM sodium acetate, 45 mM acetic acid (pH 5) and H_2O_2. Antibody secreting cells appeared as red spots and were counted with the CTL ImmunoSpot® Analyzer.

5.2.3.5. Principles of flow cytometry

The unique feature of fluorescence-activated cell sorting (FACS) and flow cytometry is the measurement of the individual light scattering and emitted fluorescence from single cells or particles enabling detailed multi-parameter analysis on single cell level mostly in the size range of 0.2 µm to 50 µm diameter. Thereby, cells tagged with fluorescent dyes are hydro-dynamically focused to the center of a sheath flow and pass through one or more beams of lasers as appropriate light excitation source. The emitted light is detected by separate fluorescence (FL-) channels consisting either of silicon photodiodes or photomultiplier tubes (PMTs) additionally controlled by optical filters.

The forward light scatter (FSC) intensity roughly equates to the cell size and can also be used to distinguish between cellular debris and living cells. The side scatter channel (SSC) provides information about the granular content within a cell. Analysis of cells with fluorochrome conjugated antibodies specific to certain intracellular and surface antigens provide additional information about the target cell population.

In the major application of flow cytometry a process called cell sorting or FACS analysis the hydrodynamically focused sample in the fluid stream is charged according to their specific

scatter and fluorescence signal. The electrostatically charged particles are deflected by passing through a strong electrostatic field and can be collected as defined populations.

5.2.3.6. Flow cytometric analysis

Cells were harvested, washed with 1% BSA in PBS and centrifuged for 10 min at 350 *g*, 4°C. After removal of the supernatant cells were stained in 1% BSA in PBS for 15 min at 4°C in the presence of the directly conjugated monoclonal antibodies (mAb) anti-human CD19 PE (LT19), anti-human CD19 FITC (4G7) anti-human CD27 APC (M-T271), anti-human CD38 FITC (HB7), anti-human CD23 APC (EBVCS-5), anti-human CD69 FITC (FN50), anti-human CD14 FITC (MφP9), anti-human CD3 APC (SK7), anti-mouse CD21/CD35 FITC (7G6), anti-mouse CD23 PE (B3B4), anti-mouse CD19 APC (1D3). Stained cells were washed and data were collected immediately using a FACSCalibur™ or MACSQuant® Analyzer. Dead cells were excluded using 1 µM propidium iodide (PI) or 1 µg/ml 4',6'-diamidino-2-phenylindole (DAPI)-dihydrochloride. Data were analyzed using FlowJo software.

5.2.3.7. 5(6)-carboxyfluorescein diacetate *N*-succinimidyl ester (CFSE) dilution analysis

The proliferation of activated B cells was monitored at a single cell level by dilution of CFSE-fluorescence. Freshly isolated B cells were washed and resuspended in PBS at a final concentration of 10^7 cells/ml. 5 µM CFSE solved in dimethylsulfoxide (DMSO) was added for 5 min at RT and the reaction was stopped by washing the cells with Advanced RPMI 1640 medium supplemented with 5% CCS. Cells were stimulated with IgE inducing conditions as described above or additionally with 50 ng/ml IL-21 and various VDR ligands. Cell proliferation was assessed after 5 days by flow cytometry and dead cells were excluded using 1 µM PI.

5.2.3.8. Flow cytometric analysis of STAT6 phosphorylation

Human peripheral B cells (1 x 10^6/ml) were stimulated with 1 µg/ml anti-CD40 (G28.5) and 5 ng/ml rhIL-4 24 h to induce the VDR expression. After starving B cells in serum free medium over night, an additional stimulation with 20 ng/ml rhIL-4 in the presence or absence of 100 nM VDR agonist or calcitriol has been carried out. After 1 h stimulation cells and the unstimulated control were harvested into the same volume prewarmed BD Phosflow Fix Buffer I. After 10 min fixation at 37°C, B cells were permeabilized with 750 µl Phosflow

Perm Buffer III for 30 min on ice. After washing with 1% FCS/PBS for 10 min at 350 *g*, and 4°C, cells were stained with anti-human pSTAT6 A647 (pY641; 18); anti-human STAT6 PE (23), anti-human CD27 PE (LG.7F9) and anti-human CD38 PE-Cy5 (HIT2) for 1 h at RT. Cells were washed and immediately analyzed by flow cytometry.

5.2.3.9. Flow cytometric analysis of IκBα degradation

$CD19^+$ B cells (1 x 10^6/ml) were stimulated with 1 µg/ml anti-CD40 (G28.5) and 5 ng/ml rhIL-4 with or without 100 nM of VDR agonist or calcitriol for 24 h. After additional 1 h preincubation in the absence or presence of the VDR agonist or calcitriol, a 50 min stimulation step with 1 µg/ml anti-CD40 (G28.5) has been carried out. Subsequently, stimulated and unstimulated cells were harvested directly into prewarmed 4% paraformaldehyde (PFA). After fixation for 10 min at 37°C, cells were washed and centrifuged for 10 min at 350 *g*, and 4°C. B cells were incubated for 15 min with anti-human CD20 FITC (2H7), anti-human CD27 PE (LG.7F9) and anti-human CD38 PerCP-Cy5.5 (HIT2) on ice. Subsequent to an additional washing step in 1% saponin/FACS buffer, cells were stained intracellularly with anti-human IκBα A647 (L35A5) in 1% saponin/FACS buffer for 30 min at 4°C. After the final washing step with 1% saponin/FACS buffer, cells were analyzed by flow cytometry.

5.2.4. Immunohistochemistry

Tissue samples were cut into 5 µm cross-sections by a cryotome at -24°C to -28°C and directly transferred on microscope slides. After drying on a hot plate, samples were stored at -80°C until further preparation.

5.2.4.1. Staining of $CD4^+$ and $CD8^+$ T cell infiltrates

Skin sections were blocked for 20 min with 5% normal goat serum in 1x TBS following the avidin/biotin blocking kit. Rat anti-mouse CD4 (RM4-5) or CD8 (53-6.7), 1:30 diluted in antibody diluent, was incubated for 1 h at RT. After washing in 1x TBS, biotin-conjugated polyclonal goat anti-rat IgG, 1:200 diluted in antibody diluent, was incubated for 30 min at RT. Negative controls were run in parallel omitting either the primary or the secondary antibody. Signals were detected by Dako REAL™ Detection System AP/RED according to the manufacture's instructions and hematoxylin counter staining to stain nuclei (blue) and eosinophilic structures (red).

5.2.4.2. Staining of Foxp3$^+$ cells

Foxp3 staining was performed by Simone Spiekermann and Christoph Loddenkemper (Charité Institute for Pathology, Campus Benjamin Franklin). Samples were additionally costained with hematoxylin and eosin (HE). In brief, skin sections were deparaffinized and subjected to a heat-induced epitope retrieval step before incubation with antibodies. Sections were immersed in sodium citrate buffer solutions at pH 6.0 and heated in a high-pressure cooker. The slides were rinsed in cool running water, washed in TBS (pH 7.4), blocked using a commercial peroxidase-blocking reagent and incubated for 30 min with rat anti-mouse Foxp3 (FJK-16s, dilution 1:100), followed by a secondary rabbit anti-rat antibody (1:200) and the EnVision peroxidase kit against rabbit antibodies[237].

5.2.4.3. Histological Analyses

Photographs from the stained samples were taken on the Axioplan light microscope at x 100 magnification. Analysis of the images was made by AxioVision software tools. In all cases, positively stained cells were counted in defined areas of the dermis at a x 100 magnification and normalized to 1 mm^2.

5.2.5. Molecular biology methods

5.2.5.1. RNA isolation from murine skin

Frozen samples of lesional skin were homogenized by pounding with a mortar and pestle in liquid nitrogen. Homogenized samples were transferred into RNase-free prechilled 15 ml conical tubes. 500 µl lysis buffer (RA1, NucleoSpin® RNA II) containing 5 µl β-mercaptoethanol (β-ME) was added to each sample following vigorous vortexing. Homogenized samples were transferred to tissue shredder columns and centrifuged at maximum speed for 3 min at RT. Proteins were digested by adding 100 µl proteinase K for 10 min at 55°C. For RNA extraction the RNeasy Mini Kit was used according to the instructions for RNA extraction from tissue samples. After binding of RNA on the column membrane an additional DNase digestion step for 15 min at RT was applied. Further steps of RNA isolation were performed according to the manufacturer's protocol. RNA was finally eluted with 50 µl of RNase-free water. RNA concentration was measured at 260 nm with the NanoDrop UV-Vis spectrophotometer. Additionally, RNA quality was checked by measuring the 260/280 ratio and by running a 1% agarose gel with 5 µl of the eluate per lane. RNA samples were stored at -80°C.

5.2.5.2. RNA isolation from cultured cells

A minimum of 2.5 x 10^5 cultured cells was transferred from cell culture plates into 1.5 ml reaction tubes and 1x PBS was added. After a centrifugation step for 10 min at 340 *g*, 4°C the supernatant was aspirated and the cell pellet was resuspended in 350 µl lysis buffer (RA1, NucleoSpin® RNA II) containing 3.5 µl β-ME. Lysed cells were stored at -20°C. RNA was isolated by using the RNA isolation kit NucleoSpin® RNA II according to manufacturer's instructions. Finally, RNA was eluted by 30 µl RNase-free water. A second elution step was performed with the same eluate.

5.2.5.3. cDNA synthesis

The cDNA synthesis was performed by a reverse transcriptase-PCR with TaqMan® Reverse Transcription Reagents containing a recombinant Moloney Murine Leukemia Virus Reverse Transcriptase, random hexamers and oligo $d(T)_{16}$. Up to 1 µg RNA in a total volume of 7.7 µl was mixed with 12.3 µl reaction mix (Table 4) and transcribed into cDNA. The reverse transcription was performed in a thermal cycler with 10 min at 25°C for initial primer-RNA template binding, 40 min at 48°C for reverse transcription, and 95°C for reverse transcriptase inactivation. cDNA samples were stored at -20°C.

Component		Volume per sample	Final concentration
10x	TaqMan RT Puffer	2.0 µl	1x
25 mM	$MgCl_2$ (or prediluted)	4.4 µl	3-6 mM
2 mM	dNTPs Mixture (each)	4.0 µl	500 µM (each)
50 µM	Random Hexamers	0.5 µl	1.25 µM
50 µM	Oligo $d(T)_{16}$	0.5 µl	1.25 µM
20 U/µl	RNase Inhibitor	0.4 µl	0.4 U/µl
50 U/µl	MultiScribe Reverse Transcriptase	0.5 µl	1.25 U/µl

Table 4 Reverse transcription reaction mix.

5.2.5.4. Real-time PCR/quantitative PCR (qPCR)

The fluorescence-based real-time polymerase chain reaction (real-time PCR/qPCR) has become one of the most widely used methods for the quantification and characterization of gene expression patterns and mRNA levels. For the assessment of gene expression levels qPCR was performed with the LightCycler® FastStart DNA Master SYBR Green I. The real-time detection of PCR product formation is monitored by measuring the increase in

fluorescence caused by the highly specific binding of SYBR Green fluorescence dye to double-stranded (ds) DNA. The 10x SYBR Green PCR Buffer also includes a passive reference dye as an internal reference to which the SYBR Green-dsDNA complex signal can be normalized. The threshold cycle value (C_T) or cycle number of crossing point (C_P) is the cycle at which a statistically significant increase of the normalized fluorescence intensity above an arbitrarily placed threshold is first detected. Based on the C_T values and the efficiency of primers in the real-time PCR/qPCR reaction relative quantification methods were applied.

Primers for the qPCR analysis were mostly designed by the Primer3 software[238] according to considerations for primer design described by Nolan *et al.*[239]. For qPCR reaction 2 µl of prediluted cDNA (1:2 to 1:4) was added to 3 µl of reaction mix (Table 5) in a LightCycler® capillary. Primer sequences for human and murine target gene analyses are shown in Table 6 and Table 7.

The target gene expression based on the C_T value was normalized to the expression of hypoxanthine-guanine phosphoribosyltransferase (*Hprt, hprt*) as a housekeeping gene. Relative expression ratio was calculated by the efficiency correction method as described[240, 241].

Component		Volume per sample	Final concentration
10x	FastStart DNA Master SYBR Green I	0.50 µl	1x
25 mM	$MgCl_2$	0.80 µl	3-5 mM
10 µM	Primer, forward	0.25 µl	100-500 nM
10 µM	Primer, reverse	0.25 µl	100-500 nM
	H_2O, PCR grade	1.20 µl	

Table 5 Real-time PCR/qPCR reaction mix.

Gene	Size	Sequence	Product size	Efficiency
aicda	20 20	for: 5'-agaggcgtgacagtgctaca-3' rev: 5'-atgtagcggaggaagagcaa-3'	93 bp	1.88
cyp24a1	23 23	for: 5'-cgggtgtaccatttacaactcgg-3' rev: 5'-ctcaacaggctcattgtctgtgg-3'	317 bp	1.88
hprt	29 23	for: 5'-atcagactgaagagctattgtaatgacca-3' rev: 5'-tggcttatatccaacacttcgtg-3'	231 bp	2.00
vdr	20 20	for: 5'-acttgcatgaggaggagcat-3' rev: 5'-aggtcggctagcttctggat-3'	199 bp	1.84

Table 6 Human primers for real-time/qPCR analyses.

Gene	Size	Sequence	Product size	Efficiency
Ccl22	20 21	for: 5'-tggtgccaatgtggaagaca-3' rev: 5'-ggcaggattttgaggtccaga-3'	101 bp	1.77
Ccl27	20 18	for: 5'-atagacagccactcccaagc-3' rev: 5'-ccaggtgaagcacgacag-3'	101 bp	1.94
Defb2	21 20	for: 5'-cactccagctgttggaagttt-3' rev: 5'-gcaacaggggttcttctctg-3'	148 bp	1.94
Defb3	20 20	for: 5'-ctccacctgcagcttttagc-3' rev: 5'-ggaactccacaactgccaat-3'	118 bp	2.09
Flg	22 20	for: 5'-cactgagcaaagaagagctgaa-3' rev: 5'-cgatgtcttggtcatctgga-3'	81 bp	1.70
Foxp3[242]	21 21	for: 5'-cccaggaaagacagcaacctt-3' rev: 5'-ttctcacaaccaggccacttg-3'	89 bp	2.00
Hprt	20 20	for: 5'-cgtcgtgattagcgatgatg-3' rev: 5'-aatccagcaggtcagcaaag-3'	221 bp	1.80
Ifng	27 21	for: 5'-aactattttaactcaagtggcatagat-3' rev: 5'-tgctgttgctgaagaaggtag-3'	217 bp	1.95
Il4	19 21	for: 5'-gactctttcgggcttttcg-3' rev: 5'-tgatgctctttaggctttcca-3'	105 bp	1.97
Ivl	22 20	for: 5'-ctcctgtgagtttgtttggtct-3' rev: 5'-ggatgtggagttggttgctt-3'	156 bp	2.10
Lor	21 21	for: 5'-tccttccctcactcatcttcc-3' rev: 5'-ctcctccaccagaggtctttc-3'	126 bp	1.86
Tgm1	21 21	for: 5'-agacccaaggtcctcaatgtc-3' rev: 5'-acttgggaaagctgtggactg-3'	131 bp	1.89
Tnfa	20 21	for: 5'-ccaccacgctcttctgtcta-3' rev: 5'-ggttgtctttgagatccatgc-3'	98 bp	2.28
Tslp	20 20	for: 5'-agagaagccctcaatgacca-3' rev: 5'-ggacttcttgtgccatttcc-3'	82 bp	2.00

Table 7 Murine primers for real-time/qPCR analyses.

5.2.6. Statistical analyses

Statistical analyses were performed using GraphPad Prism. When a non-Gaussian distribution of sample values was assumed non-parametrical two-tailed Wilcoxon matched pairs test or Mann-Whitney *U* test for independent groups was applied. For normally distributed values a two-tailed paired or unpaired t test was applied. Results are presented as scatter dot plots with median values or column bar graphs with mean ± SEM. Statistical significance was assumed at $P < 0.05$ for all tests.

6. Results

6.1. The VDR agonist mediates VDR activation in B cells

First, the expression of the VDR and the activity of the VDR agonist were assessed by investigating the effects on the expression of the vitamin D responsive gene *cyp24a1* in human naïve and memory B cells as defined by their expression of CD19 and CD27[243]. *Cyp24a1*, a classical VDR responsive gene[244], encodes the calcitriol inactivating enzyme 25-OH-D_3-24-hydoxylase[20]. In $CD27^-$ naïve B cells the VDR agonist induced *cyp24a1* to a similar extent as calcitriol after 24 h and 48 h; a slightly increased tendency of the *cyp24a1* induction in $CD27^+$ memory versus $CD27^-$ naïve B cells was observed for both VDR ligands after 48 h (Figure 9A). At the same time, *vdr* expression by itself, induced by CD40/IL-4 stimulation, was not influenced either by the VDR agonist or by calcitriol (data not shown).

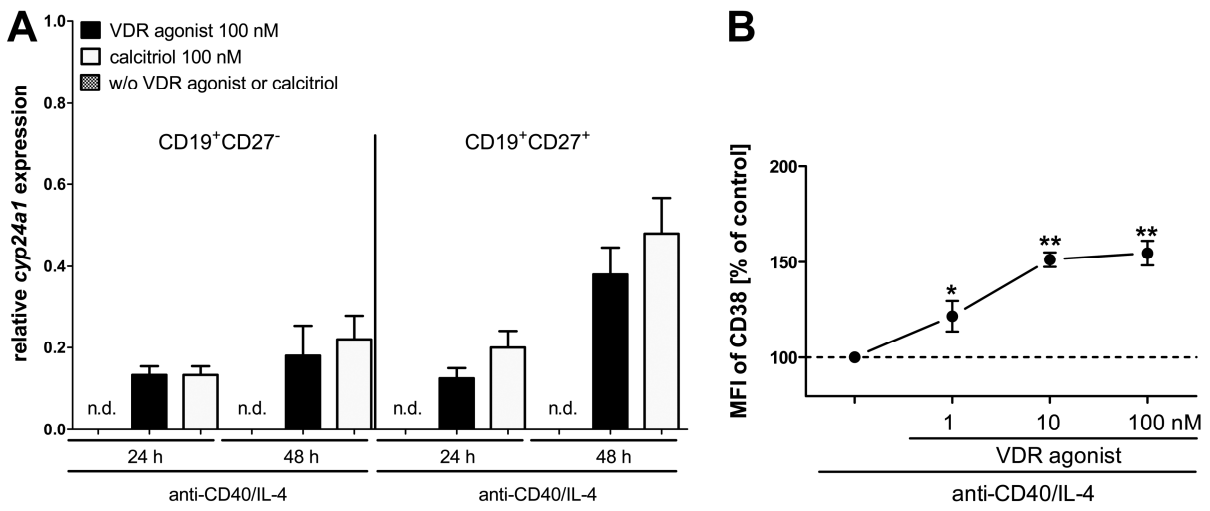

Figure 9 The VDR agonist activates the VDR in human B cells. *A*, Human naïve and memory B cells were stimulated with anti-CD40 and IL-4 in the presence or absence of the VDR agonist or calcitriol for 24 h and 48 h. The mRNA of the vitamin D responsive gene *cyp24a1* was assessed by quantitative PCR (n ≥ 4, n.d. = not detectable). *B*, Peripheral human $CD19^+$ B cells were cultured with anti-CD40 and IL-4 in the presence of increasing amounts of the VDR agonist. After 8 d of culture, the expression of CD38 was analyzed by flow cytometry. The median fluorescence intensity (MFI) was measured and is given in % of stimulated control (100%, n ≥ 3, $P < 0.05$ *, $P < 0.01$ **).

Additionally, the induction of another well-known vitamin D-induced molecule, namely CD38[47, 245] was determined at the protein level. As shown in Figure 9B, the VDR agonist induced expression of CD38 on the cell surface of anti-CD40/IL-4 stimulated $CD19^+$ B cells dose-dependently.

6.2. VDR activation by the VDR agonist inhibits IgE production in B cells

After showing that human B cells express the VDR and respond to the VDR agonist, its impact on B cell function was assessed. As we have previously shown that VDR targeting in B cells modulates IgE production[144], the VDR agonist in comparison to the natural ligand calcitriol was studied. Indeed, the data shown in Figure 10 demonstrate that calcitriol but also the VDR agonist inhibits the anti-CD40/IL-4-induced IgE production in human B cells in a dose-dependent manner. A maximum of inhibition was reached with 70.1 ± 6.0% (VDR agonist) and 59.9 ± 11.6% (calcitriol) (Figure 10A). In contrast, by addition of the VDR antagonist no inhibition of IgE secretion was observed, suggesting a specific VDR-dependent effect. To address the question whether VDR signaling alters IgE secretion per cell or inhibits differentiation of IgE secreting cells, ELISPOT analyses were performed. VDR ligation by the agonist strongly reduced IgE secreting cells by 68.1 ± 12.7% (Figure 10B). Furthermore, in the presence of calcitriol the number of IgE secreting cells was reduced by 81.3 ± 5.8% (Figure 10B). Taken together, these data show that VDR activation by the low-calcemic agonist strongly inhibits IgE production and reduces the number of IgE secreting cells with a comparable efficacy to calcitriol.

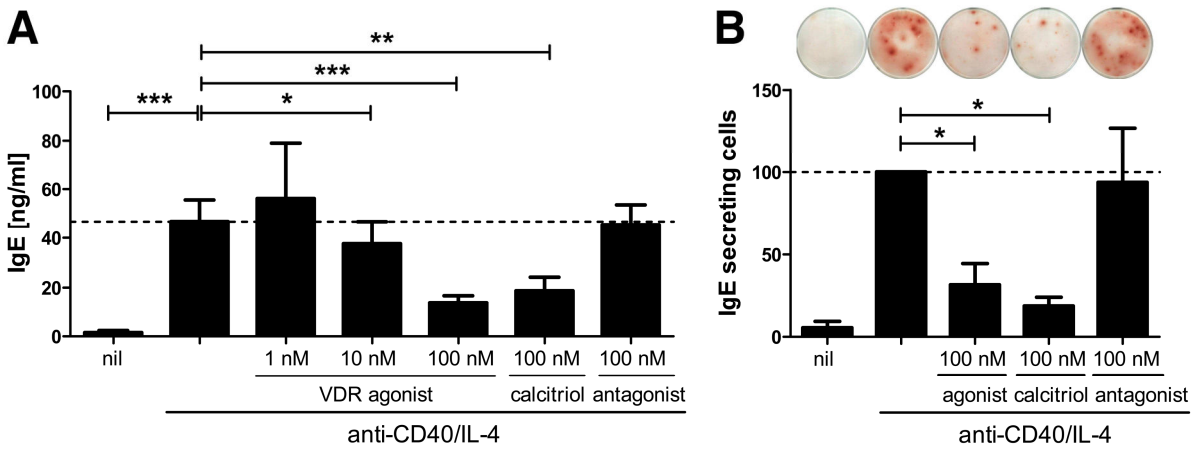

Figure 10 VDR activation by the VDR agonist inhibits IgE production in B cells. $CD19^+$ B cells were activated by CD40/IL-4 in the presence of various VDR ligands. *A*, IgE concentrations in the cell free supernatants were determined by ELISA after 8 d of culture. The dashed line indicates the mean stimulated IgE concentration. Mean values ± SEM are given (n ≥ 3). *B*, B cells were cultured for 5 d as described before and analyzed after 5 d by ELISPOT assay. Data are shown as mean ± SEM in % of the anti-CD40/IL-4 stimulated control (n = 6 – 7, $P < 0.05$ *, $P < 0.01$ **, $P < 0.001$ ***).

To investigate the effect of the VDR agonist on other Ig isotypes than IgE, ELISA and ELISPOT analyses from the same samples were performed. The secretion of IgG was inhibited upon VDR activation by the VDR agonist (64.0 ± 5.6%), whereas IgA was affected to a lesser extent (27.6 ± 8.5%) (Figure 11A). These data were confirmed by ELISPOT analyses showing a reduction of IgG secreting cells by 70.4 ± 6.5% whereas IgA secreting cells were decreased by 26.6 ± 8.0% upon stimulation with the VDR agonist (Figure 11B and C). Calcitriol diminished the IgG secreting cells by 62.2 ± 6.9% and IgA secreting cells by 40 ± 9.5% (Figure 11B and C). Conversely, IgM secretion was also reduced but did not reach statistical significance (Figure 11A).

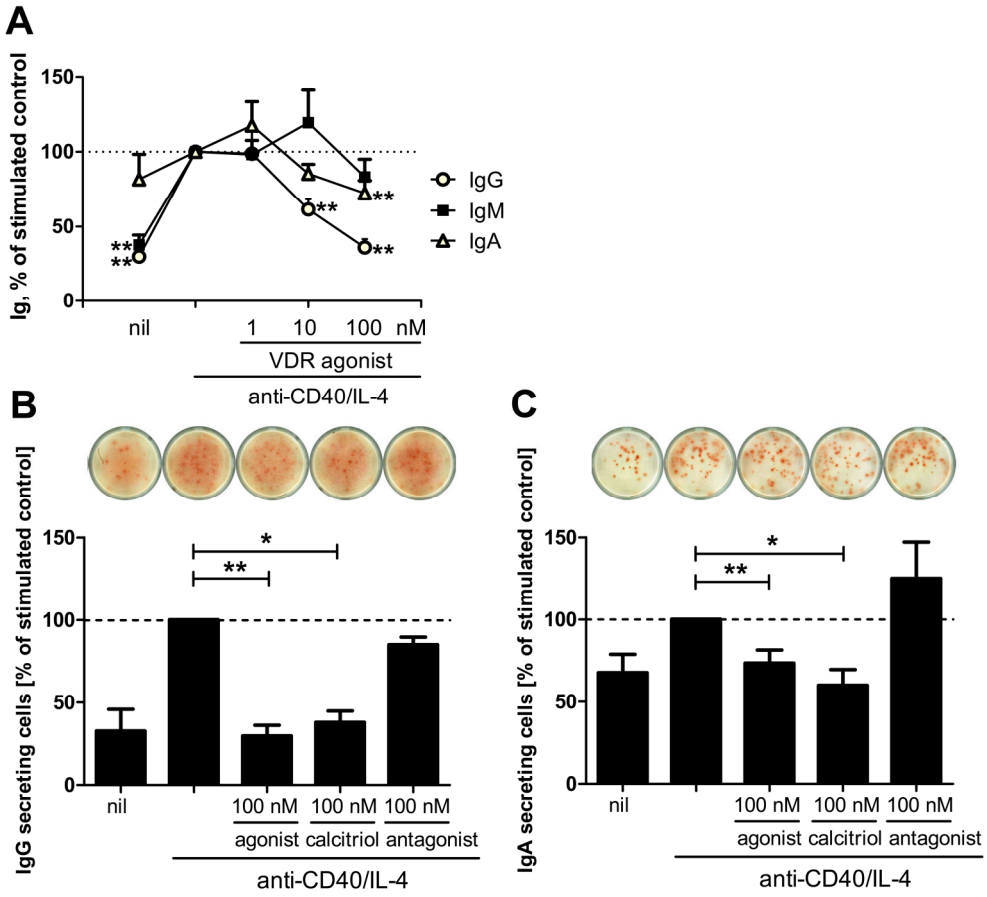

Figure 11 Analysis of other isotypes than IgE. *A*, Peripheral CD19$^+$ B cells were activated by anti-CD40 and IL-4 in the presence of increasing amounts of the VDR agonist. Ig concentrations in the cell free supernatants were determined by ELISA after 8 d of culture (n ≥ 3). Data are normalized on the anti-CD40/IL-4 stimulated control indicated by the dotted line. It corresponds to a mean concentration of IgG = 257.6 ± 94.4 ng/ml (○), IgM = 629.4 ± 271.4 ng/ml (■) and IgA = 452.5 ± 98.4 ng/ml (△), respectively. *B* and *C*, Peripheral CD19$^+$ B cells were activated as described above in the presence or absence of 100 nM VDR agonist, calcitriol or VDR antagonist. After 5 d of culture B cells were analyzed for IgG (*B*) and IgA (*C*) secreting B cells by ELISPOT assay. Data are shown as mean ± SEM in % of the anti-CD40/IL-4 stimulated control (n ≥ 6, $P < 0.05$ *, $P < 0.01$ **).

6.3. STAT6 phosphorylation and IκBα degradation is not modulated

As IL-4 and CD40 signaling are important for the induction of class switch recombination (CSR) towards IgE[155], key molecules of the downstream signaling pathway of IL-4 and CD40 in human B cells were analyzed.

IL-4 receptors, consisting of the IL-4Rα and common γ (γ_c) chain, induce phosphorylation of the signal transducer and activator of transcription 6 (STAT6) following ligation by IL-4. Subsequently, phosphorylated STAT6 (pSTAT6) dimerizes and translocates into the nucleus, where it acts as transcription factor to modulate transcriptional activity[157].

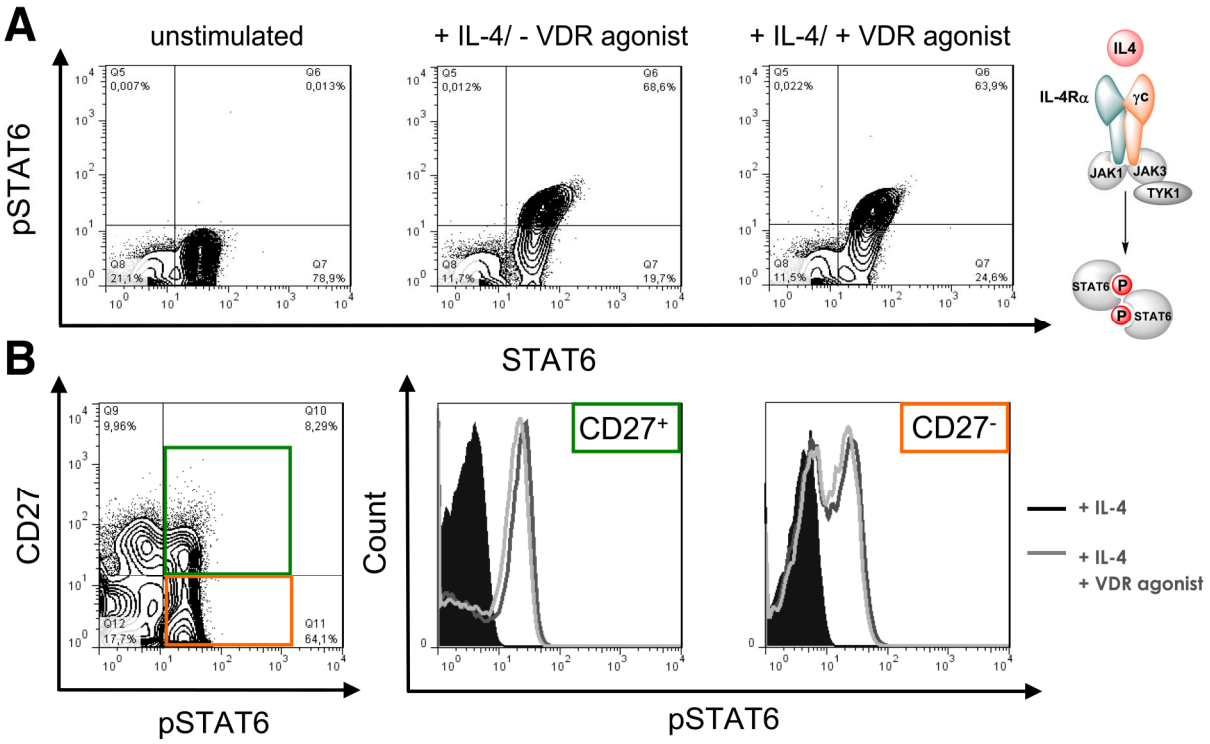

Figure 12 Analysis of STAT6 phosphorylation. *A*, Peripheral $CD19^+$ B cells were activated by anti-CD40 and IL-4 for 24 h. After starving over night, cells were stimulated with IL-4 for 1 h in the absence or presence of the VDR agonist. Cells were harvested immediately and stained for flow cytometry analysis. Cells were gated on the $CD19^+$ population. *B*, $CD19^+$ B cells were activated as described in (*A*). Cells were gated on $CD19^+$ and $STAT6^+$, and pSTAT6 in $CD27^-$ as well as $CD27^+$ B cells was analyzed. Shown is one representative out of three independent experiments.

As depicted in Figure 12A IL-4 receptor activation results in a substantial activation of STAT6 molecules by phosphorylation. In contrast, STAT6 remained in an unphosphorylated inactive state in unstimulated B cells. Additional stimulation by the VDR agonist did not change the percentages of phosphorylated STAT6 significantly (Figure 12A). Detailed analyses of

pSTAT6 in CD27$^-$ naïve and CD27$^+$ memory B cells did not demonstrate any inhibitory effect of the VDR agonist on STAT6 phosphorylation in this setting (Figure 12B).

In the next step, CD40-induced degradation of the dominant inhibitor of nuclear factor-κB (NF-κB), IκBα, which sequesters the inactive p50-p65 NF-κB dimer in the cytoplasm[246] was determined by flow cytometry.

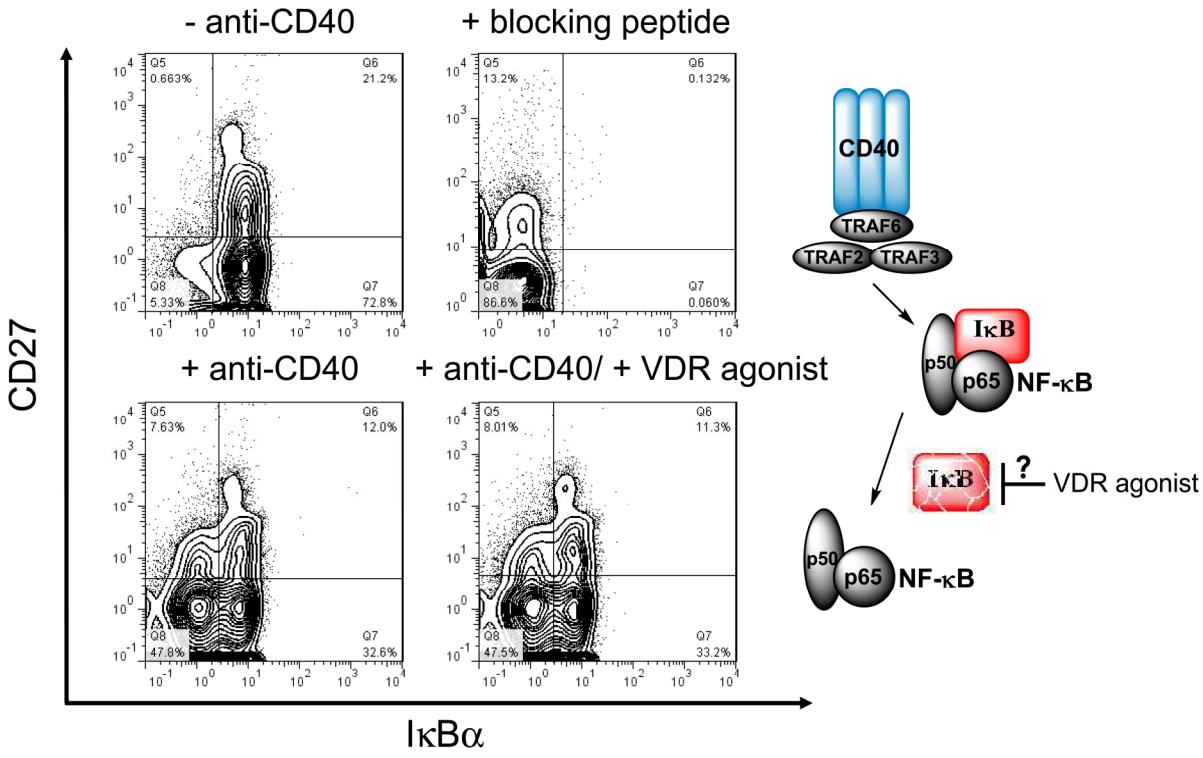

Figure 13 Analysis of IκBα degradation. Peripheral CD19$^+$ B cells were activated by anti-CD40 and IL-4 for 24 h. After additional 60 min preincubation in the absence or presence of the VDR agonist, cells were stimulated with 1 µg/ml anti-CD40 for 50 min. Cells were harvested immediately and stained for flow cytometry analysis. Cells were gated on the CD19$^+$ population. The expression of IκBα in CD27$^-$ as well as CD27$^+$ B cells was analyzed. Shown is one representative out of three independent experiments.

After 24 h stimulation with anti-CD40/IL-4, almost all human CD27$^-$ and CD27$^+$ B cells expressed IκBα in the cytoplasm (Figure 13, upper left), suggesting an inactive state regarding CD40 signaling. Upon additional stimulation with anti-CD40, cells were strongly activated as shown by the reduction of IκBα (Figure 13, lower left). More importantly, no impact of the VDR agonist on IκBα degradation was detected (Figure 13, lower right). Taken together, VDR activation by the VDR agonist does not influence the downstream signaling of IL-4 and CD40 at the level of STAT6 phosphorylation and IκBα degradation.

6.4. Reduction of *aicda* expression by calcitriol and the VDR agonist

Previously, it has been shown that calcitriol inhibits the expression of the epsilon germline transcript (εGLT) by direct binding of the VDR on the εGLT promoter and subsequent recruitment of transrepressing factors[144, 145]. To answer the question whether inhibition of other subtypes than IgE by the VDR agonist is due to common mechanisms, which are also involved in IgE class switch recombination, the expression of *aicda* was analyzed. *Aicda* encodes the enzyme activation-induced cytidine deaminase (AID), which is essential for somatic hypermutation and class switching towards IgE but also other subtypes[155, 175].

The expression of *aicda* in anti-CD40/IL-4 stimulated $CD19^+$ $CD27^-$ naïve B cells was inhibited by 33.2 ± 3.0% after 24 h and by 39.6 ± 7.6% after 48 h of culture in the presence of the VDR agonist (Figure 14A). Calcitriol also reduced the expression of *aicda* in $CD19^+$ $CD27^-$ B cells by 27.9 ± 6.6% after 48 h (Figure 14A). The *aicda* expression in $CD19^+$ $CD27^+$ memory B cells was inhibited by 29.1 ± 5.7% after 24 h and by 35.7 ± 3.8% after 48 h of incubation with the VDR agonist and to a comparable extent (28.1 ± 8.3%) with calcitriol after 48 h (Figure 14B). Together, both calcitriol and the low-calcemic VDR agonist interfere with the switching process by reducing *aicda* expression.

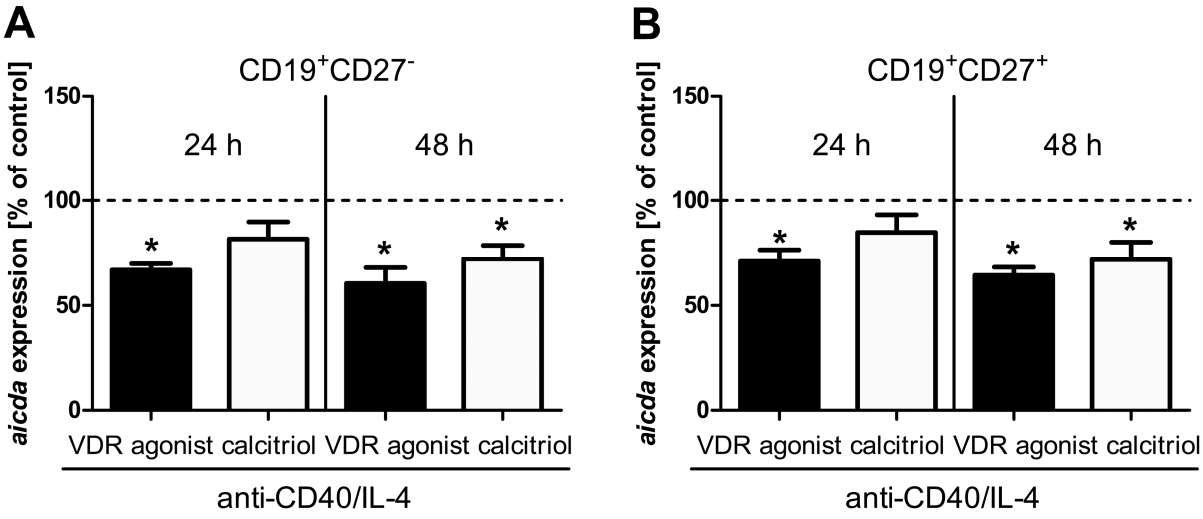

Figure 14 Inhibition of *aicda* expression. *A*, Human naïve B cells ($CD19^+$ $CD27^-$) were stimulated with anti-CD40 and IL-4 in the presence or absence of the VDR agonist or calcitriol for 24 h and 48 h. Gene expression of the activation-induced cytidine deaminase (*aicda*) was assessed by quantitative PCR. *B*, Memory B cells ($CD19^+$ $CD27^+$) were analyzed as described in *A*. The relative quantification was calculated and is given in % of the anti-CD40/IL-4 stimulated control. The percentages are shown as mean ± SEM ($n \geq 6$, $P < 0.05$, *).

6.5. Reduction of the CD19$^+$ CD27^{high} CD38$^+$ B cell population by activated VDRs

Having found a suppressive effect on *aicda* expression, but even more potently, on the production of distinctive Ig subclasses themselves, the question whether additional events may also be targets of VDR dependent action was addressed.

Therefore, B cell proliferation was analyzed by CFSE dilution assays. As shown in Figure 15A, little proliferation of B cells upon anti-CD40/IL-4 stimulation was observed. Application of the VDR agonist resulted in a slightly reduced frequency of proliferating cells to 10.8 ± 1.0% compared to 12.4 ± 1.2% ($P > 0.05$), while the percentages of PI-positive cells remained stable (Figure 15B).

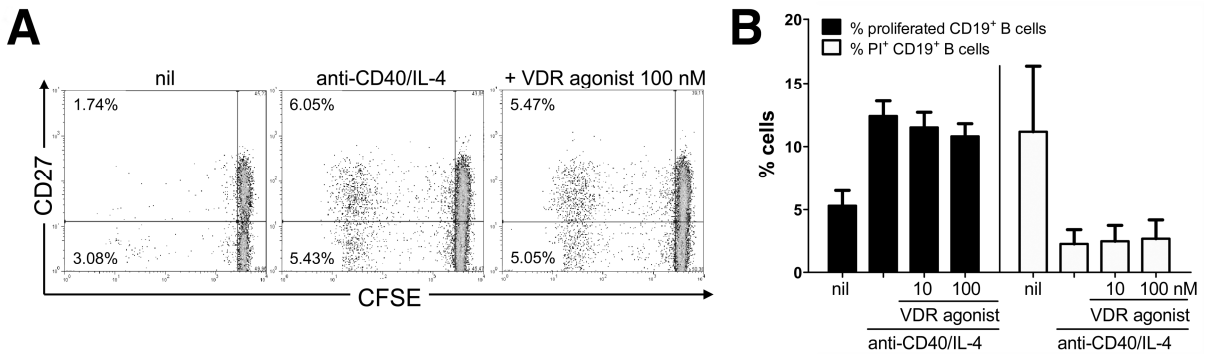

Figure 15 Impact of the VDR agonist on proliferation and cell viability. *A* and *B,* Cells were labeled with CFSE and stimulated with anti-CD40 and IL-4 in the presence or absence of 100 nM VDR agonist. After a 5-day-culture, cells were analyzed by flow cytometry and the frequency of proliferated and PI$^+$ cells was determined. The percentages of proliferated and PI-positive cells were measured and are shown as mean ± SEM (n = 4).

As IL-21 is known to facilitate IgE production and B cell proliferation in humans[158, 159, 247-249], the effect of VDR activation under highly proliferative conditions through simultaneous treatment with IL-21 and anti-CD40/IL-4 was delineated. As expected, B cell proliferation was 4.6-fold more pronounced under these conditions compared to the stimulation with anti-CD40/IL-4 (Figure 15), as determined by increased CFSE dilution corresponding to a higher number of proliferating cells (Figure 16A and B). The most pronounced induction of proliferation by IL-21 was observed in the naïve B cell compartment (Figure 16A). This may result from the higher expression level of IL-21R on naive, compared to memory, B cells[249]. Notably, in B cells treated with the VDR agonist, a slight, but not significant antiproliferative effect of 16.8 ± 7.4% (100 nM) was observed under these conditions (Figure 16B). A minor,

but also slight inhibitory effect (9.5 ± 8.0%) on B cell proliferation was observed for calcitriol (Figure 16B).

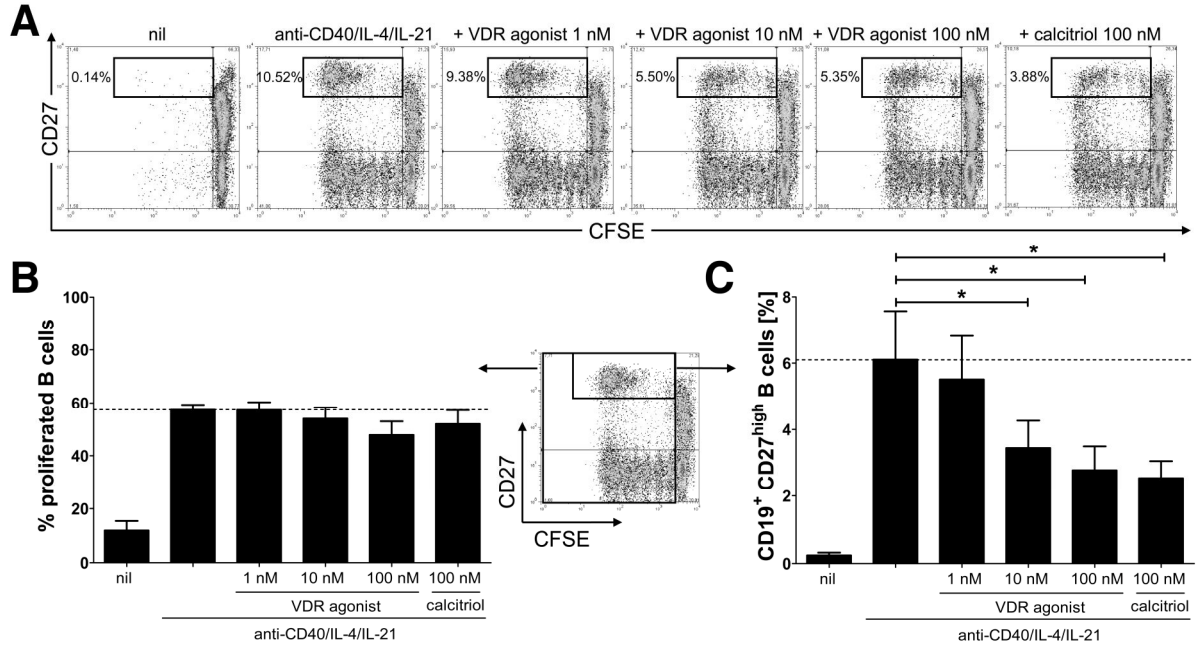

Figure 16 VDR agonist signaling inhibits the generation of CD27^{high} cells. *A*, Peripheral human CD19^{+} B cells were cultured with anti-CD40/IL-4/IL-21 in the absence or presence of the VDR agonist and calcitriol and analyzed after 5 d by flow cytometry. Shown is one representative density plot. *B*, The percentages of proliferated CD19^{+} B cells are shown as mean ± SEM (n = 4). *C*, The frequency of CD19^{+} CD27^{high} B cells is shown as mean ± SEM (n = 7; $P < 0.05$, *).

Additionally, IL-21 is known to promote the differentiation of human B cells into immunoglobulin-secreting cells (ISCs)[248, 250] which are characterized as CD27^{high} at their transitional stage to ISCs[250, 251]. Interestingly, by stimulation with anti-CD40/IL-4 and IL-21, a CD27^{high} population comprising 6.1 ± 1.5% of CD19^{+} B cells at d 5, appeared approximately after three division cycles (Figure 16C). Additional data show that if CD27^{high} cells were depleted by FACSsort before stimulation under equal conditions, a newly formed CD27^{high} subset was induced (data not shown). These data suggest an induced formation of the CD27^{high} cells by stimulation rather than a maintenance or expansion of preexisting cells. More importantly, additional activation by the VDR agonist diminished the generation of CD27^{high} cells dose-dependently, with a maximum inhibition of 51.1 ± 6.3%. The natural ligand calcitriol inhibited the CD27^{high} population by 64.6 ± 3.3%.

In vitro generated human Ig-producing blasts or ISCs, however, are also characterized by the surface expression of CD38[252, 253]. Therefore, CD19^{+} B cells were stimulated with anti-CD40/IL-4 and IL-21 to induce CD27^{high} CD38^{+} cells, and the impact of VDR activation was examined.

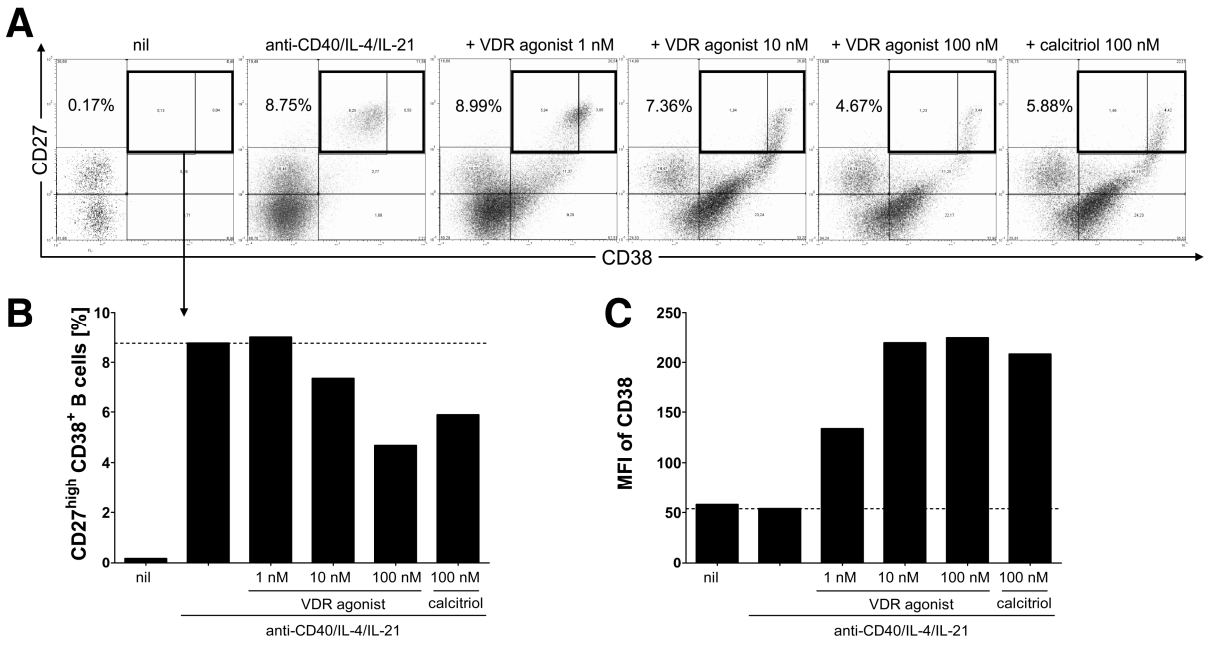

Figure 17 VDR agonist signaling reduces the frequency of CD27^{high} CD38^{+} B cells while increasing the expression of CD38. *A*, Human peripheral CD19^{+} B cells were stimulated with anti-CD40/IL-4 and IL-21 in the presence or absence of increasing amounts of the VDR agonist and calcitriol. After a 5-day-culture, cells were analyzed by flow cytometry. *B*, Representative percentages of CD19^{+}, PI^{-}, CD27^{high}, CD38^{+} B cells are shown. *C*, The MFI of CD38, gated on CD19^{+}, PI^{-}, CD27^{high} cells, was determined. Shown is one representative out of 3 experiments. MFI = median fluorescence intensity.

In consequence of stimulation with anti-CD40/IL-4 and IL-21, about 8.75% CD27^{high} CD38^{+} cells were induced, shown by one representative experiment (Figure 17A and B). Upon addition of the VDR agonist and calcitriol, this population was strongly reduced by 46.6% and 32.8%. In contrast, surface expression of the VDR target gene CD38[47, 245] on these cells was increased upon treatment with the VDR agonist or calcitriol, as determined by a 2-fold increase in the median fluorescence intensity (MFI) (Figure 17C). In summary, VDR activation profoundly interferes with the generation of ISCs *in vitro* as shown by the reduced frequency of CD27^{high} CD38^{+} cells. These results correlate with the reduced Ig secretion and numbers of Ig secreting cells determined by ELISA and ELISPOT.

6.6. VDR activation reduces the IgE response in a type I allergy mouse model without calcemic side effects

Based on the potency to counteract the IgE production *in vitro*, the impact of the low-calcemic VDR agonist on the allergic immune response *in vivo* was delineated. Mice were

sensitized and treated as depicted in Figure 6. The low-calcemic nature of the VDR agonist was confirmed by measurement of serum calcium concentrations on day 47.

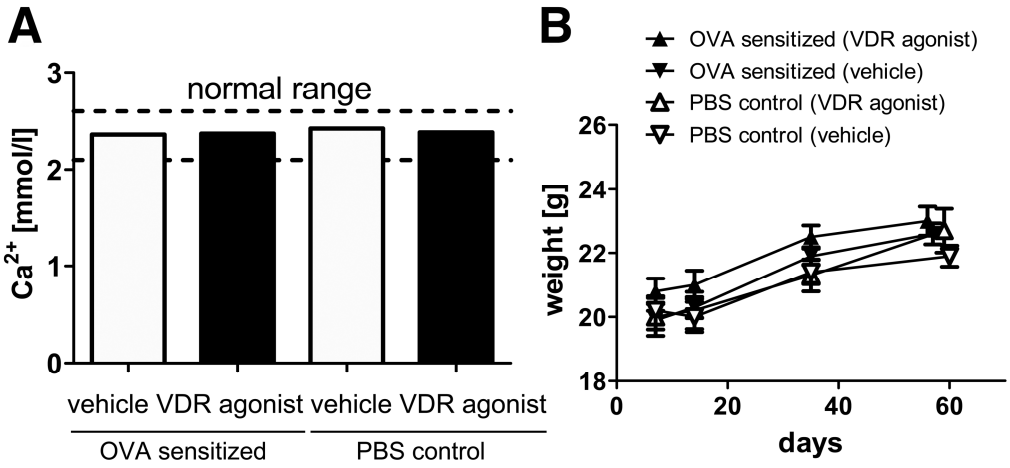

Figure 18 The VDR agonist is well tolerated *in vivo*. *A*, Ca^{2+}-levels in pooled sera from sensitized and non-sensitized BALB/c mice on d 47, treated with the VDR agonist or vehicle control. *B*, Weight gain over time of VDR agonist-treated mice compared to vehicle-treated control groups. Data represent means ± SEM of 8 mice per group.

Both, the VDR agonist and PBS treated groups showed comparable serum Ca^{2+}-levels, confirming the low-calcemic character of the VDR agonist (Figure 18A). In addition, the mice remained healthy and displayed a comparable development of weight gain throughout the experiment (Figure 18B). As depicted in Figure 19 the therapeutic treatment regimen led to a profound inhibition of the allergen-specific IgE response by 46.7% ($P = 0.03$; Figure 19A, right). As expected, no allergen-specific Ig production was detected in non-sensitized control mice (data not shown). Total IgE levels were also reduced by 35.5% ($P = 0.05$; Figure 19A, left). Although the effect on the IgE level was most distinctive, an inhibition of the allergen-specific IgG_1 levels by 20.7% ($P = 0.04$; Figure 19B) was also observed. A similar tendency as for IgG_1 was found for IgG_{2a} and IgA, but overall levels of these isotypes were barely detectable and variable (data not shown). To investigate whether the suppressing effects on IgE production were accompanied by alterations in the B cell compartment, the composition of splenic B cells was assessed. As shown in Figure 19C, the B cell compartment consisted of 5.3 ± 0.2% marginal zone B cells, expressing high levels of CD21 but no CD23, and 80.9 ± 0.9% of follicular B cells, expressing CD21 and CD23. This pattern did not change upon VDR activation, demonstrating that the suppression of IgE production is not the result of overt changes in B cell subpopulations, further emphasizing the specificity of the Ig reducing effect.

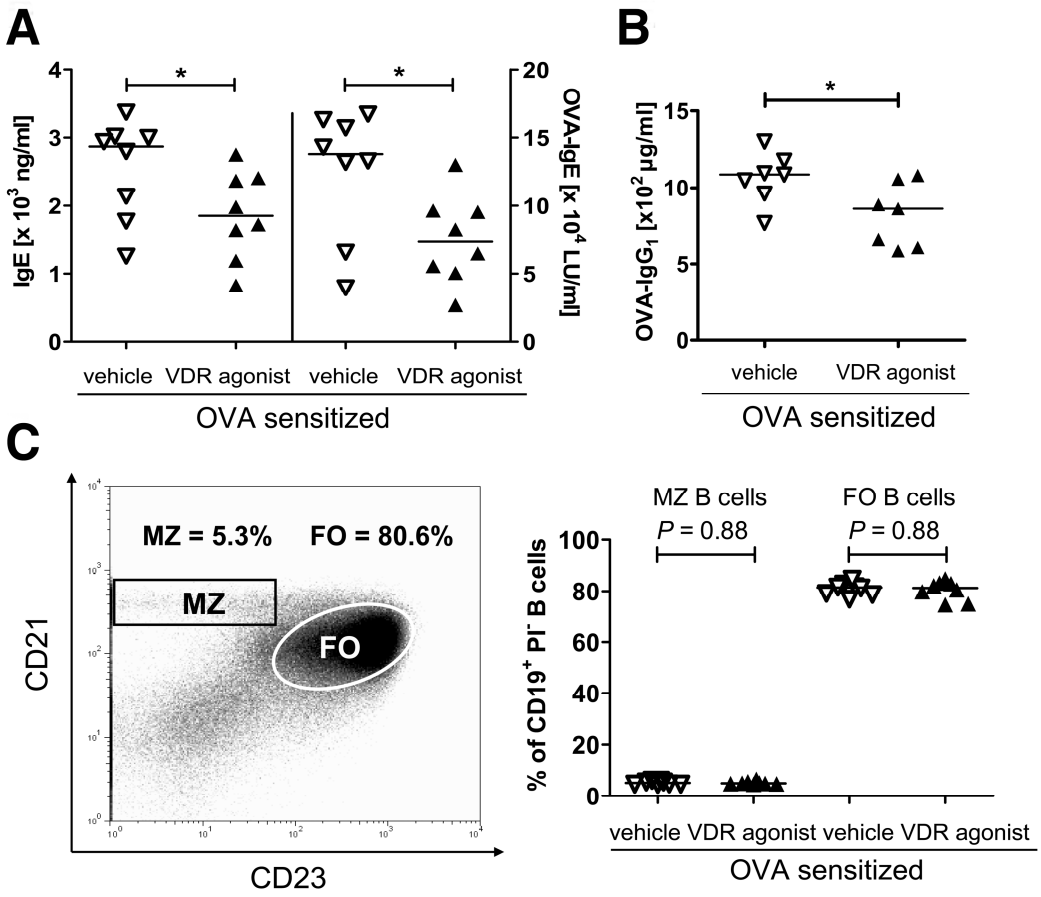

Figure 19 The VDR agonist reduces total and allergen-specific IgE in a mouse model of type I allergy. *A* and *B*, Total IgE (*A*, left), allergen-specific IgE (*A*, right) and IgG1 levels (*B*) in sera of treated mice on d 47 were determined by ELISA. *C*, The splenic B cell compartment gated on living $CD19^+$ B cells was analyzed by flow cytometry. Follicular (FO, $CD21^{mid}$, $CD23^+$) and marginal zone (MZ, $CD21^{hi}$, $CD23^-$) B cells were identified by different expression levels of CD21 and CD23. Bars in the scatter plot represent medians ($n \geq 7$), triangles represent single values ($P < 0.05$, *).

6.7. VDR agonist treatment ameliorates allergen-triggered skin eczema in mice

Although vitamin D_3 and its metabolites are known for their substantial impact on the immune system[39, 254] and the skin differentiation and function[209], the effects of VDR ligands on atopic dermatitis (AD) have not been studied in detail. Using the VDR agonist, which was proven low-calcemic but nevertheless exhibiting strong immunomodulatory effects, the role of VDR signaling in a defined model of allergen-driven dermatitis (Figure 7) was investigated. In accordance with previous results[234], a strong induction of the eczema by epicutaneous application of OVA compared to PBS as reflected by the increased clinical skin score (median OVA-patched mice: 10.0, range: 8.0 – 12.0; median PBS-patched mice: 4.25, range: 1.5 – 6.5; $P = 0.0003$) was observed (Figure 20A). The clinical skin score of 4.25, induced by

the patch itself in the absence of the allergen (antigen), corresponds to an allergen-independent, mild dermatitis.

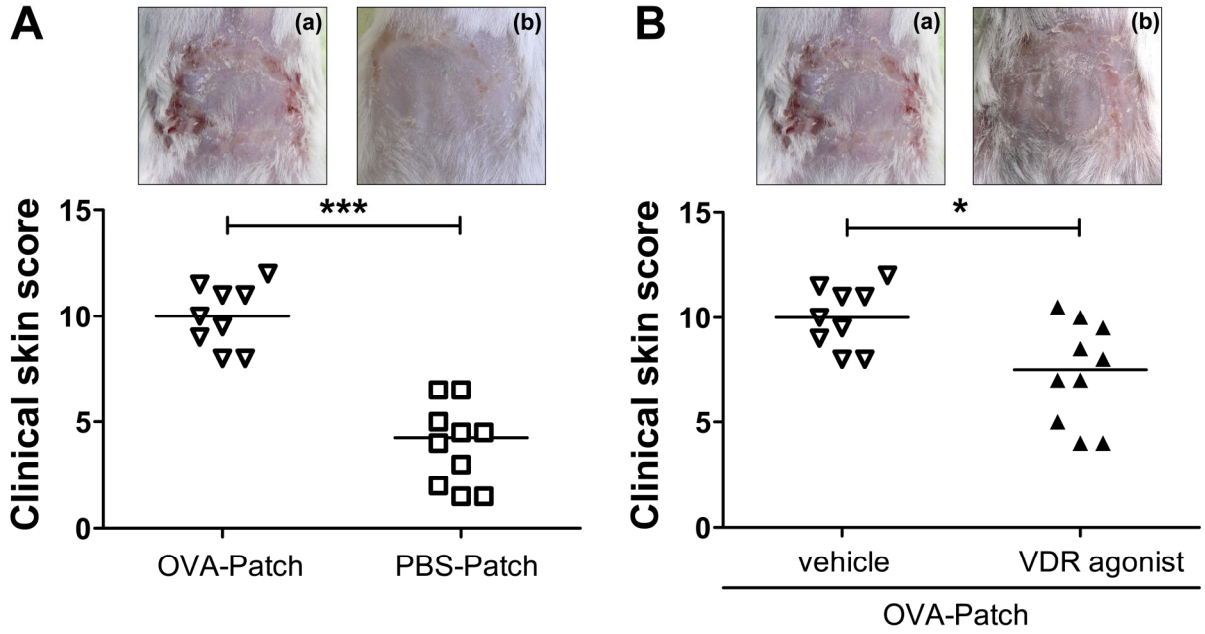

Figure 20 The VDR agonist ameliorates allergen-triggered skin eczema in mice. *A*, Mice were sensitized with OVA/alum and challenged with either OVA/alum (OVA-Patch) or PBS/alum (PBS-Patch) locally, according to the scheme in Figure 7. *B*, Mice were sensitized with OVA/alum as described above, followed by treatment with VDR agonist or vehicle control, according to the method section (see also Figure 7). On day 71 mice were sacrificed and the severity of the eczema was evaluated as described in methods. The index of severity (clinical skin score) is shown as the median for each group ($n \geq 9$; $P < 0.05$ *, $P < 0.001$ ***). One representative picture of each group is shown.

To delineate the effect of the VDR agonist on the allergen-induced eczema, following results are shown from OVA-sensitized mice treated with either the VDR agonist or a vehicle control. VDR activation by the VDR agonist led to a clear improvement of all signs and symptoms of the OVA-induced eczema, including erythema, edema, excoriation, dryness and extension, as evidenced by a reduced clinical skin score (median VDR agonist-treated mice: 7.5, range: 4.0 – 10.5; median vehicle-treated mice: 10.0, range: 8.0 – 12.0; $P = 0.0195$) (Figure 20B). Taken together, the data clearly show that the low-calcemic VDR agonist significantly modulates the local immune response as shown by improvement of the allergen-induced eczema.

6.8. VDR activation does not change the numbers of infiltrating T cells in lesional skin

Immunohistochemistry was employed to analyze the relative distribution of different T cell subsets in lesional skin. As shown in Figure 21A, there was no significant difference between VDR agonist-treated and control mice in terms of total $CD4^+$ T cells. Nevertheless, a tendency of higher numbers of $CD4^+$ T cells (1.8-fold increase compared to vehicle-treated group) was observed in the VDR agonist-treated group (median VDR agonist-treated mice: 612.8, range: 369.8 – 740.5; median vehicle-treated mice: 347.9, range: 128.0 – 764.5; $P = 0.1628$). In line with previous results[234], $CD8^+$ T cells were strongly induced upon epicutaneous sensitization with OVA ($P = 0.0068$; data not shown) homing into the dermis and epidermis. There was a slight tendency of $CD8^+$ T cells to decrease in the skin of VDR agonist-treated mice, which did not reach statistical significance (Figure 21B).

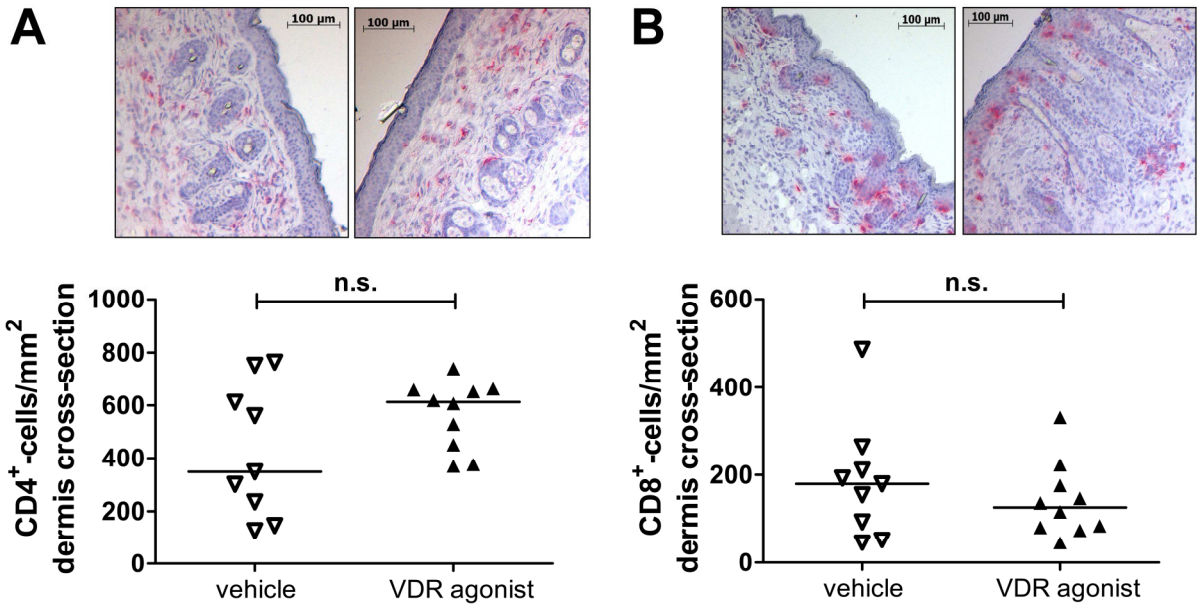

Figure 21 $CD4^+$ and $CD8^+$ cells in skin lesions of OVA-sensitized and VDR ligand treated mice. $CD4^+$ (*A*) and $CD8^+$ T cells (*B*) were stained and quantified in the dermis of lesional skin of VDR agonist-treated and untreated mice. Numbers of cells per mm^2 are shown as the median for each group ($n \geq 9$). One representative photograph of each group is shown; n.s.: not significant.

6.9. Increased numbers of $Foxp3^+$ cells in skin lesions of VDR agonist-treated mice

As VDR agonist treatment was associated with only minor changes in the skin infiltrating $CD4^+$ and $CD8^+$ T cells, the question for other mechanisms and changes in defined cell types

that might contribute to the amelioration of the dermatitis was asked. As Foxp3$^+$ T_{reg} cells are known to inhibit both T_H1 and T_H2 cells by reducing their cytokine production[255], and due to its crucial role in the maintenance of immune homeostasis in normal skin[256], the number of Foxp3$^+$ cells in lesional skin was analyzed.

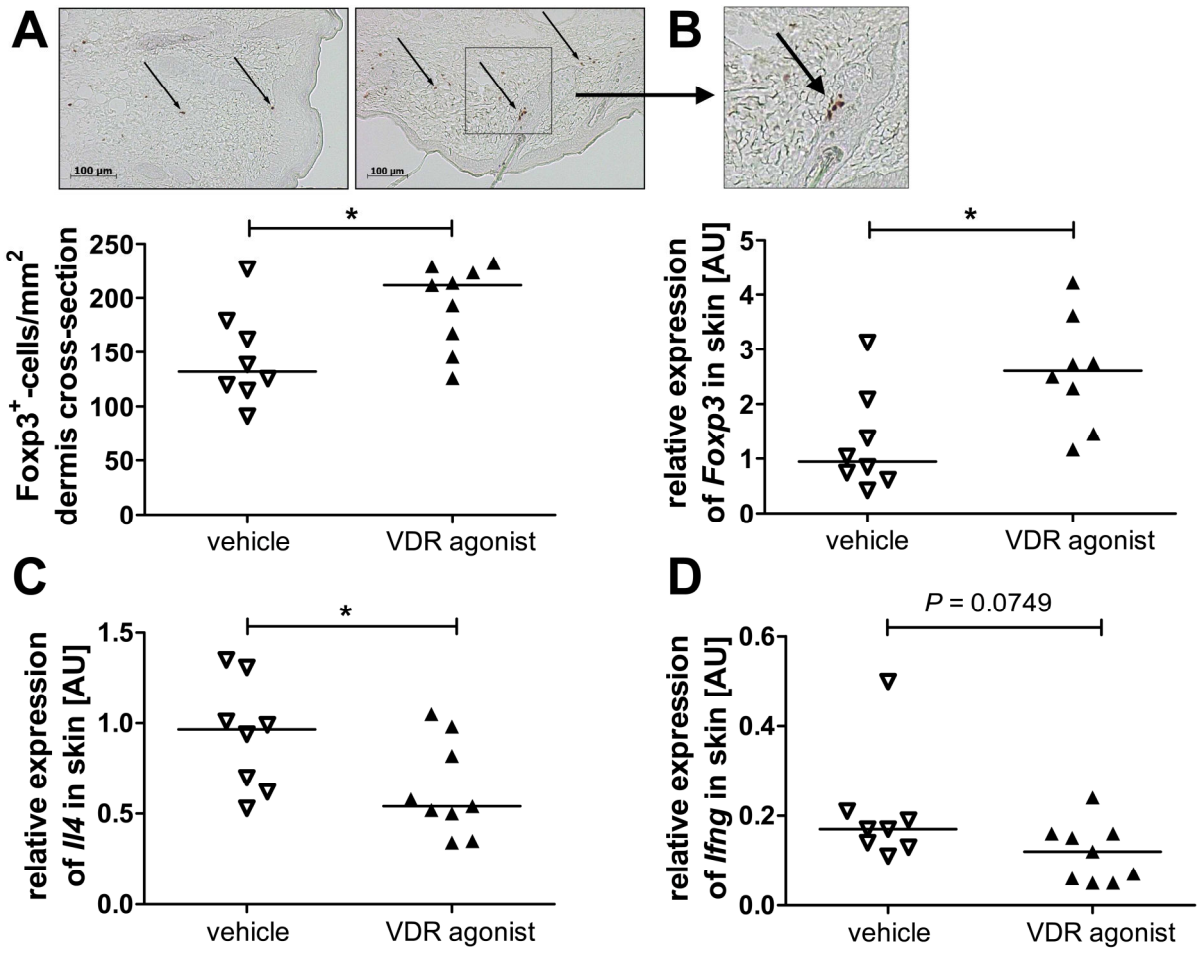

Figure 22 The VDR agonist increases the number of Foxp3$^+$ cells in lesional skin. *A*, Foxp3$^+$ cells were stained and quantified in the dermis of lesional skin of VDR agonist-treated and untreated mice. Numbers of cells per mm^2 are shown as the median for each group (n ≥ 8; $P < 0.05$ *). One representative photograph of each group is shown (arrows indicate Foxp3$^+$ cells). Expression levels of *Foxp3* (*B*), *Il4* (*C*) and *Ifng* (*D*) in lesional skin of each group were assessed by quantitative PCR. Shown is the relative expression of the target gene compared to the housekeeping gene *Hprt* in arbitrary units (AU) (n ≥ 8; $P < 0.05$ *).

Indeed, there was a clear-cut increase in the number of Foxp3$^+$ cells by 60.0% upon therapeutic treatment with the VDR agonist (median VDR agonist-treated mice: 211.9, range: 126.0 – 232.3; median vehicle-treated mice: 132.0, range: 91.1 – 226.9; $P = 0.026$) (Figure 22A) which might explain the 1.8-fold increase in infiltrating CD4$^+$ T cells (Figure 21A). This observation is also supported by a significantly 2.5-fold increased expression of *Foxp3* in

the skin of VDR agonist-treated mice (median VDR agonist-treated mice: 2.61, range: 1.17 – 4.22; median vehicle-treated mice: 0.94, range: 0.42 – 3.13; $P = 0.0148$) (Figure 22B).

To delineate possible functions of the Foxp3$^+$ cells in the lesional skin the expression of the T_H1 and T_H2 signature cytokines IFNγ and IL-4, known to be involved in skin inflammation[232], was examined. The VDR agonist strongly reduced *Il4* expression in lesional skin by 44.0% (median VDR agonist-treated mice: 0.54, range: 0.34 – 1.05; median vehicle-treated mice: 0.97, range: 0.53 – 1.35; $P = 0.0435$) (Figure 22C). Additionally, *Ifng* expression was reduced by 29.4%, but this did not reach statistical significance (median VDR agonist-treated mice: 0.12, range: 0.05 – 0.24; median vehicle-treated mice: 0.17, range: 0.11 – 0.50; $P = 0.0749$) (Figure 22D). The data show that the selective increase in Foxp3$^+$ cells and *Foxp3* expression may have contributed to reduce T_H1 and T_H2 cytokine expression in lesional skin and subsequent improvement of the eczema.

6.10. Modulation of cytokine and chemokine expression in lesional skin

Having found only minor differences in CD8$^+$ T cell numbers in lesional skin, whereas CD4$^+$ T cells and Foxp3$^+$ cells were increased, chemokines attracting skin-homing CD4$^+$ T cells, in particular CCL22 and CCL27[257-260] were analyzed. *Ccl22* expression (MDC, macrophage-derived chemokine), encoding the ligand for the chemokine receptor CCR4, was 1.8-fold increased in the VDR agonist-treated mice (median VDR agonist-treated mice: 0.28, range: 0.15 – 0.36; median vehicle-treated mice: 0.15, range: 0.07 – 0.39; $P = 0.2523$) but this did not reach statistical significance (Figure 23A). The expression of *Ccl27*, the ligand for the skin-homing receptor CCR10, was 2.1-fold increased in VDR agonist-treated mice compared to vehicle-treated mice (median VDR agonist-treated mice: 0.75, range: 0.4 – 1.01; median vehicle-treated mice: 0.37, range: 0.21 – 0.49; $P = 0.0012$) (Figure 23B).

As TSLP is known to promote T_H2 cell responses[198, 199] and is induced by topical VDR activation[261], its expression in lesion skin was assessed. A 2.4-fold induction in *Tslp* expression was observed upon VDR agonist treatment (median VDR agonist-treated mice: 1.71, range: 1.13 – 2.54; median vehicle-treated mice: 0.71, range: 0.52 – 1.51; $P = 0.0016$) (Figure 23C). In addition, the expression of the proinflammatory cytokine TNFα, involved in AD as well as psoriasis[190, 262], was analyzed in lesional skin of VDR agonist-treated and vehicle-treated mice. *Tnfa* expression was 2.9-fold increased in skin samples of VDR agonist-treated compared to control mice (median VDR agonist-treated mice: 0.004, range:

0.001 – 0.008; median vehicle-treated mice: 0.001, range: 0.0002 – 0.004; $P = 0.0079$) (Figure 23D).

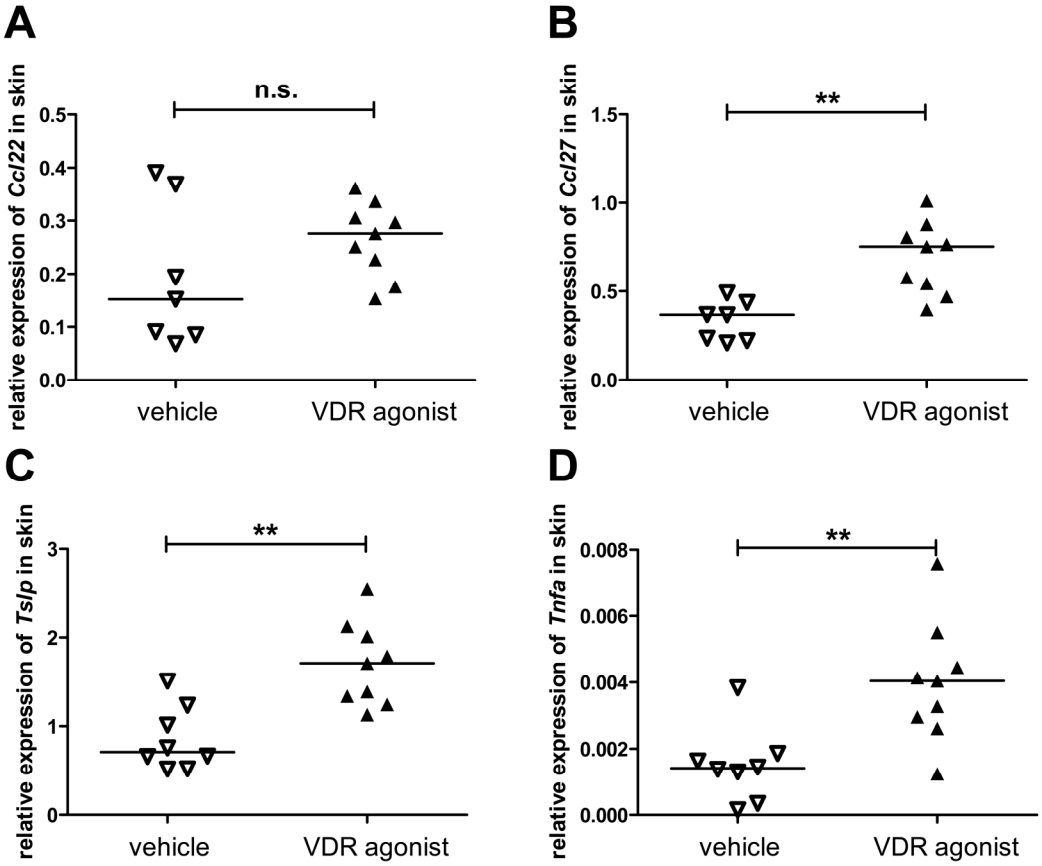

Figure 23 Systemically applied VDR agonist modulates cytokine and chemokine expression in lesional skin. Expression levels of cytokines and chemokines in lesional skin were analyzed by quantitative PCR. The relative expression of CCL22 (*Ccl22*, *A*), CCL27 (*Ccl27*, *B*), TSLP (*Tslp*, *C*), and TNFα (*Tnfa*, *D*) was measured in comparison to the housekeeping gene *Hprt* and is shown as the median for each group (n ≥ 7; $P < 0.01$ **).

6.11. VDR agonist treatment induces barrier and antimicrobial peptide gene expression

The VDR and its ligands are described to induce several genes important for skin barrier function and integrity[209]. Disruption of the skin barrier is involved in the development of allergic skin inflammation, such as AD[194]. Finally, the impact of the VDR agonist on barrier and antimicrobial peptide gene expression in lesional skin was determined. Therapeutic treatment with the VDR agonist robustly induced the expression of the skin barrier genes loricrin (*Lor*), involucrin (*Ivl*), transglutaminase 1 (*Tgm1*) and filaggrin (*Flg*), and the antimicrobial peptides β-defensin 2 (*Defb2*) and β-defensin 3 (*Defb3*) (Figure 24).

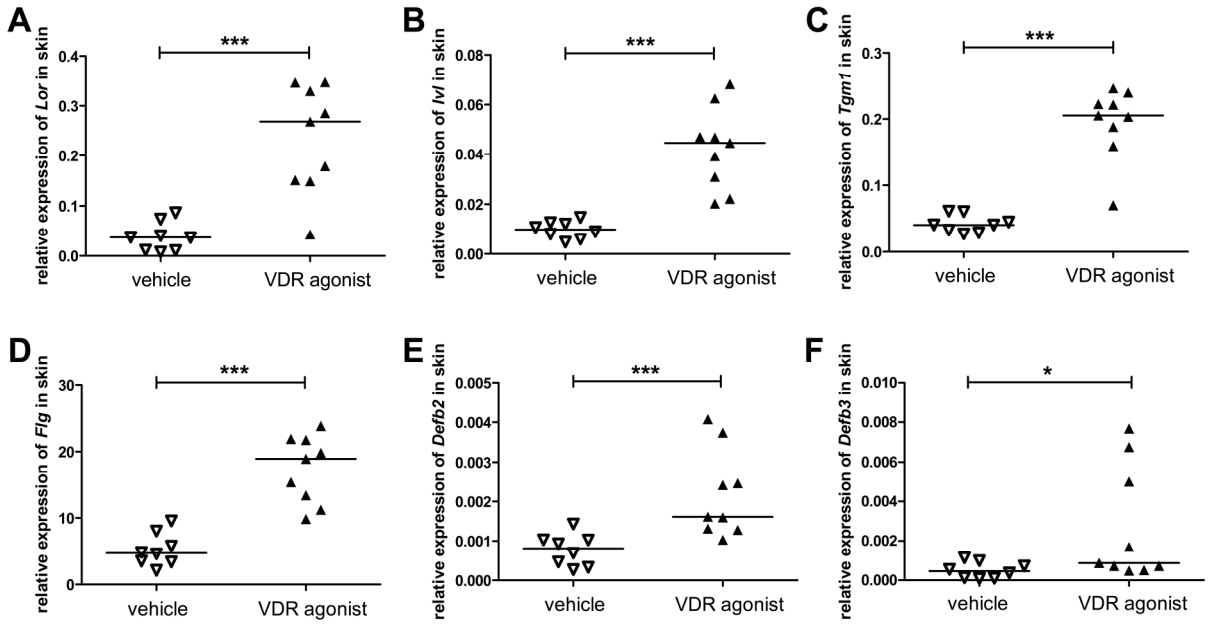

Figure 24 Systemic VDR agonist application induces barrier and antimicrobial peptide genes in lesional skin. Expression levels of skin barrier genes and antimicrobial peptides in lesional skin were analyzed by quantitative PCR. The relative expression of loricrin (*Lor*, *A*), involucrin (*Ivl*, *B*), transglutaminase 1 (*Tgm1*, *C*), filaggrin (*Flg*, *D*), β-defensin 2 (*Defb2*, *E*) and β-defensin 3 (*Defb3*, *F*) was measured in comparison to the housekeeping gene *Hprt* and is shown as the median for each group ($n \geq 8$; $P < 0.05$ *, $P < 0.001$ ***).

Thereby, the highest induction in gene expression of 7.2-fold was examined for loricrin ($P = 0.0003$) and transglutaminase 1 (5-fold, $P < 0.0001$) (Figure 24A and C). Filaggrin (Figure 24D) and involucrin (Figure 24B) were 4.0-fold ($P < 0.0001$) and 4.5-fold ($P < 0.0001$) induced by the VDR agonist in lesional skin. The expression of β-defensin 2 was 2.0-fold ($P = 0.0006$, Figure 24E) and β-defensin 3 0.5-fold ($P = 0.0464$, Figure 24F) increased by the VDR agonist compared to the vehicle control while the overall expression of these antimicrobial peptides was barely detectable.

Taken together, these data show that VDR activation induces the skin barrier and antimicrobial peptide gene expression in allergen-induced AD-like skin lesions.

7. Discussion

7.1. Targeting the VDR inhibits the humoral immune response, preferentially IgE, *in vitro* and *in vivo*

IgE antibodies, normally present at low levels in the plasma, are the key effector molecules of type I allergic diseases[155]. Epidemiological data suggest that vitamin D insufficiency, as defined by less than 30 ng/ml of the circulating precursor 25-hydroxyvitamin D_3, is associated with elevated IgE levels[176]. Other reports show a beneficial association between higher maternal vitamin D intake during pregnancy and protection from childhood asthma and allergic diseases in the offspring[180-182]. In addition, genetic variants at the vitamin D receptor (VDR) locus but also at a number of genes involved in the vitamin D pathway have been shown to be associated with asthma and atopy[263, 264]. In VDR knockout mice, total and antigen-specific IgE serum levels are increased[178]. Taken together, these studies clearly support a potential and probably beneficial role of VDR signaling in IgE dependent diseases. Therefore, the VDR might be a promising target for the prevention and treatment of allergic diseases.

The active metabolite of vitamin D, calcitriol, mediates anti-inflammatory functions on adaptive immune responses including IgE synthesis[39, 40, 144, 254], but its use is limited by hypercalcemic side effects in pharmacological dosages resulting in significant toxicity when systemically applied[265, 266]. Consequently, synthetic analogs with reduced hypercalcemic activity were developed for systemic application. The actions of vitamin D analogs with regard to selective immunomodulatory versus hypercalcemic effects are determined by their interactions with the nuclear VDR, the serum vitamin D binding protein (DBP), the 25-hydroxyvitamin D_3-24-hydroxylase (CYP24A1) and perhaps other metabolizing enzymes, the membrane receptor(s) (MARRS) that mediate the rapid actions of vitamin D compounds, and intracellular vitamin D binding proteins that can facilitate both metabolism and VDR activation[267, 268].

The VDR agonist used in the present study has been recently shown to exert immunomodulatory properties *in vitro* and *in vivo*[226, 269]. The advantage of the VDR agonist in comparison to calcitriol is its dissociated profile (immunomodulatory vs. calcemic)[226]. Thus, the VDR agonist being immunomodulatory while not being hypercalcemic suggests a potential therapeutic window[226].

In line with previous reports, the expression of the VDR in human peripheral B cells was induced by stimulation with anti-CD40/IL-4[144]. More recent results show that the binding affinity of the used VDR agonist to the VDR is in the same range as for calcitriol[226].
The results of the present work show that the VDR agonist activates the VDR in naïve and memory human B cells, reflected by *cyp24a1* gene expression and the induction of CD38 on the surface of $CD19^+$ B cells, analogous to calcitriol[110, 245].
To induce IgE synthesis in human peripheral B cells, monoclonal anti-CD40 antibodies and recombinant human IL-4 were used[270]. Furthermore, these stimuli are known to induce the switch to IgG in human B cells[271], resulting in IgG production[270, 272, 273]. The present results clearly demonstrate that the VDR agonist strongly inhibits the anti-CD40/IL-4 induced IgE production dose-dependently, as shown by reduced secreted IgE and a diminished number of IgE secreting B cells. The efficacy of the VDR agonist to inhibit the IgE response *in vitro* was comparable to that of the natural ligand calcitriol which is in line with a previous report showing the inhibitory effect of calcitriol on the IgE response *in vitro*[144]. In contrast, the use of a carboxylic ester VDR antagonist, binding to the VDR with a potency similar to that of calcitriol[274], showed no impact on stimulated B cell responses. This observation is in accordance with previous reports showing a selective stabilization of an antagonistic conformation of the ligand-binding domain (LBD) of the VDR within VDR-RXR-VDRE complexes by disturbing the helix 12 position[275], which in turn inhibits the interaction of the VDR with coactivator proteins and an induction of transactivation[227, 276]. In conclusion, these data suggest that direct involvement of the liganded VDR and its downstream signaling events are responsible for the observed inhibition of IgE production.

Nevertheless, besides IgE, IgG and to a lesser extent IgA were also reduced following VDR activation. IgA which is considered rather protective in allergic diseases[277, 278] was far less affected in the context of VDR stimulation than IgE. A skewing effect on isotype switching away from IgE towards IgA must have occurred. In fact, the IgA/IgE ratio increased upon VDR activation from 1.0 to 2.2 in human B cells. In comparison to IgA, IgM was as strongly induced as IgG by this kind of stimulation but lacked a statistically significant inhibition upon treatment with the VDR agonist in the same experimental setup.

STAT6-mediated IL-4 and NF-κB-mediated CD40 signaling synergize to induce IgE switching and production[167, 171, 270]. Therefore, critical downstream events were analyzed by applying flow cytometry. The results indicate that the VDR agonist does not have an impact on either STAT6 phosphorylation or IκBα degradation. These data were also confirmed by the observation of the stable IL-4 and CD40-dependent expression of the surface markers

CD23 (FcεRII) and CD69[279-281] upon VDR agonist treatment in the initial phase of B cell activation (data not shown).

Therefore, the question whether other downstream events of anti-CD40/IL-4 signaling, necessary for class switch recombination and terminal differentiation, are impaired by the VDR agonist was addressed. A previous report has shown that VDR activation by calcitriol inhibits the expression of the εGLT[144]. These data were confirmed by a subsequent report showing direct binding of the liganded VDR to the εGL promoter, exhibiting transrepressive activity[145]. However, the assessment of the εGLT expression is only suitable to a limited extent to evaluate IgE production caused by the fact that although IL-4 induces the transcription of germline ε mRNA by CD40-stimulated human B cells, two-thirds of these B cells fail to produce IgE[282].

Thus, more general mechanisms involved in class switch recombination and differentiation were analyzed. At the molecular level, an inhibition of *aicda* expression, encoding the activation-induced cytidine deaminase (AID), which is indispensable for somatic hypermutation and class switching towards IgE but also other subtypes[155, 175], was observed in both B cell subsets. AID deficiency causes the autosomal recessive form of the Hyper-IgM syndrome (HIGM2) which is characterized by normal or elevated serum IgM levels in the absence of IgG, IgA, and IgE[174]. It is likely that the diminished expression of *aicda* may contribute to the decreased immunoglobulin production of all isotypes other than IgM and IgD, as determined here.

As B cell proliferation is another key factor associated with isotype class switching as well as immunoglobulin secretion[253, 272] the impact of VDR activation on proliferation was investigated in more detail. The proliferation of anti-CD40/IL-4 activated human B cells with or without additional mitogenic IL-21 was altered only to a minor extent in the presence of the VDR agonist, which did not reach statistical significance. Nevertheless, such slight antiproliferative effects of the VDR agonist may contribute to the observed reduction in Ig production as well. In fact, a strong link between differentiation of human B cells to IgE-secreting cells and the degree of cell division has been described previously[159]. However, this antiproliferative effect cannot fully explain the remarkable inhibition of immunoglobulin E secretion by 70.1 ± 6.0% and the reduction of other isotypes like IgG and IgA.

Due to the strong reduction in the number of immunoglobulin-secreting cells (ISCs), the differentiation of $CD27^{high}$ $CD38^{+}$ B cells which define *in vitro* generated ISCs that express a transcriptional profile comparable to plasma cells[251, 253] was analyzed. In fact, diminished

frequencies of $CD27^{high}$ $CD38^{+}$ B cells were detected, although CD38 expression, a well-known target of VDR activation[47, 247], was increased on the $CD27^{high}$ subset, suggesting a recent VDR activation in these cells. The clear reduction of this cell population may contribute to the reduced number of Ig secreting cells resulting in a reduced Ig secretion of activated B cells. Such reduction of plasmablasts is in accordance with previous data using calcitriol[46]. Taken together, two potential mechanisms by which the VDR agonist may inhibit the IgE response should be taken into consideration, first the interference with the switching machinery and second a reduction of the differentiation into Ig secreting cells. Unravelling the mechanistic details in their entire complexity and the determination of their relative contribution upon VDR activation will require future experiments. First, the contribution of AID expression to the inhibition of class switching to IgE and other subtypes should be confirmed at the protein level, e.g., by western blotting or intracellular flow cytometry. Furthermore, it has been shown that VDR signaling most likely plays a role in controlling proliferation, supporting the potential role of calcitriol and analogs as preventative and therapeutic anticancer agents[95]. Cheng and colleagues have shown that calcitriol can increase the expression of p27, a cyclin-dependent kinase (CDK) inhibitor, while suppressing cyclin D1, cyclin D2, cyclin T1, cyclin T2, CDK4, and CDK6 in human B cells[46]. Although different stimuli were used in the present work, an effect on cell cycle progression by VDR agonist signaling cannot be excluded. Therefore, the impact of the VDR agonist on the cell cycle progression should be examined by flow cytometric cell cycle analysis and cell cycle-related gene expression. In addition, the impact of VDR signaling on terminal differentiation of B cells into plasma cells, as shown in the present work, should be determined in more detail by gene expression analysis of the key transcription factors X-box-binding protein 1 (XBP1), paired box protein 5 (PAX5), B cell lymphoma 6 (BCL6), B lymphocyte-induced maturation protein 1 (BLIMP1), and interferon-regulatory factor 4 (IRF4). Recent data indicate that the calcitriol-mediated inhibition of IgE production can only be achieved by activating VDRs at the beginning of the B cell culture[144]. This suggests that there might also be a modulation of early cellular responses, e.g. the activation of the mitogen-activated protein kinase (MAPK)-extracellular signal-regulated kinase (ERK) cascade, which may engage in cross talk with the classical VDR pathway to modulate gene expression or directly affect various signaling molecules.

Based on these *in vitro* observations, the immune modulation by the low-calcemic VDR agonist in a murine model of type I sensitization was assessed. As IgE, normally present at low levels in the plasma, is elevated in type I allergic diseases, BALB/c as an IgE high responder mouse strain was used in this study. BALB/c mice are known as a T_H2-biased mouse strain. The susceptibility to develop a T_H2-biased immune response is caused by different gene loci, one of which is the MYC-induced nuclear antigen (*Mina*) locus on chromosome 16[283]. Mina, which binds to the *Il4* promoter in a NFAT-dependent fashion, is expressed at lower levels in BALB/c mice, which leads to a higher IL-4 production influencing the balance between T_H1 and T_H2.

The serum calcium concentration as well as the weight gain over time in VDR agonist-treated mice remained stable. Thus, hypercalcemic or toxic side effects were excluded, clearly supporting the advantage of this low-calcemic VDR agonist in pharmacological doses in accordance with previous data[226]. In contrast, numerous previous studies have shown calcium mobilizing side effects upon calcitriol treatment when it was used at immunomodulatory dosages. For example, Osborn *et al.* observed hypercalcemia (grade I) as the most common side effect of oral treatment with calcitriol[284]. They used a daily dose ranging from 0.5 µg to 1.5 µg calcitriol. Calculated to a normal average body weight of 70 kg, they used between 0.007 µg/kg/d and 0.02 µg/kg/d in their study. In the present study 6 µg/kg/d of the VDR agonist was used. This is a 280-fold excess over the dose of calcitriol used by Osborn and colleagues. Boehm *et al.* showed that a 5-day treatment of 5 µg/kg calcitriol induces significant changes of the serum Ca^{2+}-level in BALB/c mice[285]. As mentioned above, two 5-day treatments with the VDR agonist (6 µg/kg/d) were performed in the present work. The 10% toxic dose (TD10, 10% loss of bodyweight) for calcitriol in SJL mice was determined as 0.1 µg/kg/d[286]. In addition, these authors showed that the maximal dose of calcitriol that could be administered intraperitoneally during 7 consecutive days in NMRI mice, without inducing hypercalcemia, was 0.1 µg/kg/d[286]. Thus, a 60-fold lower amount of the VDR ligand was used here. Furthermore, other studies also show hypercalcemic effects by the administration of calcitriol above 8 µg (0.11 µg/kg, s.c.)[287]. Using a model of rodent contact hypersensitivity (CHS) other studies showed that a therapeutic efficacy of calcitriol occurs at 0.1 µg/kg/d only, i.e. when calcium excretion is already enhanced[226, 288]. In contrast, the VDR agonist exerted full therapeutic efficacy at doses up to 60 µg/kg/d, and even these high doses did not cause hypercalciuria[226]. Thus, a 60-fold excess of the VDR agonist over the immunomodulatory dose of calcitriol that causes hypercalcemic side effects was applied by using 6 µg/kg/d.

In summary, these data evidently indicate the limitation of the systemic treatment with calcitriol *in vivo*. Thus, the great benefit of the VDR agonist used in this study is its dissociated character, clearly separating the calcemic from its immunomodulatory properties.

Importantly, a strong VDR agonist-mediated reduction of the antigen-specific IgE response and to a lesser degree total serum IgE production was observed. Moreover, a reduction of the antigen-specific IgG_1 response was determined, although the extent of suppression was 2.3-fold more pronounced on specific IgE than IgG_1, suggesting a predominance for specific IgE. IgG, however, can also induce the alternative pathway of systemic anaphylaxis in mice and there is some evidence this may also occur in humans, at least when the antigen is available in abundant quantities[289]. Besides anaphylaxis, IgG also plays a role in type II hypersensitivity triggering a variety of autoimmune diseases such as blistering skin diseases like pemphigus vulgaris or bullous pemphigoid, autoimmune hemolytic anemia, autoimmune-mediated chronic urticaria and certain types of drug allergy[290]. Therefore, IgG may contribute to allergic symptoms, at least under certain conditions as well. In addition, the molecular mechanisms that govern murine IgE and IgG_1 production are, in fact, quite similar[228, 291]. Hence, a partially coordinated VDR agonist-induced change in the levels of these two isotypes *in vivo* is not surprising – and it does in no way imply a generalized immune suppression.

There are only a few reports that directly addressed the role of VDR signaling for allergic immune responses *in vivo*, but these support the notion that VDR triggering possesses anti-allergic effects. Accordingly, type I sensitized VDR knockout mice have higher serum IgE concentrations than wild type controls in an allergic asthma model[178], suggesting an important role for VDR signaling in regulating IgE responses *in vivo*. Additionally, allergen-specific immunotherapy has been suggested to be more efficient upon calcitriol treatment[179]. However, so far no data are available on such a concept in human allergic patients.

In conclusion, these data provide evidence that VDR activation by a low-calcemic agonist modulates the humoral immune response including IgE. Thus, targeting vitamin D receptors by low-calcemic ligands may be a promising strategy for novel therapeutic approaches. However, VDR expression and subsequent VDR-mediated immunomodulatory effects are not limited to B cells, but also relevant in T cells, DCs and myeloid cells. Hence, to carefully dissect the *in vivo* effects of VDR activation on the immune response it will be necessary to use animal models in which VDR deficiency is restricted to T cells, B cells and myeloid cells.

7.2. VDR activation ameliorates allergen-induced skin eczema

VDR signaling has been shown to be important not only in the immune system, but also in the skin and in particular keratinocytes[209, 254]. Atopic dermatitis (AD) is a common chronic inflammatory skin disease caused by a combination of epidermal barrier dysfunction and immune dysregulation[190, 194]. Therefore, the effect of VDR activation by the low-calcemic VDR agonist on allergen-induced eczema was delineated in a mouse model of OVA-induced skin inflammation, mimicking AD in humans. Importantly, AD and psoriasis, another inflammatory skin disease, are both skin disorders sharing many similarities. They are common, chronic, inflammatory, and proliferative skin disorders in which both genetic and environmental factors have an important pathogenetic role[190, 192, 262, 292, 293]. In both diseases T cells might play an important role as well. Psoriasis is primarily characterized by T_H1-mediated responses but T_H17 cells have also been implicated in the pathogenesis of psoriasis. In AD, a biphasic T cell response, marked by an acute phase with a T_H2-dominated milieu and a chronic phase with T_H1-mediated responses have been described[190]. Altough the presence of T_H17 cells in AD skin lesions is less prominent than in psoriasis, they might contribute to skin inflammation in AD patients[294, 295]. An additional overlap in both disorders is the impairment of the skin barrier formation[193, 296]. Moreover, topically applied calcitriol and analogs are known to be successful therapeutic approaches in psoriasis[267, 297]. Thus, it is likely that VDR activation by systemic application of low-calcemic agonists may also be of potential benefit for the treatment of AD. To analyze potential modulatory effects on AD, the immunmodulatory, low-calcemic VDR agonist was therapeutically applied in a mouse model of allergen-induced eczema.

Indeed, there was a clear-cut improvement of the symptom severity of AD-like skin lesions, indicated by a decreased clinical skin score. This improvement of the clinical skin score was associated with a decreased transepidermal water loss (TEWL) ([298] and own unpublished data), one critical hallmark to determine barrier function. T cell receptor (TCR)$\alpha\beta^+$ T cells are critical for skin inflammation and T_H2 responses in AD[299]. Furthermore, a role for epidermal $CD8^+$ T cells in the pathogenesis of atopic eczema has been suggested[300, 301]. $CD8^+$ T cell-depleted mice show no skin inflammation upon allergen exposure in a mouse model of allergen-induced AD, indicating a crucial role of $CD8^+$ cells in the development of AD[302]. In accordance with previous results[234], an increase in skin-infiltrating $CD8^+$ T cells by epicutaneous OVA challenge was observed (data not shown), which only slightly decreased upon therapeutic VDR agonist treatment. However, these data suggest that the slightly

decreased numbers of $CD8^+$ T cells are most likely not the major mechanism resulting in the VDR agonist-mediated improvement of the allergen-induced eczema in this mouse model. Nevertheless, a contribution to the decreased skin inflammation by a direct or indirect suppressive effect of VDR activation on $CD8^+$ T cells cannot be completely excluded.

Dermal $CD4^+$ T cell infiltration is known to be involved in skin lesion development[196]. In contrast, the present data show a minor increase of infiltrating $CD4^+$ T cells simultaneously with a clear-cut improvement of the symptom severity upon VDR agonist treatment. $CD4^+$ T cells consist of several subsets of T helper (T_H) cells modulating the immune response[303, 304]. Natural $CD4^+$ $CD25^+$ $Foxp3^+$ T_{reg} cells, comprising 5 – 10% and 1 – 2% of the $CD4^+$ T cell pool in mice and humans[142], and other subtypes of induced T_{reg} cells are known to inhibit both T_H1 and T_H2 cells by reducing their cytokine production or by direct interaction with effector T cells[255, 305, 306]. Importantly, they also have a crucial role in the maintenance of immune homeostasis in normal skin[256]. Thus, it is likely that the minor increase of $CD4^+$ T cells is reflected by the increased number of $Foxp3^+$ T_{reg} cells, observed in the lesional skin of VDR agonist-treated mice.

Recent work has shown the importance of the *forkhead* family transcription factor Foxp3 for the development and function of T_{reg} cells. Scurfy mice, carrying a recessive mutation that involves a 2-bp insertion in the *Foxp3* gene[307], develop an intense multiorgan inflammatory response associated with allergic airway inflammation, a striking hyper-immunoglobulinemia E, eosinophilia, and dysregulated T_H1 and T_H2 cytokine production as well as scaly and inflamed skin resulting in eczema[308]. Moreover, the number of natural T_{regs} is decreased in lesional skin of patients with AD or psoriasis[309]. Another study, using mixed $CCR4^-/Foxp3^-$ bone marrow chimeras, showed that mice lacking $Foxp3^+$ T cells in the skin spontaneously develop a cutaneous inflammatory disease with red, scaly skin, hyperkeratosis, lymphocytic and eosinophilic infiltration, and elevated local levels of IL-4[310]. Thus, the increased number of $Foxp3^+$ cells upon VDR agonist treatment might contribute to the amelioration of AD-like skin lesions by the reduction of *Il4* and *Ifng* expression and/or inhibiting $CD8^+$ T cell priming and activation in the skin. Interestingly, VDR knockout mice fail to increase $Foxp3^+$ T_{regs} in skin-draining lymph nodes (SDLN) following UV-irradiation[142]. Additionally, topical calcitriol or calcipotriol treatment was shown to enhance the suppressive activity of T_{regs} in SDLN whereas calcipotriol caused the expansion of antigen-specific T_{reg} cells[142, 143]. Thereby, keratinocyte expression of receptor activator of NF-κB ligand (RANKL; also known as CD254, OPGL and TRANCE) and its subsequent interaction with RANK seem to be critically involved in the maintenance and/or peripheral

expansion as well as function of $CD4^+$ $CD25^+$ T_{regs} by changing epidermal DC function[142, 311, 312]. It has been shown that the *RankL* gene includes a unique VDRE sequence mediating sensitivity to agonistic VDR activation[313]. Notably, there was a slight increase of *RankL* expression in lesional skin of VDR agonist-treated mice (data not shown) which did not reach statistical significance but it might be of importance in contributing to the increased number of $Foxp3^+$ cells in the skin. Another explanation for increased numbers of $Foxp3^+$ cells in the lesional skin of VDR agonist-treated mice might be a change in the migratory behavior of these cells, induced in the SDLN. Gene expression analyses from VDR agonist-treated mice revealed an up-regulation of CCL22 (MDC, macrophage-derived chemokine) and CCL27 (CTACK, cutaneous T cell-attracting chemokine) in lesional skin. CCL22, expressed by activated T cells and professional APCs such as DCs and monocytes/macrophages, is known to preferentially attract T_{reg} cells expressing the chemokine receptor CCR4[124]. The importance of CCR4 expression on T_{reg} cells has been demonstrated by $CCR4^{-/-}$ mice developing lymphocytic infiltration and severe inflammatory disease in the skin and lungs, accompanied by peripheral lymphadenopathy and increased differentiation of skin-tropic $CD4^+$ $Foxp3^-$ T cells[314]. Recent reports have shown that the exposure of myeloid DCs to calcitriol upregulated the production of CCL22 whereas production of CCL17, the other CCR4 ligand, was reduced[126, 315]. Besides CCR4 and CCR8, cutaneous T cells have been shown to preferentially express CCR10[259]. In addition to cutaneous T cells, T_{reg} subsets in tissues can also express CCR10[316]. Skin-specific CCL27, the ligand for CCR10, is constitutively produced by keratinocytes but can also be induced upon stimulation with TNFα and IL-1β and is thought to mediate the "epidermotropism" (chemoattraction to the epidermis)[259, 260, 317]. A recent report from Sigmundsdottir *et al.* has shown that calcitriol can induce CCR10 expression on activated human T cells whereas calcitriol is capable of, but relatively inefficient at, inducing CCR10 on mouse T cells *in vitro*[45]. Thus, the expression of CCL22 and CCL27 in VDR agonist-treated mice may influence the migration of T_{reg} but also T_{eff} cells by the interaction with CCR4 and CCR10[318, 319].

TSLP, an IL-7-like type I cytokine of the IL-2 "cytokine family", which was induced upon VDR agonist treatment in lesional skin, is known to promote T_H2 cell responses resulting in the promotion of allergic skin inflammation[198, 199]. Blockade of TSLP by a neutralizing antibody and $TSLPR^{-/-}$ mice have shown an inhibition in the development of allergic skin inflammation in a mouse model of AD[320]. Inducible overexpression of TSLP on BALB/c background leads to AD-like changes with a T_H2 cell profile even in the absence of T cells

when crossed with TCRβ$^{-/-}$ mice[321]. These data suggest that TSLP could amplify skin inflammation, independently of T cells. Notably, in addition to a dramatic increase in T_H2 CD4$^+$ T cells expressing the cutaneous homing receptor CCR4, CCL17 but not CCL22 was detectable in inflamed skin of TSLP transgenic mice[321]. This may support the idea of preferential migration of suppressive T_{reg} cells towards CCL22. However, several studies support a potential role for TSLP in the direct promotion of Foxp3$^+$ T_{reg} cell development in the thymus[322-324] but the precise role of TSLP in the development of T_{reg} cells, still remains controversial.

However, Chambon *et al.* reported that topical calcitriol and MC903, another VDR agonist, induce TSLP gene expression[261]. In addition, serum TSLP levels were increased after treatment with topical MC903. The authors show that TSLP promoter regions contain putative VDREs that may bind RXR/VDR heterodimers in mouse keratinocytes and trigger an AD-like phenotype. In their model, TSLP production and skin inflammation induced by VDR activation were T and B cell-independent supporting a direct effect on keratinocytes. Notably, topical application of calcitriol at a dose of 4 nmol (1.7 µg) per ear in their study resulted in mouse death within 7 days. Therefore, 0.25 nmol (0.1 µg) to 0.4 nmol (0.17 µg) of calcitriol were applied. In contrast, in the present study 0.15 µg of the low-calcemic VDR agonist was systemically applied. Thus, it is not likely that such a high local concentration was achieved by the VDR agonist treatment resulting in AD-like skin inflammation by TSLP induction in keratinocytes. Moreover, treatment for mild to moderate psoriasis with calcitriol 3 µg/g ointment was considered as effective and safe with only mild local adverse effects in a small number of patients[297]. These results suggest that there may also be other VDR agonist-mediated compensating mechanisms which modulate various responses and processes resulting in an improved clinical outcome.

A major hallmark of both AD and psoriasis is a change of the epidermal barrier function[193, 296]. The epidermal barrier is ensured by the correct formation and function of the cornified enevelope (CE), consisting of proteins such as filaggrin, involucrin, loricrin and transglutaminases and a complex series of lipids[203]. Its crucial role in AD, however, is underscored by a spontaneous mouse model of AD in which NC/Nga mice show skin barrier abnormalities with increased TEWL and abnormal skin conductivity under conventional conditions, but not under specific pathogen-free conditions, which might predispose these mice to the development of AD-like skin lesions[325]. Furthermore, flaky tail mice (*ft/ft*) are characterized by dry, flaky skin associated with increased TEWL, as observed in patients with AD and filaggrin mutations[326, 327]. In addition, loss-of-function genetic variants of the

filaggrin gene (*FLG*) have been reported to be strong predisposing factors for atopic dermatitis[205-207] whereas others showed a reduced expression of antimicrobial peptides, involucrin and loricrin in AD skin[193, 328]. As numerous functions of the skin, including formation of the permeability barrier, are regulated by VDR signaling[209] the effect of the low-calcemic VDR agonist on the regulation of skin barrier genes was assessed. Indeed, there was a strong increase in the gene expression of the CE-forming proteins filaggrin, loricrin, involucrin and transglutaminase I in skin lesions of VDR agonist-treated mice. Importantly, there are evidences for the direct increase of involucrin and transglutaminase expression by VDR activation in keratinocytes[210-212]. Silencing of the VDR and VDR coactivators led to decreased filaggrin expression and subsequently decreased keratinocyte differentiation[213]. Moreover, data from $VDR^{-/-}$ and $CYP27B1^{-/-}$ ($1\alpha OHase^{-/-}$) mice exhibit a defect in epidermal differentiation as shown by reduced levels of involucrin, filaggrin, and loricrin[214, 215]. In line with these data, VDR agonist treatment in a mouse model of allergen-induced eczema may improve the clinical outcome by modulating the expression of skin barrier genes. Whether these effects are mediated by a direct rather than indirect modulation induced by activated VDRs needs to be elucidated. Notably, it is also likely that VDR agonist treatment affects the cytokine milieu in the skin, as shown by reduced expression of *Il4* and *Ifng* which may contribute to the upregulation of genes forming the CE. This is in accordance with recent results from Kim *et al.* showing that T_H2 cytokines, such as IL-4, downregulate the gene expression of loricrin and involucrin[328]. This was further supported by a report from Sehra *et al.* demonstrating that expression of filaggrin and involucrin is increased in the absence of endogenous IL-4[329].

In contrast to psoriasis patients, demonstrating a marked upregulation of cathelicidin and defensin expression in their skin lesions, AD skin lesions are associated with a decrease in the expression of human β-defensin (HBD) 2 and 3, and LL-37[216, 218]. Expression of T_H2 cytokines, such as IL-4 and IL-13, have been shown to downregulate AMP expression *in vitro* whereas proinflammatory cytokines, such as TNFα, IFNγ, and IL-1β, can increase AMP expression. Thus, the T_H2 dominated cytokine milieu in AD might account for low AMP levels in the skin of AD patients. In the present study, murine β-defensin 2 and 3 were shown to be increased in skin lesions of VDR agonist-treated mice. Likewise, the lower expression level of IL-4 and the increased expression of TNFα in VDR agonist-treated mice may have contributed to the elevated expression of β-defensin 2 and 3. Interestingly, a recent report from Hata *et al.* showed a significant induction of cathelicidin expression in lesional skin of AD patients by oral vitamin D_3 administration[330], suggesting a local effect by systemic

administration of vitamin D_3. However, whether AMP expression in the present work is directly induced by VDR activation or results from alterations of the local cytokine milieu needs to be elucidated. Additionally, the impact of increased AMP expression on the severity of allergen-induced eczema in specific pathogen-free mice remains to be clarified in detail.

Taken together, these data suggest that systemically applied low-calcemic VDR agonists may contribute to the improvement of the clinical outcome in allergen-induced eczema. The detailed mechanisms responsible for the benefical effect of VDR activation on allergen-induced eczema *in vivo* are not completely clear. However, it is likely that a direct modulation of immune cells (e.g. DCs, T cells, B cells) in draining lymph nodes, resulting in changes of the cytokine milieu and/or induction of T_{reg} cells, and/or a local modulation of immune cells and keratinocytes, altering the local cytokine milieu and/or skin barrier function are involved.

In conclusion, the data from the present thesis support the crucial role of VDR signaling in the modulation of immune responses, in particular with regard to B cells, but also other cells like T_{regs} and keratinocytes. Accordingly, VDR activation by low-calcemic agonists may have a promising potential for the therapeutic intervention of immune-mediated disorders.

8. Bibliography

1. Lehmann, B. and Meurer, M., Vitamin D metabolism. *Dermatol Ther*, **2010**. 23(1): p. 2-12.

2. Baeke, F., Etten, E.v., Gysemans, C.*, et al.*, Vitamin D signaling in immune-mediated disorders: Evolving insights and therapeutic opportunities. *Mol Aspects Med*, **2008**. 29(6): p. 376-387.

3. Holick, M.F., MacLaughlin, J.A., Clark, M.B.*, et al.*, Photosynthesis of previtamin D3 in human skin and the physiologic consequences. *Science*, **1980**. 210(4466): p. 203-205.

4. Lehmann, B., Role of the vitamin D3 pathway in healthy and diseased skin - facts, contradictions and hypotheses. *Exp Dermatol*, **2009**. 18(2): p. 97-108.

5. Holick, M.F., The Cutaneous Photosynthesis of Previtamin D3: A Unique Photoendocrine System. *J Invest Dermatol*, **1981**. 77(1): p. 51-58.

6. Bonjour, J.P., Trechsel, U., Granzer, E.*, et al.*, The increase in skin 7-dehydrocholesterol induced by an hypocholesterolemic agent is associated with elevated 25-hydroxyvitamin D3 plasma level. *Pflugers Arch*, **1987**. 410(1): p. 165-168.

7. MacLaughlin, J.A., Anderson, R.R., and Holick, M.F., Spectral character of sunlight modulates photosynthesis of previtamin D3 and its photoisomers in human skin. *Science*, **1982**. 216(4549): p. 1001-1003.

8. Chen, T.C., Chimeh, F., Lu, Z.*, et al.*, Factors that influence the cutaneous synthesis and dietary sources of vitamin D. *Arch Biochem Biophys*, **2007**. 460(2): p. 213-217.

9. Webb, A.R., Decosta, B.R., and Holick, M.F., Sunlight Regulates the Cutaneous Production of Vitamin D3 by Causing Its Photodegradation. *J Clin Endocrinol Metab*, **1989**. 68(5): p. 882-887.

10. Webb, A.R., Kline, L., and Holick, M.F., Influence of Season and Latitude on the Cutaneous Synthesis of Vitamin D3: Exposure to Winter Sunlight in Boston and Edmonton Will Not Promote Vitamin D3 Synthesis in Human Skin. *J Clin Endocrinol Metab*, **1988**. 67(2): p. 373-378.

11. Clemens, T.L., Henderson, S.L., Adams, J.S.*, et al.*, Increased skin pigment reduces the capacity of skin to synthesize vitamin D3. *Lancet*, **1982**. 319(8263): p. 74-76.

12. Matsuoka, L.Y., Ide, L., Wortsman, J.*, et al.*, Sunscreens Suppress Cutaneous Vitamin D3 Synthesis. *J Clin Endocrinol Metab*, **1987**. 64(6): p. 1165-1168.

13. Matsuoka, L.Y., Wortsman, J., Hanifan, N.*, et al.*, Chronic Sunscreen Use Decreases Circulating Concentrations of 25-Hydroxyvitamin D: A Preliminary Study. *Arch Dermatol*, **1988**. 124(12): p. 1802-1804.

14. MacLaughlin, J. and Holick, M.F., Aging decreases the capacity of human skin to produce vitamin D3. *J Clin Invest*, **1985**. 76(4): p. 1536-1538.

15. Holick, M.F., MacLaughlin, J.A., and Doppelt, S.H., Regulation of cutaneous previtamin D3 photosynthesis in man: skin pigment is not an essential regulator. *Science*, **1981**. 211(4482): p. 590-593.

16. Cooke, N.E. and Haddad, J.G., Vitamin D Binding Protein (Gc-Globulin). *Endocr Rev*, **1989**. 10(3): p. 294-307.

17. Haddad, J.G., Plasma vitamin D-binding protein (Gc-globulin): Multiple tasks. *J Steroid Biochem Mol Biol*, **1995**. 53(1-6): p. 579-582.

18. Mizwicki, M.T. and Norman, A.W., Two Key Proteins of the Vitamin D Endocrine System Come Into Crystal Clear Focus: Comparison of the X-ray Structures of the Nuclear Receptor for 1α,25(OH)2 Vitamin D3, the Plasma Vitamin D Binding Protein, and Their Ligands. *J Bone Miner Res*, **2003**. 18(5): p. 795-806.

19. Holick, M.F., Resurrection of vitamin D deficiency and rickets. *J Clin Invest*, **2006**. 116(8): p. 2062-2072.

20. Prosser, D.E. and Jones, G., Enzymes involved in the activation and inactivation of vitamin D. *Trends Biochem Sci*, **2004**. 29(12): p. 664-673.

21. Schuster, I., Cytochromes P450 are essential players in the vitamin D signaling system. *Biochim Biophys Acta*, **2011**. 1814(1): p. 186-199.

22. Ohyama, Y. and Yamasaki, T., Eight cytochrome P450s catalyze vitamin D metabolism. *Front Biosci*, **2004**. 9: p. 3007-3018.

23. Jones, G., Pharmacokinetics of vitamin D toxicity. *Am J Clin Nutr*, **2008**. 88(2): p. 582S-586.

24. Holick, M.F., Vitamin D Deficiency. *N Engl J Med*, **2007**. 357(3): p. 266-281.

25. Holick, M.F., Vitamin D Status: Measurement, Interpretation, and Clinical Application. *Ann Epidemiol*, **2009**. 19(2): p. 73-78.

26. Nykjaer, A., Dragun, D., Walther, D.*, et al.*, An Endocytic Pathway Essential for Renal Uptake and Activation of the Steroid 25-(OH) Vitamin D3. *Cell*, **1999**. 96(4): p. 507-515.

27. Nykjaer, A., Fyfe, J.C., Kozyraki, R.*, et al.*, Cubilin dysfunction causes abnormal metabolism of the steroid hormone 25(OH) vitamin D3. *Proc Natl Acad Sci U S A*, **2001**. 98(24): p. 13895-13900.

28. Christensen, E.I. and Birn, H., Megalin and cubilin: multifunctional endocytic receptors. *Nat Rev Mol Cell Biol*, **2002**. 3(4): p. 258-268.

29. Norman, A.W., Evidence for a new kidney-produced hormone, 1,25-dihydroxycholecalciferol, the proposed biologically active form of vitamin D. *Am J Clin Nutr*, **1971**. 24(11): p. 1346-1351.

30. Holick, M.F., Schnoes, H.K., DeLuca, H.F.*, et al.*, Isolation and identification of 1,25-dihydroxycholecalciferol. A metabolite of vitamin D active in intestine. *Biochemistry*, **1971**. 10(14): p. 2799-2804.

31. Bouillon, R., Carmeliet, G., Verlinden, L.*, et al.*, Vitamin D and Human Health: Lessons from Vitamin D Receptor Null Mice. *Endocr Rev*, **2008**. 29(6): p. 726-776.

32. Kim, M.-S., Fujiki, R., Kitagawa, H.*, et al.*, 1[alpha],25(OH)2D3-induced DNA methylation suppresses the human CYP27B1 gene. *Mol Cell Endocrinol*, **2007**. 265-266: p. 168-173.

33. Norman, A.W., From vitamin D to hormone D: fundamentals of the vitamin D endocrine system essential for good health. *Am J Clin Nutr*, **2008**. 88(2): p. 491S-499.

34. Norman, A.W. and Bouillon, R., Vitamin D nutritional policy needs a vision for the future. *Exp Biol Med*, **2010**. 235(9): p. 1034-1045.

35. Kogawa, M., Findlay, D.M., Anderson, P.H., *et al.*, Osteoclastic Metabolism of 25(OH)-Vitamin D3: A Potential Mechanism for Optimization of Bone Resorption. *Endocrinology*, **2010**. 151(10): p. 4613-4625.

36. Kogawa, M., Anderson, P.H., Findlay, D.M., *et al.*, The metabolism of 25-(OH)vitamin D3 by osteoclasts and their precursors regulates the differentiation of osteoclasts. *J Steroid Biochem Mol Biol*, **2010**. 121(1-2): p. 277-280.

37. Holick, M.F. and Bikle, D.D., Extrarenal Synthesis of 1,25-Dihydroxyvitamin D and Its Health Implications, in *Vitamin D*, Bendich, A., Editor. **2010**, Humana Press. p. 277-295.

38. Stoffels, K., Overbergh, L., Giulietti, A., *et al.*, Immune Regulation of 25-Hydroxyvitamin-D3-1α-Hydroxylase in Human Monocytes. *J Bone Miner Res*, **2006**. 21(1): p. 37-47.

39. Hewison, M., Vitamin D and the intracrinology of innate immunity. *Mol Cell Endocrinol*, **2010**. 321(2): p. 103-111.

40. Adams, J.S. and Hewison, M., Unexpected actions of vitamin D: new perspectives on the regulation of innate and adaptive immunity. *Nat Clin Pract Endocrinol Metab*, **2008**. 4(2): p. 80-90.

41. Liu, P.T., Stenger, S., Li, H., *et al.*, Toll-Like Receptor Triggering of a Vitamin D-Mediated Human Antimicrobial Response. *Science*, **2006**. 311(5768): p. 1770-1773.

42. Hewison, M., Burke, F., Evans, K.N., *et al.*, Extra-renal 25-hydroxyvitamin D3-1[alpha]-hydroxylase in human health and disease. *J Steroid Biochem Mol Biol*, **2007**. 103(3-5): p. 316-321.

43. Hewison, M., Freeman, L., Hughes, S.V., *et al.*, Differential Regulation of Vitamin D Receptor and Its Ligand in Human Monocyte-Derived Dendritic Cells. *J Immunol*, **2003**. 170(11): p. 5382-5390.

44. Fritsche, J., Mondal, K., Ehrnsperger, A., *et al.*, Regulation of 25-hydroxyvitamin D3-1{alpha}-hydroxylase and production of 1{alpha},25-dihydroxyvitamin D3 by human dendritic cells. *Blood*, **2003**. 102(9): p. 3314-3316.

45. Sigmundsdottir, H., Pan, J., Debes, G.F., *et al.*, DCs metabolize sunlight-induced vitamin D3 to 'program' T cell attraction to the epidermal chemokine CCL27. *Nat Immunol*, **2007**. 8(3): p. 285-293.

46. Chen, S., Sims, G.P., Chen, X.X., *et al.*, Modulatory Effects of 1,25-Dihydroxyvitamin D3 on Human B Cell Differentiation. *J Immunol*, **2007**. 179(3): p. 1634-1647.

47. Heine, G., Niesner, U., Chang, H.D., *et al.*, 1,25-dihydroxyvitamin D(3) promotes IL-10 production in human B cells. *Eur J Immunol*, **2008**. 38(8): p. 2210-2218.

48. Baeke, F., Korf, H., Overbergh, L., *et al.*, Human T lymphocytes are direct targets of 1,25-dihydroxyvitamin D3 in the immune system. *J Steroid Biochem Mol Biol*, **2010**. 121(1-2): p. 221-227.

49. Gottfried, E., Rehli, M., Hahn, J., *et al.*, Monocyte-derived cells express CYP27A1 and convert vitamin D3 into its active metabolite. *Biochem Biophys Res Commun*, **2006**. 349(1): p. 209-213.

50. Tokar, E. and Webber, M., Chemoprevention of prostate cancer by cholecalciferol (vitamin D3): 25-hydroxylase (CYP27A1) in human prostate epithelial cells. *Clin Exp Metastasis*, **2005**. 22(3): p. 265-273.

51. Lehmann, B. and Meurer, M., Extrarenal sites of calcitriol synthesis: the particular role of the skin. *Recent Results Cancer Res*, **2003**. 164: p. 135-145.

52. Bikle, D.D., Nemanic, M.K., Gee, E.*, et al.*, 1,25-Dihydroxyvitamin D3 production by human keratinocytes. Kinetics and regulation. *J Clin Invest*, **1986**. 78(2): p. 557-566.

53. Fu, G.K., Lin, D., Zhang, M.Y.H.*, et al.*, Cloning of Human 25-Hydroxyvitamin D-1{alpha}-Hydroxylase and Mutations Causing Vitamin D-Dependent Rickets Type 1. *Mol Endocrinol*, **1997**. 11(13): p. 1961-1970.

54. Flanagan, J.N., Young, M.V., Persons, K.S.*, et al.*, Vitamin D Metabolism in Human Prostate Cells: Implications for Prostate Cancer Chemoprevention by Vitamin D. *Anticancer Res*, **2006**. 26(4A): p. 2567-2572.

55. Lehmann, B., Knuschke, P., and Meurer, M., UVB-induced Conversion of 7-Dehydrocholesterol to 1α,25-Dihydroxyvitamin D3 (Calcitriol) in the Human Keratinocyte Line HaCaT. *Photochem Photobiol*, **2000**. 72(6): p. 803-809.

56. Lehmann, B., Genehr, T., Knuschke, P.*, et al.*, UVB-Induced Conversion of 7-Dehydrocholesterol to 1α,25-Dihydroxyvitamin D3 in an In Vitro Human Skin Equivalent Model. *J Invest Dermatol*, **2001**. 117(5): p. 1179-1185.

57. Schuessler, M., Astecker, N., Herzig, G.*, et al.*, Skin is an autonomous organ in synthesis, two-step activation and degradation of vitamin D3: CYP27 in epidermis completes the set of essential vitamin D3-hydroxylases. *Steroids*, **2001**. 66(3-5): p. 399-408.

58. Lehmann, B., Sauter, W., Knuschke, P.*, et al.*, Demonstration of UVB induced synthesis of 1α,25-dihydroxyvitamin D3 (calcitriol) in human skin by microdialysis. *Arch Dermatol Res*, **2003**. 295(1): p. 24-28.

59. Vantieghem, K., De Haes, P., Bouillon, R.*, et al.*, Dermal fibroblasts pretreated with a sterol Δ^7-reductase inhibitor produce 25-hydroxyvitamin D3 upon UVB irradiation. *J Photochem Photobiol B*, **2006**. 85(1): p. 72-78.

60. Lou, Y.-R., Molnár, F., Peräkylä, M.*, et al.*, 25-Hydroxyvitamin D3 is an agonistic vitamin D receptor ligand. *J Steroid Biochem Mol Biol*, **2010**. 118(3): p. 162-170.

61. Henry, H.L., Taylor, A.N., and Norman, A.W., Response of Chick Parathyroid Glands to the Vitamin D Metabolites, 1,25-Dihydroxycholecalciferol and 24,25-Dihydroxycholecalciferol. *J. Nutr.*, **1977**. 107(10): p. 1918-1926.

62. Uchida, M., Ozono, K., and Pike, W.J., Activation of the human osteocalcin gene by 24R,25-dihydroxyvitamin D_3 occurs through the vitamin d receptor and the vitamin D-responsive element. *J Bone Miner Res*, **1994**. 9(12): p. 1981-1987.

63. Norman, A.W., Okamura, W.H., Bishop, J.E.*, et al.*, Update on biological actions of 1[alpha],25(OH)2-vitamin D3 (rapid effects) and 24R,25(OH)2-vitamin D3. *Mol Cell Endocrinol*, **2002**. 197(1-2): p. 1-13.

64. Haussler, M.R. and Norman, A.W., Chromosomal receptor for a vitamin D metabolite. *Proc Natl Acad Sci U S A*, **1969**. 62(1): p. 155-162.

65. Lawson, D.E. and Wilson, P.W., Intranuclear localization and receptor proteins for 1,25-dihydroxycholecalciferol in chick intestine. *Biochem J*, **1974**. 144(3): p. 573-583.

66. Brumbaugh, P.F. and Haussler, M.R., Specific binding of 1alpha,25-dihydroxycholecalciferol to nuclear components of chick intestine. *J Biol Chem*, **1975**. 250(4): p. 1588-1594.

67. Evans, R.M., The steroid and thyroid hormone receptor superfamily. *Science*, **1988**. 240(4854): p. 889-895.

68. Mangelsdorf, D.J., Thummel, C., Beato, M.*, et al.*, The nuclear receptor superfamily: The second decade. *Cell*, **1995**. 83(6): p. 835-839.

69. Losel, R. and Wehling, M., Nongenomic actions of steroid hormones. *Nat Rev Mol Cell Biol*, **2003**. 4(1): p. 46-55.

70. Mizwicki, M.T. and Norman, A.W., The Vitamin D Sterol-Vitamin D Receptor Ensemble Model Offers Unique Insights into Both Genomic and Rapid-Response Signaling. *Sci. Signal.*, **2009**. 2(75): p. re4.

71. Mizwicki, M.T., Menegaz, D., Yaghmaei, S.*, et al.*, A molecular description of ligand binding to the two overlapping binding pockets of the nuclear vitamin D receptor (VDR): Structure-function implications. *J Steroid Biochem Mol Biol*, **2010**. 121(1-2): p. 98-105.

72. Issa, L.L., Leong, G.M., and Eisman, J.A., Molecular mechanism of vitamin D receptor action. *Inflamm Res*, **1998**. 47(12): p. 451-475.

73. Esteban, L.M., Fong, C., Amr, D.*, et al.*, Promoter-, cell-, and ligand-specific transactivation responses of the VDRB1 isoform. *Biochem Biophys Res Commun*, **2005**. 334(1): p. 9-15.

74. Sunn, K.L., Cock, T.A., Crofts, L.A.*, et al.*, Novel N-Terminal Variant of Human VDR. *Mol Endocrinol*, **2001**. 15(9): p. 1599-1609.

75. Haussler, M.R., Haussler, C.A., Bartik, L.*, et al.*, Vitamin D receptor: molecular signaling and actions of nutritional ligands in disease prevention. *Nutr Rev*, **2008**. 66: p. S98-S112.

76. Aranda, A. and Pascual, A., Nuclear Hormone Receptors and Gene Expression. *Physiol Rev.*, **2001**. 81(3): p. 1269-1304.

77. Germain, P., Staels, B., Dacquet, C.*, et al.*, Overview of Nomenclature of Nuclear Receptors. *Pharmacol Rev*, **2006**. 58(4): p. 685-704.

78. Quack, M., Szafranski, K., Rouvinen, J.*, et al.*, The role of the T-box for the function of the vitamin D receptor on different types of response elements. *Nucleic Acids Res*, **1998**. 26(23): p. 5372-5378.

79. Mizwicki, M.T., Bishop, J.E., and Norman, A.W., Applications of the Vitamin D sterol-Vitamin D receptor (VDR) conformational ensemble model. *Steroids*, **2005**. 70(5-7): p. 464-471.

80. Norman, A.W., Okamura, W.H., Hammond, M.W.*, et al.*, Comparison of 6-s-cis- and 6-s-trans-Locked Analogs of 1{alpha},25-Dihydroxyvitamin D3 Indicates That the 6-s-cis Conformation Is Preferred for Rapid Nongenomic Biological Responses and That Neither 6-s-cis- nor 6-s-trans-Locked Analogs Are Preferred for Genomic Biological Responses. *Mol Endocrinol*, **1997**. 11(10): p. 1518-1531.

81. Norman, A.W., Henry, H.L., Bishop, J.E., *et al.*, Different shapes of the steroid hormone 1[alpha],25(OH)2-vitamin D3 act as agonists for two different receptors in the vitamin D endocrine system to mediate genomic and rapid responses. *Steroids*, **2001**. 66(3-5): p. 147-158.

82. Mizwicki, M.T., Keidel, D., Bula, C.M., *et al.*, Identification of an alternative ligand-binding pocket in the nuclear vitamin D receptor and its functional importance in 1α,25(OH)2-vitamin D3 signaling. *Proc Natl Acad Sci U S A*, **2004**. 101(35): p. 12876-12881.

83. Norman, A.W., Bishop, J.E., Bula, C.M., *et al.*, Molecular tools for study of genomic and rapid signal transduction responses initiated by 1[alpha],25(OH)2-vitamin D3. *Steroids*, **2002**. 67(6): p. 457-466.

84. Hsieh, J.-C., Shimizu, Y., Minoshima, S., *et al.*, Novel nuclear localization signal between the two DNA-binding zinc fingers in the human vitamin D receptor. *J Cell Biochem*, **1998**. 70(1): p. 94-109.

85. Michigami, T., Suga, A., Yamazaki, M., *et al.*, Identification of Amino Acid Sequence in the Hinge Region of Human Vitamin D Receptor That Transfers a Cytosolic Protein to the Nucleus. *J Biol Chem*, **1999**. 274(47): p. 33531-33538.

86. Hsieh, J.C., Jurutka, P.W., Galligan, M.A., *et al.*, Human vitamin D receptor is selectively phosphorylated by protein kinase C on serine 51, a residue crucial to its trans-activation function. *Proc Natl Acad Sci U S A*, **1991**. 88(20): p. 9315-9319.

87. Jurutka, P.W., Hsieh, J.C., MacDonald, P.N., *et al.*, Phosphorylation of serine 208 in the human vitamin D receptor. The predominant amino acid phosphorylated by casein kinase II, in vitro, and identification as a significant phosphorylation site in intact cells. *J Biol Chem*, **1993**. 268(9): p. 6791-6799.

88. Desvergne, B. and Gerald, L., RXR: From Partnership to Leadership in Metabolic Regulations, in *Vitamins & Hormones*. **2007**, Academic Press. p. 1-32.

89. Mizwicki, M.T., Bula, C.M., Mahinthichaichan, P., *et al.*, On the Mechanism Underlying (23S)-25-Dehydro-1α(OH)-vitamin D3-26,23-lactone Antagonism of hVDRwt Gene Activation and Its Switch to a Superagonist. *J Biol Chem*, **2009**. 284(52): p. 36292-36301.

90. Kim, M.-s., Fujiki, R., Murayama, A., *et al.*, 1{alpha},25(OH)2D3-Induced Transrepression by Vitamin D Receptor through E-Box-Type Elements in the Human Parathyroid Hormone Gene Promoter. *Mol Endocrinol*, **2007**. 21(2): p. 334-342.

91. Kato, S., Kim, M.S., Yamaoka, K., *et al.*, Mechanisms of transcriptional repression by 1,25(OH)2 vitamin D. *Curr Opin Nephrol Hypertens*, **2007**. 16(4): p. 297-304.

92. Huhtakangas, J.A., Olivera, C.J., Bishop, J.E., *et al.*, The Vitamin D Receptor Is Present in Caveolae-Enriched Plasma Membranes and Binds 1{alpha},25(OH)2-Vitamin D3 in Vivo and in Vitro. *Mol Endocrinol*, **2004**. 18(11): p. 2660-2671.

93. Buitrago, C. and Boland, R., Caveolae and caveolin-1 are implicated in 1α,25(OH)2-vitamin D3-dependent modulation of Src, MAPK cascades and VDR localization in skeletal muscle cells. *J Steroid Biochem Mol Biol*, **2010**. 121(1-2): p. 169-175.

94. Patel, H.H., Murray, F., and Insel, P.A., Caveolae as Organizers of Pharmacologically Relevant Signal Transduction Molecules. *Annu Rev Pharmacol Toxicol*, **2008**. 48(1): p. 359-391.

95. Deeb, K.K., Trump, D.L., and Johnson, C.S., Vitamin D signalling pathways in cancer: potential for anticancer therapeutics. *Nat Rev Cancer*, **2007**. 7(9): p. 684-700.

96. Nemere, I., Safford, S.E., Rohe, B.*, et al.*, Identification and characterization of 1,25D3-membrane-associated rapid response, steroid (1,25D3-MARRS) binding protein. *J Steroid Biochem Mol Biol*, **2004**. 89-90: p. 281-285.

97. Nemere, I., Farach-Carson, M.C., Rohe, B.*, et al.*, Ribozyme knockdown functionally links a 1,25(OH)2D3 membrane binding protein (1,25D3-MARRS) and phosphate uptake in intestinal cells. *Proc Natl Acad Sci U S A*, **2004**. 101(19): p. 7392-7397.

98. Rohe, B., Safford, S.E., Nemere, I.*, et al.*, Identification and characterization of 1,25D3-membrane-associated rapid response, steroid (1,25D3-MARRS)-binding protein in rat IEC-6 cells. *Steroids*, **2005**. 70(5-7): p. 458-463.

99. Wu, W., Beilhartz, G., Roy, Y.*, et al.*, Nuclear translocation of the 1,25D3-MARRS (membrane associated rapid response to steroids) receptor protein and NF[kappa]B in differentiating NB4 leukemia cells. *Exp Cell Res*, **2010**. 316(7): p. 1101-1108.

100. Coppari, S., Altieri, F., Ferraro, A.*, et al.*, Nuclear localization and DNA interaction of protein disulfide isomerase ERp57 in mammalian cells. *J Cell Biochem*, **2002**. 85(2): p. 325-333.

101. Coe, H. and Michalak, M., ERp57, a multifunctional endoplasmic reticulum resident oxidoreductase. *Int J Biochem Cell Biol*, **2010**. 42(6): p. 796-799.

102. Bouillon, R., Bischoff-Ferrari, H., and Willett, W., Vitamin D and Health: Perspectives From Mice and Man. *J Bone Miner Res*, **2008**. 23(7): p. 974-979.

103. Verstuyf, A., Carmeliet, G., Bouillon, R.*, et al.*, Vitamin D: a pleiotropic hormone. *Kidney Int*, **2010**. 78(2): p. 140-145.

104. Baeke, F., Takiishi, T., Korf, H.*, et al.*, Vitamin D: modulator of the immune system. *Curr Opin Pharmacol*, **2010**. 10(4): p. 482-496.

105. Adams, J.S. and Hewison, M., Update in Vitamin D. *J Clin Endocrinol Metab*, **2010**. 95(2): p. 471-478.

106. Brennan, A., Katz, D.R., Nunn, J.D.*, et al.*, Dendritic cells from human tissues express receptors for the immunoregulatory vitamin D3 metabolite, dihydroxycholecalciferol. *Immunology*, **1987**. 61(4): p. 457-461.

107. Kreutz, M., Andreesen, R., Krause, S.W.*, et al.*, 1,25-dihydroxyvitamin D3 production and vitamin D3 receptor expression are developmentally regulated during differentiation of human monocytes into macrophages. *Blood*, **1993**. 82(4): p. 1300-1307.

108. Babina, M., Krautheim, M., Grützkau, A.*, et al.*, Human Leukemic (HMC-1) Mast Cells Are Responsive to 1[alpha],25-Dihydroxyvitamin D3: Selective Promotion of ICAM-3 Expression and Constitutive Presence of Vitamin D3 Receptor. *Biochem Biophys Res Commun*, **2000**. 273(3): p. 1104-1110.

109. Veldman, C.M., Cantorna, M.T., and DeLuca, H.F., Expression of 1,25-Dihydroxyvitamin D3 Receptor in the Immune System. *Arch Biochem Biophys*, **2000**. 374(2): p. 334-338.

110. Morgan, J.W., Morgan, D.M., Lasky, S.R.*, et al.*, Requirements for induction of vitamin D-mediated gene regulation in normal human B lymphocytes. *J Immunol*, **1996**. 157(7): p. 2900-2908.

111. Provvedini, D.M., Tsoukas, C.D., Deftos, L.J.*, et al.*, 1,25-dihydroxyvitamin D3 receptors in human leukocytes. *Science*, **1983**. 221(4616): p. 1181-1183.

112. Krutzik, S.R., Hewison, M., Liu, P.T.*, et al.*, IL-15 Links TLR2/1-Induced Macrophage Differentiation to the Vitamin D-Dependent Antimicrobial Pathway. *J Immunol*, **2008**. 181(10): p. 7115-7120.

113. Gombart, A.F., Borregaard, N., and Koeffler, H.P., Human cathelicidin antimicrobial peptide (CAMP) gene is a direct target of the vitamin D receptor and is strongly up-regulated in myeloid cells by 1,25-dihydroxyvitamin D3. *FASEB J*, **2005**. 19(9): p. 1067-1077.

114. Wang, T.-T., Nestel, F.P., Bourdeau, V.*, et al.*, Cutting Edge: 1,25-Dihydroxyvitamin D3 Is a Direct Inducer of Antimicrobial Peptide Gene Expression. *J Immunol*, **2004**. 173(5): p. 2909-2912.

115. Liu, P.T., Schenk, M., Walker, V.P.*, et al.*, Convergence of IL-1beta and VDR activation pathways in human TLR2/1-induced antimicrobial responses. *PLoS ONE*, **2009**. 4(6): p. e5810.

116. Wang, T.-T., Tavera-Mendoza, L.E., Laperriere, D.*, et al.*, Large-Scale in Silico and Microarray-Based Identification of Direct 1,25-Dihydroxyvitamin D3 Target Genes. *Mol Endocrinol*, **2005**. 19(11): p. 2685-2695.

117. Almerighi, C., Sinistro, A., Cavazza, A.*, et al.*, 1[alpha],25-Dihydroxyvitamin D3 inhibits CD40L-induced pro-inflammatory and immunomodulatory activity in Human Monocytes. *Cytokine*, **2009**. 45(3): p. 190-197.

118. D'Ambrosio, D., Cippitelli, M., Cocciolo, M.G.*, et al.*, Inhibition of IL-12 production by 1,25-dihydroxyvitamin D3. Involvement of NF-kappaB downregulation in transcriptional repression of the p40 gene. *J Clin Invest*, **1998**. 101(1): p. 252-262.

119. Giulietti, A., van Etten, E., Overbergh, L.*, et al.*, Monocytes from type 2 diabetic patients have a pro-inflammatory profile: 1,25-Dihydroxyvitamin D3 works as anti-inflammatory. *Diabetes Res Clin Pract*, **2007**. 77(1): p. 47-57.

120. Penna, G. and Adorini, L., 1α,25-Dihydroxyvitamin D3 Inhibits Differentiation, Maturation, Activation, and Survival of Dendritic Cells Leading to Impaired Alloreactive T Cell Activation. *J Immunol*, **2000**. 164(5): p. 2405-2411.

121. Pedersen, A.W., Holmstrom, K., Jensen, S.S.*, et al.*, Phenotypic and functional markers for 1alpha,25-dihydroxyvitamin D(3)-modified regulatory dendritic cells. *Clin Exp Immunol*, **2009**. 157(1): p. 48-59.

122. Berer, A., Stöckl, J., Majdic, O.*, et al.*, 1,25-Dihydroxyvitamin D3 inhibits dendritic cell differentiation and maturation in vitro. *Exp Hematol*, **2000**. 28(5): p. 575-583.

123. Bartels, L.E., Hvas, C.L., Agnholt, J.*, et al.*, Human dendritic cell antigen presentation and chemotaxis are inhibited by intrinsic 25-hydroxy vitamin D activation. *Int Immunopharmacol*, **2010**. 10(8): p. 922-928.

124. Iellem, A., Mariani, M., Lang, R.*, et al.*, Unique Chemotactic Response Profile and Specific Expression of Chemokine Receptors Ccr4 and Ccr8 by Cd4+Cd25+ Regulatory T Cells. *J Exp Med*, **2001**. 194(6): p. 847-854.

125. Hirahara, K., Liu, L., Clark, R.A., *et al.*, The Majority of Human Peripheral Blood CD4+CD25highFoxp3+ Regulatory T Cells Bear Functional Skin-Homing Receptors. *J Immunol*, **2006**. 177(7): p. 4488-4494.

126. Penna, G., Amuchastegui, S., Giarratana, N., *et al.*, 1,25-Dihydroxyvitamin D3 Selectively Modulates Tolerogenic Properties in Myeloid but Not Plasmacytoid Dendritic Cells. *J Immunol*, **2007**. 178(1): p. 145-153.

127. Lombardi, G., Riffo-Vasquez, Y., Adorini, L., *et al.*, Induction of Tolerogenic Dendritic Cells by Vitamin D Receptor Agonists, in *Dendritic Cells*, Starke, K., Born, G.V.R., Eichelbaum, M., Ganten, D., Hofmann, F., Kobilka, B., Rosenthal, W., and Rubanyi, G., Editors. **2009**, Springer Berlin Heidelberg. p. 251-273.

128. Rigby, W.F., Stacy, T., and Fanger, M.W., Inhibition of T lymphocyte mitogenesis by 1,25-dihydroxyvitamin D3 (calcitriol). *J Clin Invest*, **1984**. 74(4): p. 1451-1455.

129. Alroy, I., Towers, T.L., and Freedman, L.P., Transcriptional repression of the interleukin-2 gene by vitamin D3: direct inhibition of NFATp/AP-1 complex formation by a nuclear hormone receptor. *Mol. Cell. Biol.*, **1995**. 15(10): p. 5789-5799.

130. Lemire, J.M., Adams, J.S., Kermani-Arab, V., *et al.*, 1,25-Dihydroxyvitamin D3 suppresses human T helper/inducer lymphocyte activity in vitro. *J Immunol*, **1985**. 134(5): p. 3032-3035.

131. Cippitelli, M. and Santoni, A., Vitamin D3: a transcriptional modulator of the interferon-γ gene. *Eur J Immunol*, **1998**. 28(10): p. 3017-3030.

132. Jeffery, L.E., Burke, F., Mura, M., *et al.*, 1,25-Dihydroxyvitamin D3 and IL-2 Combine to Inhibit T Cell Production of Inflammatory Cytokines and Promote Development of Regulatory T Cells Expressing CTLA-4 and FoxP3. *J Immunol*, **2009**. 183(9): p. 5458-5467.

133. Meehan, M.A., Kerman, R.H., and Lemire, J.M., 1,25-Dihydroxyvitamin D3 enhances the generation of nonspecific suppressor cells while inhibiting the induction of cytotoxic cells in a human MLR. *Cell Immunol*, **1992**. 140(2): p. 400-409.

134. Urry, Z., Xystrakis, E., Richards, D.F., *et al.*, Ligation of TLR9 induced on human IL-10-secreting Tregs by 1alpha,25-dihydroxyvitamin D3 abrogates regulatory function. *J Clin Invest*, **2009**. 119(2): p. 387-398.

135. Matilainen, J.M., Räsänen, A., Gynther, P., *et al.*, The genes encoding cytokines IL-2, IL-10 and IL-12B are primary 1[alpha],25(OH)2D3 target genes. *J Steroid Biochem Mol Biol*, **2010**. 121(1-2): p. 142-145.

136. Mahon, B.D., Wittke, A., Weaver, V., *et al.*, The targets of vitamin D depend on the differentiation and activation status of CD4 positive T cells. *J Cell Biochem*, **2003**. 89(5): p. 922-932.

137. Boonstra, A., Barrat, F.J., Crain, C., *et al.*, 1{alpha},25-Dihydroxyvitamin D3 Has a Direct Effect on Naive CD4+ T Cells to Enhance the Development of Th2 Cells. *J Immunol*, **2001**. 167(9): p. 4974-4980.

138. Staeva-Vieira, T.P. and Freedman, L.P., 1,25-Dihydroxyvitamin D3 Inhibits IFN-{gamma} and IL-4 Levels During In Vitro Polarization of Primary Murine CD4+ T Cells. *J Immunol*, **2002**. 168(3): p. 1181-1189.

139. Barrat, F.J., Cua, D.J., Boonstra, A.*, et al.*, In Vitro Generation of Interleukin 10-producing Regulatory CD4+ T Cells Is Induced by Immunosuppressive Drugs and Inhibited by T Helper Type 1 (Th1)- and Th2-inducing Cytokines. *J. Exp. Med.*, **2002**. 195(5): p. 603-616.

140. Gregori, S., Casorati, M., Amuchastegui, S.*, et al.*, Regulatory T Cells Induced by 1α,25-Dihydroxyvitamin D3 and Mycophenolate Mofetil Treatment Mediate Transplantation Tolerance. *J Immunol*, **2001**. 167(4): p. 1945-1953.

141. Gregori, S., Giarratana, N., Smiroldo, S.*, et al.*, A 1α,25-Dihydroxyvitamin D3 Analog Enhances Regulatory T-Cells and Arrests Autoimmune Diabetes in NOD Mice. *Diabetes*, **2002**. 51(5): p. 1367-1374.

142. Ghoreishi, M., Bach, P., Obst, J.*, et al.*, Expansion of Antigen-Specific Regulatory T Cells with the Topical Vitamin D Analog Calcipotriol. *J Immunol*, **2009**. 182(10): p. 6071-6078.

143. Gorman, S., Kuritzky, L.A., Judge, M.A.*, et al.*, Topically applied 1,25-dihydroxyvitamin D3 enhances the suppressive activity of CD4+CD25+ cells in the draining lymph nodes. *J Immunol*, **2007**. 179(9): p. 6273-6283.

144. Heine, G., Anton, K., Henz, B.M.*, et al.*, 1alpha,25-dihydroxyvitamin D3 inhibits anti-CD40 plus IL-4-mediated IgE production in vitro. *Eur J Immunol*, **2002**. 32(12): p. 3395-3404.

145. Milovanovic, M., Heine, G., Hallatschek, W.*, et al.*, Vitamin D receptor binds to the [epsilon] germline gene promoter and exhibits transrepressive activity. *J Allergy Clin Immunol*, **2010**. 126(5): p. 1016-1023.e1014.

146. Shirakawa, A.-K., Nagakubo, D., Hieshima, K.*, et al.*, 1,25-Dihydroxyvitamin D3 Induces CCR10 Expression in Terminally Differentiating Human B Cells. *J Immunol*, **2008**. 180(5): p. 2786-2795.

147. Galli, S.J., Tsai, M., and Piliponsky, A.M., The development of allergic inflammation. *Nature*, **2008**. 454(7203): p. 445-454.

148. Cookson, W., The immunogenetics of asthma and eczema: a new focus on the epithelium. *Nat Rev Immunol*, **2004**. 4(12): p. 978-988.

149. Vercelli, D., Discovering susceptibility genes for asthma and allergy. *Nat Rev Immunol*, **2008**. 8(3): p. 169-182.

150. Kuriakose, J.S. and Miller, R.L., Environmental epigenetics and allergic diseases: recent advances. *Clin Exp Allergy*, **2010**. 40(11): p. 1602-1610.

151. Martino, D.J. and Prescott, S.L., Silent mysteries: epigenetic paradigms could hold the key to conquering the epidemic of allergy and immune disease. *Allergy*, **2010**. 65(1): p. 7-15.

152. Okada, H., Kuhn, C., Feillet, H.*, et al.*, The 'hygiene hypothesis' for autoimmune and allergic diseases: an update. *Clin Exp Immunol*, **2010**. 160(1): p. 1-9.

153. Tesse, R., Pandey, R.C., and Kabesch, M., Genetic variations in toll-like receptor pathway genes influence asthma and atopy. *Allergy*, **2010**(DOI: 10.1111/j.1398-9995.2010.02489.x).

154. Paul, W.E. and Zhu, J., How are TH2-type immune responses initiated and amplified? *Nat Rev Immunol*, **2010**. 10(4): p. 225-235.

155. Geha, R.S., Jabara, H.H., and Brodeur, S.R., The regulation of immunoglobulin E class-switch recombination. *Nat Rev Immunol*, **2003**. 3(9): p. 721-732.

156. Minton, K., Allergy and Asthma: What 'drives' IL-4 versus IL-13 signalling? *Nat Rev Immunol*, **2008**. 8(3): p. 166-167.

157. Hebenstreit, D., Wirnsberger, G., Horejs-Hoeck, J.*, et al.*, Signaling mechanisms, interaction partners, and target genes of STAT6. *Cytokine Growth Factor Rev*, **2006**. 17(3): p. 173-188.

158. Kobayashi, S., Haruo, N., Sugane, K.*, et al.*, Interleukin-21 stimulates B-cell immunoglobulin E synthesis in human beings concomitantly with activation-induced cytidine deaminase expression and differentiation into plasma cells. *Hum Immunol*, **2009**. 70(1): p. 35-40.

159. Avery, D.T., Ma, C.S., Bryant, V.L.*, et al.*, STAT3 is required for IL-21-induced secretion of IgE from human naive B cells. *Blood*, **2008**. 112(5): p. 1784-1793.

160. Bishop, G.A., The multifaceted roles of TRAFs in the regulation of B-cell function. *Nat Rev Immunol*, **2004**. 4(10): p. 775-786.

161. Takeda, K., Tanaka, T., Shi, W.*, et al.*, Essential role of Stat6 in IL-4 signalling. *Nature*, **1996**. 380(6575): p. 627-630.

162. Snapper, C.M., Zelazowski, P., Rosas, F.R.*, et al.*, B cells from p50/NF-kappa B knockout mice have selective defects in proliferation, differentiation, germ-line CH transcription, and Ig class switching. *J Immunol*, **1996**. 156(1): p. 183-191.

163. Sha, W.C., Liou, H.-C., Tuomanen, E.I.*, et al.*, Targeted disruption of the p50 subunit of NF-[kappa]B leads to multifocal defects in immune responses. *Cell*, **1995**. 80(2): p. 321-330.

164. Dedeoglu, F., Horwitz, B., Chaudhuri, J.*, et al.*, Induction of activation-induced cytidine deaminase gene expression by IL-4 and CD40 ligation is dependent on STAT6 and NF{kappa}B. *Int Immunol*, **2004**. 16(3): p. 395-404.

165. Messner, B., Stutz, A.M., Albrecht, B.*, et al.*, Cooperation of binding sites for STAT6 and NF kappa B/rel in the IL-4- induced up-regulation of the human IgE germline promoter. *J Immunol*, **1997**. 159(7): p. 3330-3337.

166. Shen, C.-H. and Stavnezer, J., Interaction of Stat6 and NF-kappa B: Direct Association and Synergistic Activation of Interleukin-4-Induced Transcription. *Mol Cell Biol*, **1998**. 18(6): p. 3395-3404.

167. Iciek, L.A., Delphin, S.A., and Stavnezer, J., CD40 cross-linking induces Ig epsilon germline transcripts in B cells via activation of NF-kappaB: synergy with IL-4 induction. *J Immunol*, **1997**. 158(10): p. 4769-4779.

168. Gould, H.J., Beavil, R.L., and Vercelli, D., IgE isotype determination: {varepsilon}-germline gene transcription, DNA recombination and B-cell differentiation. *Br Med Bull*, **2000**. 56(4): p. 908-924.

169. Stavnezer, J., Guikema, J.E.J., and Schrader, C.E., Mechanism and Regulation of Class Switch Recombination. *Annu Rev Immunol*, **2008**. 26(1): p. 261-292.

170. Hellman, L., Regulation of IgE homeostasis, and the identification of potential targets for therapeutic intervention. *Biomed Pharmacother*, **2007**. 61(1): p. 34-49.

171. Gauchat, J.F., Lebman, D.A., Coffman, R.L.*, et al.*, Structure and expression of germline epsilon transcripts in human B cells induced by interleukin 4 to switch to IgE production. *J Exp Med*, **1990**. 172(2): p. 463-473.

172. Oettgen, H.C., Regulation of the IgE isotype switch: new insights on cytokine signals and the functions of [var epsilon] germline transcripts. *Curr Opin Immunol*, **2000**. 12(6): p. 618-623.

173. Chaudhuri, J. and Alt, F.W., Class-switch recombination: interplay of transcription, DNA deamination and DNA repair. *Nat Rev Immunol*, **2004**. 4(7): p. 541-552.

174. Revy, P., Muto, T., Levy, Y.*, et al.*, Activation-Induced Cytidine Deaminase (AID) Deficiency Causes the Autosomal Recessive Form of the Hyper-IgM Syndrome (HIGM2). *Cell*, **2000**. 102(5): p. 565-575.

175. Muramatsu, M., Kinoshita, K., Fagarasan, S.*, et al.*, Class Switch Recombination and Hypermutation Require Activation-Induced Cytidine Deaminase (AID), a Potential RNA Editing Enzyme. *Cell*, **2000**. 102(5): p. 553-563.

176. Brehm, J.M., Celedon, J.C., Soto-Quiros, M.E.*, et al.*, Serum Vitamin D Levels and Markers of Severity of Childhood Asthma in Costa Rica. *Am J Respir Crit Care Med*, **2009**. 179(9): p. 765-771.

177. Hypponen, E., Berry, D.J., Wjst, M.*, et al.*, Serum 25-hydroxyvitamin D and IgE - a significant but nonlinear relationship. *Allergy*, **2009**. 64(4): p. 613-620.

178. Wittke, A., Weaver, V., Mahon, B.D.*, et al.*, Vitamin D Receptor-Deficient Mice Fail to Develop Experimental Allergic Asthma. *J Immunol*, **2004**. 173(5): p. 3432-3436.

179. Taher, Y.A., van Esch, B.C.A.M., Hofman, G.A.*, et al.*, 1{alpha},25-Dihydroxyvitamin D3 Potentiates the Beneficial Effects of Allergen Immunotherapy in a Mouse Model of Allergic Asthma: Role for IL-10 and TGF-{beta}. *J Immunol*, **2008**. 180(8): p. 5211-5221.

180. Erkkola, M., Kaila, M., Nwaru, B.I.*, et al.*, Maternal vitamin D intake during pregnancy is inversely associated with asthma and allergic rhinitis in 5-year-old children. *Clin Exp Allergy*, **2009**. 39(6): p. 875-882.

181. Camargo, C.A., Jr., Rifas-Shiman, S.L., Litonjua, A.A.*, et al.*, Maternal intake of vitamin D during pregnancy and risk of recurrent wheeze in children at 3 y of age. *Am J Clin Nutr*, **2007**. 85(3): p. 788-795.

182. Devereux, G., Litonjua, A.A., Turner, S.W.*, et al.*, Maternal vitamin D intake during pregnancy and early childhood wheezing. *Am J Clin Nutr*, **2007**. 85(3): p. 853-859.

183. Hyppönen, E., Sovio, U., Wjst, M.*, et al.*, Infant Vitamin D Supplementation and Allergic Conditions in Adulthood: Northern Finland Birth Cohort 1966. *Ann N Y Acad Sci*, **2004**. 1037(1): p. 84-95.

184. Kull, I., Bergström, A., Melén, E.*, et al.*, Early-life supplementation of vitamins A and D, in water-soluble form or in peanut oil, and allergic diseases during childhood. *J Allergy Clin Immunol*, **2006**. 118(6): p. 1299-1304.

185. Oren, E., Banerji, A., and Camargo Jr, C.A., Vitamin D and atopic disorders in an obese population screened for vitamin D deficiency. *J Allergy Clin Immunol*, **2008**. 121(2): p. 533-534.

186. Peroni, D.G., Piacentini, G.L., Cametti, E.*, et al.*, Correlation between serum 25 (OH)-vitamin D levels and severity of atopic dermatitis in children. *Br J Dermatol*, **2010**: p. 10.1111/j.1365-2133.2010.10147.x.

187. Sidbury, R., Sullivan, A.F., Thadhani, R.I., *et al.*, Randomized controlled trial of vitamin D supplementation for winter-related atopic dermatitis in Boston: a pilot study. *Br J Dermatol*, **2008**. 159(1): p. 245-247.

188. Vähävihu, K., Ylianttila, L., Salmelin, R., *et al.*, Heliotherapy improves vitamin D balance and atopic dermatitis. *Br J Dermatol*, **2008**. 158(6): p. 1323-1328.

189. Vähävihu, K., Ala-Houhala, M., Peric, M., *et al.*, Narrowband ultraviolet B treatment improves vitamin D balance and alters antimicrobial peptide expression in skin lesions of psoriasis and atopic dermatitis. *Br J Dermatol*, **2010**. 163(2): p. 321-328.

190. Bieber, T., Atopic Dermatitis. *N Engl J Med*, **2008**. 358(14): p. 1483-1494.

191. Leung, D.Y.M., Boguniewicz, M., Howell, M.D., *et al.*, New insights into atopic dermatitis. *J Clin Invest*, **2004**. 113(5): p. 651-657.

192. Bieber, T., Atopic dermatitis. *Ann Dermatol*, **2010**. 22(2): p. 125-137.

193. De Benedetto, A., Agnihothri, R., McGirt, L.Y., *et al.*, Atopic Dermatitis: A Disease Caused by Innate Immune Defects? *J Invest Dermatol*, **2009**. 129(1): p. 14-30.

194. Cork, M.J., Danby, S.G., Vasilopoulos, Y., *et al.*, Epidermal Barrier Dysfunction in Atopic Dermatitis. *J Invest Dermatol*, **2009**. 129(8): p. 1892-1908.

195. Tokura, Y., Extrinsic and intrinsic types of atopic dermatitis. *J Dermatol Sci*, **2010**. 58(1): p. 1-7.

196. Oyoshi, M.K., He, R., Kumar, L., *et al.*, Cellular and Molecular Mechanisms in Atopic Dermatitis, in *Adv Immunol*. **2009**, Academic Press. p. 135-226.

197. Novak, N. and Bieber, T., Allergic and nonallergic forms of atopic diseases. *J Allergy Clin Immunol*, **2003**. 112(2): p. 252-262.

198. Rui, H. and Raif, S.G., Thymic stromal lymphopoietin. *Ann N Y Acad Sci*, **2009**. 1183(The Year in Immunology 2): p. 13-24.

199. Ziegler, S.F. and Artis, D., Sensing the outside world: TSLP regulates barrier immunity. *Nat Immunol*, **2010**. 11(4): p. 289-293.

200. Ziegler, S.F., FOXP3: Of Mice and Men. *Annu Rev Immunol*, **2006**. 24(1): p. 209-226.

201. Oscar, P., Görkem, Y., Ahmet, K.A., *et al.*, Role of Treg in immune regulation of allergic diseases. *Eur J Immunol*, **2010**. 40(5): p. 1232-1240.

202. Verhagen, J., Akdis, M., Traidl-Hoffmann, C., *et al.*, Absence of T-regulatory cell expression and function in atopic dermatitis skin. *Journal of Allergy and Clinical Immunology*, **2006**. 117(1): p. 176-183.

203. Candi, E., Schmidt, R., and Melino, G., The cornified envelope: a model of cell death in the skin. *Nat Rev Mol Cell Biol*, **2005**. 6(4): p. 328-340.

204. Hitomi, K., Transglutaminases in skin epidermis. *Eur J Dermatol*, **2005**. 15(5): p. 313-319.

205. Palmer, C.N.A., Irvine, A.D., Terron-Kwiatkowski, A., *et al.*, Common loss-of-function variants of the epidermal barrier protein filaggrin are a major predisposing factor for atopic dermatitis. *Nat Genet*, **2006**. 38(4): p. 441-446.

206. Weidinger, S., Illig, T., Baurecht, H., *et al.*, Loss-of-function variations within the filaggrin gene predispose for atopic dermatitis with allergic sensitizations. *J Allergy Clin Immunol*, **2006**. 118(1): p. 214-219.

207. O'Regan, G.M. and Irvine, A.D., The role of filaggrin loss-of-function mutations in atopic dermatitis. *Curr Opin Allergy Clin Immunol*, **2008**. 8(5): p. 406-410.

208. Weidinger, S., Rodriguez, E., Stahl, C., *et al.*, Filaggrin Mutations Strongly Predispose to Early-Onset and Extrinsic Atopic Dermatitis. *J Invest Dermatol*, **2006**. 127(3): p. 724-726.

209. Bikle, D., Vitamin D and the skin. *J Bone Miner Metab*, **2010**. 28(2): p. 117-130.

210. Su, M.J., Bikle, D.D., Mancianti, M.L., *et al.*, 1,25-Dihydroxyvitamin D3 potentiates the keratinocyte response to calcium. *J Biol Chem*, **1994**. 269(20): p. 14723-14729.

211. Bikle, D.D., Ng, D., Tu, C.L., *et al.*, Calcium- and vitamin D-regulated keratinocyte differentiation. *Mol Cell Endocrinol*, **2001**. 177(1-2): p. 161-171.

212. Bikle, D.D., Ng, D., Oda, Y., *et al.*, The Vitamin D Response Element of the Involucrin Gene Mediates its Regulation by 1,25-Dihydroxyvitamin D3. *J Invest Dermatol*, **2002**. 119(5): p. 1109-1113.

213. Oda, Y., Ishikawa, M.H., Hawker, N.P., *et al.*, Differential role of two VDR coactivators, DRIP205 and SRC-3, in keratinocyte proliferation and differentiation. *J Steroid Biochem Mol Biol*, **2007**. 103(3-5): p. 776-780.

214. Xie, Z., Komuves, L., Yu, Q.-C., *et al.*, Lack of the Vitamin D Receptor is Associated with Reduced Epidermal Differentiation and Hair Follicle Growth. *J Invest Dermatol*, **2002**. 118(1): p. 11-16.

215. Bikle, D.D., Chang, S., Crumrine, D., *et al.*, 25 Hydroxyvitamin D 1 [alpha]-Hydroxylase Is Required for Optimal Epidermal Differentiation and Permeability Barrier Homeostasis. *J Invest Dermatol*, **2004**. 122(4): p. 984-992.

216. Ong, P.Y., Ohtake, T., Brandt, C., *et al.*, Endogenous Antimicrobial Peptides and Skin Infections in Atopic Dermatitis. *N Engl J Med*, **2002**. 347(15): p. 1151-1160.

217. Hata, T.R. and Gallo, R.L., Antimicrobial Peptides, Skin Infections, and Atopic Dermatitis. *Semin Cutan Med Surg*, **2008**. 27(2): p. 144-150.

218. Nomura, I., Goleva, E., Howell, M.D., *et al.*, Cytokine Milieu of Atopic Dermatitis, as Compared to Psoriasis, Skin Prevents Induction of Innate Immune Response Genes. *J Immunol*, **2003**. 171(6): p. 3262-3269.

219. McGirt, L.Y. and Beck, L.A., Innate immune defects in atopic dermatitis. *J Allergy Clin Immunol*, **2006**. 118(1): p. 202-208.

220. Sonkoly, E., Muller, A., Lauerma, A.I., *et al.*, IL-31: A new link between T cells and pruritus in atopic skin inflammation. *J Allergy Clin Immunol*, **2006**. 117(2): p. 411-417.

221. Neis, M.M., Peters, B., Dreuw, A., *et al.*, Enhanced expression levels of IL-31 correlate with IL-4 and IL-13 in atopic and allergic contact dermatitis. *J Allergy Clin Immunol*, **2006**. 118(4): p. 930-937.

222. Altrichter, S., Kriehuber, E., Moser, J., *et al.*, Serum IgE Autoantibodies Target Keratinocytes in Patients with Atopic Dermatitis. *J Invest Dermatol*, **2008**. 128(9): p. 2232-2239.

223. Aichberger, K.J., Mittermann, I., Reininger, R.*, et al.*, Hom s 4, an IgE-Reactive Autoantigen Belonging to a New Subfamily of Calcium-Binding Proteins, Can Induce Th Cell Type 1-Mediated Autoreactivity. *J Immunol*, **2005**. 175(2): p. 1286-1294.

224. Valenta, R., Natter, S., Seiberler, S.*, et al.*, Molecular characterization of an autoallergen, Hom s 1, identified by serum IgE from atopic dermatitis patients. *J Invest Dermatol*, **1998**. 111(6): p. 1178-1183.

225. Schmid-Grendelmeier, P., Flückiger, S., Disch, R.*, et al.*, IgE-mediated and T cell-mediated autoimmunity against manganese superoxide dismutase in atopic dermatitis. *J Allergy Clin Immunol*, **2005**. 115(5): p. 1068-1075.

226. Zugel, U., Steinmeyer, A., May, E.*, et al.*, Immunomodulation by a novel, dissociated Vitamin D analogue. *Exp Dermatol*, **2009**. 18(7): p. 619-627.

227. Herdick, M., Steinmeyer, A., and Carlberg, C., Antagonistic Action of a 25-Carboxylic Ester Analogue of 1α,25-Dihydroxyvitamin D_3 Is Mediated by a Lack of Ligand-induced Vitamin D Receptor Interaction with Coactivators. *J Biol Chem*, **2000**. 275(22): p. 16506-16512.

228. Beck, L. and Spiegelberg, H.L., The polyclonal and antigen-specific IgE and IgG subclass response of mice injected with ovalbumin in alum or complete Freund's adjuvant. *Cell Immunol*, **1989**. 123(1): p. 1-8.

229. Mine, Y. and Yang, M., Epitope characterization of ovalbumin in BALB/c mice using different entry routes. *Biochim Biophys Acta*, **2007**. 1774(2): p. 200-212.

230. Kool, M., Soullie, T., van Nimwegen, M.*, et al.*, Alum adjuvant boosts adaptive immunity by inducing uric acid and activating inflammatory dendritic cells. *J. Exp. Med.*, **2008**. 205(4): p. 869-882.

231. Wang, L.F., Lin, J.Y., Hsieh, K.H.*, et al.*, Epicutaneous exposure of protein antigen induces a predominant Th2-like response with high IgE production in mice. *J Immunol*, **1996**. 156(11): p. 4079-4082.

232. Spergel, J.M., Mizoguchi, E., Brewer, J.P.*, et al.*, Epicutaneous sensitization with protein antigen induces localized allergic dermatitis and hyperresponsiveness to methacholine after single exposure to aerosolized antigen in mice. *J Clin Invest*, **1998**. 101(8): p. 1614-1622.

233. Wang, G., Savinko, T., Wolff, H.*, et al.*, Repeated epicutaneous exposures to ovalbumin progressively induce atopic dermatitis-like skin lesions in mice. *Clin Exp Allergy*, **2007**. 37(1): p. 151-161.

234. Dahten, A., Koch, C., Ernst, D.*, et al.*, Systemic PPARgamma ligation inhibits allergic immune response in the skin. *J Invest Dermatol*, **2008**. 128(9): p. 2211-2218.

235. Walker, J.M. and Jordan, W., Antigen Measurement Using ELISA, in *The Protein Protocols Handbook*. **2009**, Humana Press. p. 1827-1833.

236. Kalyuzhny, A.E., Chemistry and Biology of the ELISPOT Assay, in *Handbook of ELISPOT*, Walker, J.M., Editor. **2005**, Humana Press. p. 15-31.

237. Heimesaat, M.M., Fischer, A., Siegmund, B.*, et al.*, Shift Towards Pro-inflammatory Intestinal Bacteria Aggravates Acute Murine Colitis via Toll-like Receptors 2 and 4. *PLoS ONE*, **2007**. 2(7): p. e662.

238. Rozen, S. and Skaletsky, H.J., *Primer3 on the WWW for general users and for biologist programmers.*, in *Krawetz S, Misener S (eds) Bioinformatics Methods and Protocols: Methods in Molecular Biology. Humana Press, Totowa, NJ*. **2000**. p. 365-386.

239. Nolan, T., Hands, R.E., and Bustin, S.A., Quantification of mRNA using real-time RT-PCR. *Nat Protocols*, **2006**. 1(3): p. 1559-1582.

240. Schmittgen, T.D. and Livak, K.J., Analyzing real-time PCR data by the comparative CT method. *Nat Protocols*, **2008**. 3(6): p. 1101-1108.

241. Pfaffl, M.W., A new mathematical model for relative quantification in real-time RT-PCR. *Nucleic Acids Res*, **2001**. 29(9): p. e45.

242. Abboud, G., Staumont-Salle, D., Kanda, A.*, et al.*, Fc{epsilon}RI and Fc{gamma}RIII/CD16 Differentially Regulate Atopic Dermatitis in Mice. *J Immunol*, **2009**. 182(10): p. 6517-6526.

243. Agematsu, K., Hokibara, S., Nagumo, H.*, et al.*, CD27: a memory B-cell marker. *Immunol Today*, **2000**. 21(5): p. 204-206.

244. Chen, K.S., Prahl, J.M., and DeLuca, H.F., Isolation and expression of human 1,25-dihydroxyvitamin D3 24-hydroxylase cDNA. *Proc Natl Acad Sci U S A*, **1993**. 90(10): p. 4543-4547.

245. Stoeckler, J.D., Stoeckler, H.A., Kouttab, N.*, et al.*, 1alpha,25-Dihydroxyvitamin D3 modulates CD38 expression on human lymphocytes. *J Immunol*, **1996**. 157(11): p. 4908-4917.

246. Ghosh, S. and Hayden, M.S., New regulators of NF-[kappa]B in inflammation. *Nat Rev Immunol*, **2008**. 8(11): p. 837-848.

247. Parrish-Novak, J., Dillon, S.R., Nelson, A.*, et al.*, Interleukin 21 and its receptor are involved in NK cell expansion and regulation of lymphocyte function. *Nature*, **2000**. 408(6808): p. 57-63.

248. Avery, D.T., Deenick, E.K., Ma, C.S.*, et al.*, B cell-intrinsic signaling through IL-21 receptor and STAT3 is required for establishing long-lived antibody responses in humans. *J. Exp. Med.*, **2010**. 207(1): p. 155-171.

249. Good, K.L., Bryant, V.L., and Tangye, S.G., Kinetics of Human B Cell Behavior and Amplification of Proliferative Responses following Stimulation with IL-21. *J Immunol*, **2006**. 177(8): p. 5236-5247.

250. Ettinger, R., Sims, G.P., Fairhurst, A.-M.*, et al.*, IL-21 Induces Differentiation of Human Naive and Memory B Cells into Antibody-Secreting Plasma Cells. *J Immunol*, **2005**. 175(12): p. 7867-7879.

251. Avery, D.T., Ellyard, J.I., Mackay, F.*, et al.*, Increased Expression of CD27 on Activated Human Memory B Cells Correlates with Their Commitment to the Plasma Cell Lineage. *J Immunol*, **2005**. 174(7): p. 4034-4042.

252. Arpin, C., Dechanet, J., Van Kooten, C.*, et al.*, Generation of memory B cells and plasma cells in vitro. *Science*, **1995**. 268(5211): p. 720-722.

253. Tangye, S.G., Avery, D.T., and Hodgkin, P.D., A Division-Linked Mechanism for the Rapid Generation of Ig-Secreting Cells from Human Memory B Cells. *J Immunol*, **2003**. 170(1): p. 261-269.

254. Mora, J.R., Iwata, M., and von Andrian, U.H., Vitamin effects on the immune system: vitamins A and D take centre stage. *Nat Rev Immunol*, **2008**. 8(9): p. 685-698.

255. Ozdemir, C., Akdis, M., and Akdis, C.A., T regulatory cells and their counterparts: masters of immune regulation. *Clin Exp Allergy*, **2009**. 39(5): p. 626-639.

256. Dudda, J.C., Perdue, N., Bachtanian, E.*, et al.*, Foxp3+ regulatory T cells maintain immune homeostasis in the skin. *J Exp Med*, **2008**. 205(7): p. 1559-1565.

257. Wang, X., Fujita, M., Prado, R.*, et al.*, Visualizing CD4 T-cell migration into inflamed skin and its inhibition by CCR4/CCR10 blockades using in vivo imaging model. *Br J Dermatol*, **2009**. 162(3): p. 487-496.

258. Reiss, Y., Proudfoot, A.E., Power, C.A.*, et al.*, CC chemokine receptor (CCR)4 and the CCR10 ligand cutaneous T cell-attracting chemokine (CTACK) in lymphocyte trafficking to inflamed skin. *J Exp Med*, **2001**. 194(10): p. 1541-1547.

259. Homey, B., Wang, W., Soto, H.*, et al.*, Cutting Edge: The Orphan Chemokine Receptor G Protein-Coupled Receptor-2 (GPR-2, CCR10) Binds the Skin-Associated Chemokine CCL27 (CTACK/ALP/ILC). *J Immunol*, **2000**. 164(7): p. 3465-3470.

260. Homey, B., Alenius, H., Muller, A.*, et al.*, CCL27-CCR10 interactions regulate T cell-mediated skin inflammation. *Nat Med*, **2002**. 8(2): p. 157-165.

261. Li, M., Hener, P., Zhang, Z.*, et al.*, Topical vitamin D3 and low-calcemic analogs induce thymic stromal lymphopoietin in mouse keratinocytes and trigger an atopic dermatitis. *Proc Natl Acad Sci U S A*, **2006**. 103(31): p. 11736-11741.

262. Nestle, F.O., Kaplan, D.H., and Barker, J., Psoriasis. *N Engl J Med*, **2009**. 361(5): p. 496-509.

263. Poon, A.H., Laprise, C., Lemire, M.*, et al.*, Association of Vitamin D Receptor Genetic Variants with Susceptibility to Asthma and Atopy. *Am. J. Respir. Crit. Care Med.*, **2004**. 170(9): p. 967-973.

264. Bosse, Y., Lemire, M., Poon, A.H.*, et al.*, Asthma and genes encoding components of the vitamin D pathway. *Respir Res*, **2009**. 10: p. 98.

265. van Etten, E. and Mathieu, C., Immunoregulation by 1,25-dihydroxyvitamin D3: Basic concepts. *J Steroid Biochem Mol Biol*, **2005**. 97(1-2): p. 93-101.

266. Smith, E.A., Frankenburg, E.P., Goldstein, S.A.*, et al.*, Effects of long-term administration of vitamin D3 analogs to mice. *J Endocrinol*, **2000**. 165(1): p. 163-172.

267. Brown, A.J. and Slatopolsky, E., Vitamin D analogs: Therapeutic applications and mechanisms for selectivity. *Mol Aspects Med*, **2008**. 29(6): p. 433-452.

268. Bouillon, R., Verlinden, L., Eelen, G.*, et al.*, Mechanisms for the selective action of Vitamin D analogs. *J Steroid Biochem Mol Biol*, **2005**. 97(1-2): p. 21-30.

269. Peric, M., Koglin, S., Dombrowski, Y.*, et al.*, Vitamin D analogs differentially control antimicrobial peptide/"alarmin"expression in psoriasis. *PLoS One*, **2009**. 4(7): p. e6340.

270. Jabara, H.H., Fu, S.M., Geha, R.S.*, et al.*, CD40 and IgE: synergism between anti-CD40 monoclonal antibody and interleukin 4 in the induction of IgE synthesis by highly purified human B cells. *J Exp Med*, **1990**. 172(6): p. 1861-1864.

271. Fujieda, S., Zhang, K., and Saxon, A., IL-4 plus CD40 monoclonal antibody induces human B cells gamma subclass- specific isotype switch: switching to gamma 1, gamma 3, and gamma 4, but not gamma 2. *J Immunol*, **1995**. 155(5): p. 2318-2328.

272. Tangye, S.G., Ferguson, A., Avery, D.T.*, et al.*, Isotype Switching by Human B Cells Is Division-Associated and Regulated by Cytokines. *J Immunol*, **2002**. 169(8): p. 4298-4306.

273. Fear, D.J., McCloskey, N., O'Connor, B.*, et al.*, Transcription of Ig Germline Genes in Single Human B Cells and the Role of Cytokines in Isotype Determination. *J Immunol*, **2004**. 173(7): p. 4529-4538.

274. Castillo, A.I., Sanchez-Martinez, R., Jimenez-Lara, A.M.*, et al.*, Characterization of Vitamin D Receptor Ligands with Cell-Specific and Dissociated Activity. *Mol Endocrinol*, **2006**. 20(12): p. 3093-3104.

275. Tocchini-Valentini, G., Rochel, N., Wurtz, J.-M.*, et al.*, Crystal Structures of the Vitamin D Nuclear Receptor Liganded with the Vitamin D Side Chain Analogues Calcipotriol and Seocalcitol, Receptor Agonists of Clinical Importance. Insights into a Structural Basis for the Switching of Calcipotriol to a Receptor Antagonist by Further Side Chain Modification. *J Med Chem*, **2004**. 47(8): p. 1956-1961.

276. Herdick, M., Steinmeyer, A., and Carlberg, C., Carboxylic ester antagonists of 1α,25-dihydroxyvitamin D_3 show cell-specific actions. *Chem Biol*, **2000**. 7(11): p. 885-894.

277. Kukkonen, K., Kuitunen, M., Haahtela, T.*, et al.*, High intestinal IgA associates with reduced risk of IgE-associated allergic diseases. *Pediatr Allergy Immunol*, **2010**. 21(1-Part-I): p. 67-73.

278. Janzi, M., Kull, I., Sjöberg, R.*, et al.*, Selective IgA deficiency in early life: Association to infections and allergic diseases during childhood. *Clin Immunol*, **2009**. 133(1): p. 78-85.

279. Defrance, T., Aubry, J.P., Rousset, F.*, et al.*, Human recombinant interleukin 4 induces Fc epsilon receptors (CD23) on normal human B lymphocytes. *J. Exp. Med.*, **1987**. 165(6): p. 1459-1467.

280. Kuchen, S., Robbins, R., Sims, G.P.*, et al.*, Essential Role of IL-21 in B Cell Activation, Expansion, and Plasma Cell Generation during CD4+ T Cell-B Cell Collaboration. *J Immunol*, **2007**. 179(9): p. 5886-5896.

281. Punnonen, J., Aversa, G., Cocks, B.G.*, et al.*, Interleukin 13 induces interleukin 4-independent IgG4 and IgE synthesis and CD23 expression by human B cells. *Proc Natl Acad Sci U S A*, **1993**. 90(8): p. 3730-3734.

282. Gauchat, J.-F., Aversa, G., Gascan, H.*, et al.*, Modulation of IL-4 induced germline εRNA synthesis in human B cells by tumor necrosis factor-β, anti-CD40 monoclonal antibodies or transforming growth factor-β correlates with levels of IgE production. *Int Immunol*, **1992**. 4(3): p. 397-406.

283. Okamoto, M., Van Stry, M., Chung, L.*, et al.*, Mina, an Il4 repressor, controls T helper type 2 bias. *Nat Immunol*, **2009**. 10(8): p. 872-879.

284. Osborn, J.L., Schwartz, G.G., Smith, D.C.*, et al.*, Phase II trial of oral 1,25-dihydroxyvitamin D (calcitriol) in hormone refractory prostate cancer. *Urol Oncol*, **1995**. 1(5): p. 195-198.

285. Boehm, M.F., Fitzgerald, P., Zou, A.*, et al.*, Novel nonsecosteroidal vitamin D mimics exert VDR-modulating activities with less calcium mobilization than 1,25-dihydroxyvitamin D3. *Chem Biol*, **1999**. 6(5): p. 265-275.

286. van Etten, E., Decallonne, B., Verlinden, L.*, et al.*, Analogs of 1α,25-dihydroxyvitamin D3 as pluripotent immunomodulators. *J Cell Biochem*, **2003**. 88(2): p. 223-226.

287. Smith, D.C., Johnson, C.S., Freeman, C.C.*, et al.*, A Phase I Trial of Calcitriol (1,25-Dihydroxycholecalciferol) in Patients with Advanced Malignancy. *Clin Cancer Res*, **1999**. 5(6): p. 1339-1345.

288. Zugel, U., Steinmeyer, A., Giesen, C.*, et al.*, A Novel Immunosuppressive 1[alpha],25-Dihydroxyvitamin D3 Analog with Reduced Hypercalcemic Activity. *J Invest Dermatol*, **2002**. 119(6): p. 1434-1442.

289. Finkelman, F.D., Anaphylaxis: Lessons from mouse models. *J Allergy Clin Immunol*, **2007**. 120(3): p. 506-515.

290. Averbeck, M., Gebhardt, C., Emmrich, F.*, et al.*, Immunologic Principles of Allergic Disease. *J Dtsch Dermatol Ges*, **2007**. 5(11): p. 1015-1027.

291. PanHammarström, Q., Zhao, Y., Hammarström, L.*, et al.*, Class Switch Recombination: A Comparison Between Mouse and Human, in *Adv Immunol*. **2007**, Academic Press. p. 1-61.

292. Fonacier, L.S., Dreskin, S.C., and Leung, D.Y.M., Allergic skin diseases. *J Allergy Clin Immunol*, **2010**. 125(2, Supplement 2): p. S138-S149.

293. Bowcock, A.M. and Krueger, J.G., Getting under the skin: the immunogenetics of psoriasis. *Nat Rev Immunol*, **2005**. 5(9): p. 699-711.

294. Guttman-Yassky, E., Lowes, M.A., Fuentes-Duculan, J.*, et al.*, Low Expression of the IL-23/Th17 Pathway in Atopic Dermatitis Compared to Psoriasis. *J Immunol*, **2008**. 181(10): p. 7420-7427.

295. Nograles, K.E., Zaba, L.C., Shemer, A.*, et al.*, IL-22-producing "T22" T cells account for upregulated IL-22 in atopic dermatitis despite reduced IL-17-producing TH17 T cells. *J Allergy Clin Immunol*, **2009**. 123(6): p. 1244-1252.e1242.

296. Roberson, E.D.O. and Bowcock, A.M., Psoriasis genetics: breaking the barrier. *Trends Genet*, **2010**. 26(9): p. 415-423.

297. Sigmon, J.R., Yentzer, B.A., and Feldman, S.R., Calcitriol ointment: A review of a topical vitamin D analog for psoriasis. *J Dermatolog Treat*, **2009**. 20(4): p. 208-212.

298. Gupta, J., Grube, E., Ericksen, M.B.*, et al.*, Intrinsically defective skin barrier function in children with atopic dermatitis correlates with disease severity. *J Allergy Clin Immunol*, **2008**. 121(3): p. 725-730.e722.

299. Woodward, A.L., Spergel, J.M., Alenius, H.*, et al.*, An obligate role for T-cell receptor [alpha][beta]+ T cells but not T-cell receptor [gamma][delta]+ T cells, B cells, or CD40/CD40L interactions in a mouse model of atopic dermatitis. *J Allergy Clin Immunol*, **2001**. 107(2): p. 359-366.

300. Akdis, M., Simon, H.-U., Weigl, L.*, et al.*, Skin Homing (Cutaneous Lymphocyte-Associated Antigen-Positive) CD8+ T Cells Respond to Superantigen and Contribute to Eosinophilia and IgE Production in Atopic Dermatitis. *J Immunol*, **1999**. 163(1): p. 466-475.

301. Savinko, T., Lauerma, A., Lehtimäki, S.*, et al.*, Topical Superantigen Exposure Induces Epidermal Accumulation of CD8+ T Cells, a Mixed Th1/Th2-Type Dermatitis and Vigorous Production of IgE Antibodies in the Murine Model of Atopic Dermatitis. *J Immunol*, **2005**. 175(12): p. 8320-8326.

302. Hennino, A., Vocanson, M., Toussaint, Y.*, et al.*, Skin-Infiltrating CD8+ T Cells Initiate Atopic Dermatitis Lesions. *J Immunol*, **2007**. 178(9): p. 5571-5577.

303. Zhu, J. and Paul, W.E., CD4 T cells: fates, functions, and faults. *Blood*, **2008**. 112(5): p. 1557-1569.

304. Zhu, J., Yamane, H., and Paul, W.E., Differentiation of Effector CD4 T Cell Populations. *Annu Rev Immunol*, **2010**. 28(1): p. 445-489.

305. Beissert, S., Schwarz, A., and Schwarz, T., Regulatory T Cells. *J Invest Dermatol*, **2006**. 126(1): p. 15-24.

306. Sakaguchi, S., Miyara, M., Costantino, C.M.*, et al.*, FOXP3+ regulatory T cells in the human immune system. *Nat Rev Immunol*, **2010**. 10(7): p. 490-500.

307. Brunkow, M.E., Jeffery, E.W., Hjerrild, K.A.*, et al.*, Disruption of a new forkhead/winged-helix protein, scurfin, results in the fatal lymphoproliferative disorder of the scurfy mouse. *Nat Genet*, **2001**. 27(1): p. 68-73.

308. Lin, W., Truong, N., Grossman, W.J.*, et al.*, Allergic dysregulation and hyperimmunoglobulinemia E in Foxp3 mutant mice. *J Allergy Clin Immunol*, **2005**. 116(5): p. 1106-1115.

309. Verhagen, J., Akdis, M., Traidl-Hoffmann, C.*, et al.*, Absence of T-regulatory cell expression and function in atopic dermatitis skin. *J Allergy Clin Immunol*, **2006**. 117(1): p. 176-183.

310. Freyschmidt, E.-J., Mathias, C.B., Diaz, N.*, et al.*, Skin Inflammation Arising from Cutaneous Regulatory T Cell Deficiency Leads to Impaired Viral Immune Responses. *J Immunol*, **2010**. 185(2): p. 1295-1302.

311. Loser, K., Mehling, A., Loeser, S.*, et al.*, Epidermal RANKL controls regulatory T-cell numbers via activation of dendritic cells. *Nat Med*, **2007**. 12(12): p. 1372-1379.

312. Totsuka, T., Kanai, T., Nemoto, Y.*, et al.*, RANK-RANKL Signaling Pathway Is Critically Involved in the Function of CD4+CD25+ Regulatory T Cells in Chronic Colitis. *J Immunol*, **2009**. 182(10): p. 6079-6087.

313. Kitazawa, R., Kitazawa, S., and Maeda, S., Promoter structure of mouse RANKL/TRANCE/OPGL/ODF gene. *Biochim Biophys Acta*, **1999**. 1445(1): p. 134-141.

314. Sather, B.D., Treuting, P., Perdue, N.*, et al.*, Altering the distribution of Foxp3+ regulatory T cells results in tissue-specific inflammatory disease. *J. Exp. Med.*, **2007**. 204(6): p. 1335-1347.

315. Széles, L., Keresztes, G., Töröcsik, D.*, et al.*, 1,25-Dihydroxyvitamin D3 Is an Autonomous Regulator of the Transcriptional Changes Leading to a Tolerogenic Dendritic Cell Phenotype. *J Immunol*, **2009**. 182(4): p. 2074-2083.

316. Eksteen, B., Miles, A., Curbishley, S.M.*, et al.*, Epithelial Inflammation Is Associated with CCL28 Production and the Recruitment of Regulatory T Cells Expressing CCR10. *J Immunol*, **2006**. 177(1): p. 593-603.

317. Morales, J., Homey, B., Vicari, A.P., *et al.*, CTACK, a skin-associated chemokine that preferentially attracts skin-homing memory T cells. *Proc Natl Acad Sci U S A*, **1999**. 96(25): p. 14470-14475.

318. Sigmundsdottir, H. and Butcher, E.C., Environmental cues, dendritic cells and the programming of tissue-selective lymphocyte trafficking. *Nat Immunol*, **2008**. 9(9): p. 981-987.

319. Sells, R.E. and Hwang, S.T., Paradoxical Increase in Skin Inflammation in the Absence of CCR4. *J Invest Dermatol*, **2010**. 130(12): p. 2697-2699.

320. He, R., Oyoshi, M.K., Garibyan, L., *et al.*, TSLP acts on infiltrating effector T cells to drive allergic skin inflammation. *Proc Natl Acad Sci U S A*, **2008**. 105(33): p. 11875-11880.

321. Yoo, J., Omori, M., Gyarmati, D., *et al.*, Spontaneous atopic dermatitis in mice expressing an inducible thymic stromal lymphopoietin transgene specifically in the skin. *J Exp Med*, **2005**. 202(4): p. 541-549.

322. Watanabe, N., Wang, Y.-H., Lee, H.K., *et al.*, Hassall's corpuscles instruct dendritic cells to induce CD4+CD25+ regulatory T cells in human thymus. *Nature*, **2005**. 436(7054): p. 1181-1185.

323. Hanabuchi, S., Ito, T., Park, W.-R., *et al.*, Thymic Stromal Lymphopoietin-Activated Plasmacytoid Dendritic Cells Induce the Generation of FOXP3+ Regulatory T Cells in Human Thymus. *J Immunol*, **2010**. 184(6): p. 2999-3007.

324. Lee, J.-Y., Lim, Y.-M., Park, M.-J., *et al.*, Murine thymic stromal lymphopoietin promotes the differentiation of regulatory T cells from thymic CD4+CD8-CD25- naive cells in a dendritic cell-independent manner. *Immunol Cell Biol*, **2007**. 86(2): p. 206-213.

325. Aioi, A., Tonogaito, H., Suto, H., *et al.*, Impairment of skin barrier function in NC/Nga Tnd mice as a possible model for atopic dermatitis. *Br J Dermatol*, **2001**. 144(1): p. 12-18.

326. Kezic, S., Kemperman, P.M.J.H., Koster, E.S., *et al.*, Loss-of-Function Mutations in the Filaggrin Gene Lead to Reduced Level of Natural Moisturizing Factor in the Stratum Corneum. *J Invest Dermatol*, **2008**. 128(8): p. 2117-2119.

327. Presland, R.B., Boggess, D., Lewis, S.P., *et al.*, Loss of Normal Profilaggrin and Filaggrin in Flaky Tail (ft/ft) Mice: an Animal Model for the Filaggrin-Deficient Skin Disease Ichthyosis Vulgaris. *J Invest Dermatol*, **2000**. 115(6): p. 1072-1081.

328. Kim, B.E., Leung, D.Y.M., Boguniewicz, M., *et al.*, Loricrin and involucrin expression is down-regulated by Th2 cytokines through STAT-6. *Clin Immunol*, **2008**. 126(3): p. 332-337.

329. Sehra, S., Yao, Y., Howell, M.D., *et al.*, IL-4 Regulates Skin Homeostasis and the Predisposition toward Allergic Skin Inflammation. *J Immunol*, **2010**. 184(6): p. 3186-3190.

330. Hata, T.R., Kotol, P., Jackson, M., *et al.*, Administration of oral vitamin D induces cathelicidin production in atopic individuals. *J Allergy Clin Immunol*, **2008**. 122(4): p. 829-831.

9. Danksagung

In erster Linie gilt mein Dank Frau Prof. Dr. med. Margitta Worm für die Überlassung dieses Themas sowie die Möglichkeit, diese Arbeit in ihrer Arbeitsgruppe an der Charité in Berlin anzufertigen. Weiterhin möchte ich Frau Prof. Worm für ihre Unterstützung in allen Phasen dieser Arbeit danken. Des Weiteren gilt mein besonderer Dank Herrn Prof. Dr. rer. nat. Roland Lauster, für die Bereitschaft meine Arbeit zu betreuen.
Ein herzliches Dankeschön an Herrn Dr. med. Guido Heine für die Einführung in die facettenreiche Welt von Vitamin D, mit zahlreichen Diskussionen über die experimentelle Herangehensweise und aktuelle Daten. Bei Herrn Prof. Dr. rer. nat. Andreas Radbruch möchte ich mich für die hilfreichen, wissenschaftlichen Diskussionen insbesondere im Rahmen des B-Zellclubs im DRFZ bedanken. Ein ganz besonderer Dank an Dr. Magda Babina für die großartige Unterstützung bei der Anfertigung der Publikationen.

Meinen herzlichsten Dank an René Riedel und Katharina Jörß, die im Rahmen ihrer Diplomarbeiten, einen wesentlichen Beitrag zum Gelingen dieser Arbeit geleistet haben. Der Arbeitsgruppe von Prof. Dr. med. Christoph Loddenkemper, im Speziellen Simone Spieckermann und Frau Dr. rer. medic. Anja Kühl, danke ich für die Anfertigung der Foxp3-Färbungen in der Haut. Ein ganz großes Dankeschön den Mitgliedern der AG Worm, vor allem Dr. rer. nat. Christin Weise, Dr. rer. nat. Verena Fokuhl, Dr. med. Zhu Yan, Milena Milovanovic, M.D., Gennadiy Drozdenko, Maria Nassiri, Kiran Kumar, Vandana Kumari, Sabine Dölle, Pascal Klaus, Tim Hollstein, Dr. med. vet. Friederike Kirn, Dana Hoser, Carolin Hobe und Carolin Heunemann für viele gemeinsame Stunden im Labor, in Seminaren, Vitamin D-Treffen und Arbeitsgruppenbesprechungen sowie bei außerwissenschaftlichen Zusammenkünften. Weiterhin möchte ich Dennis Ernst, dem guten Geist im Labor der AG Worm, für seine außergewöhnliche Hilfsbereitschaft und seinen ansteckenden Humor, der stets für gute Laune im Labor sorgte, danken. Meiner Bürogenossin und Mitstreiterin, Kerstin Geldmeyer-Hilt (Hilti), danke ich recht herzlich für die sehr angenehme Zeit im 5. Stock, für all die Diskussionen, gegenseitige Hilfestellung (wissenschaftlich und mental), die Kaffeepausen und für das Teilen jeglicher Art von Süßigkeiten, Obst und anderen Nahrungsmitteln zur Nervenstärkung.

Schließlich möchte ich den Personen danken, ohne die ich nicht da wäre, wo ich jetzt bin, meiner Familie und Katharina. Danke für Eure Geduld, für das Zuhören und den Rückhalt, den Ihr mir während dieser Zeit entgegengebracht habt.

10. Publications

Hartmann, B., Heine, G., Babina, M., Steinmeyer, A., Zügel, U., Radbruch, A., and Worm, M., Targeting the vitamin D receptor inhibits the B cell-dependent allergic immune response. *Allergy*, **2010**: p. DOI: 10.1111/j.1398-9995.2010.02513.x. [Epub ahead of print]

Heine, G., Dahten, A., Hilt, K., Ernst, D., Milovanovic, M., Hartmann, B., and Worm, M., Liver X Receptors Control IgE Expression in B Cells. *J Immunol*, **2009**. 182(9): p. 5276-5282.